博 士 学 位 論 文

Doctoral Dissertation

Study on Mechanical Properties of Fiber-Cement Stabilized Soil Produced by Using Agricultural By-Products (農業廃棄物を用いた繊維質固化処理土の機械的特性に関する研究)

東北大学大学院環境科学研究科

Graduate School of Environmental Studies, Tohoku University

先進社会環境学専攻

氏　名
Name

Duong Thanh Nga

指　導　教　員 Supervisor at Tohoku Univ.	高橋 弘 教授
研 究 指 導 教 員 Research Advisor at Tohoku Univ.	
審　査　委　員 （○印は主査） Dissertation Committee Members Name marked with "○" is the Chief Examiner	○　高橋 弘 教授 1　駒井 武 教授　　2　岡本 敦 教授 3　里見 知昭 助教　　4 5　　6

THESIS

STUDY ON MECHANICAL PROPERTIES OF FIBER-CEMENT STABILIZED SOIL PRODUCED BY USING AGRICULTURAL BY-PRODUCTS

JULY 2021

TOHOKU UNIVERSITY
GRADUATE SCHOOL OF ENVIRONMENTAL STUDIES
TAKAHASHI LABORATORY

BY

DUONG THANH NGA

CONTENTS

LIST OF FIGURES

LIST OF TABLES

CHAPTER 1
INTRODUCTION

1.1 Problem statement

1.1.1 Sludge disposal

Vietnam is located in Southwest Asia 14.0583°N, 108.2772°E and has a border with Laos, Cambodia, and China (Fig. 1-1). Every year, the sludge and soft soil produced from construction sites and canal dredging in The South of Viet Nam are very huge. Nguyen Viet Trung et al. (2013) [1] reported that in Ho Chi Minh City, the canal dredging sludge are sandy soil in 30 - 50 cm of the surface and clay-soil in the bottom layer. Sludge volume of canal dredging and construction is up to about 1750 m^3 per day and up to millions of m^3, respectively. Sludge is discharged to final disposal (i.e., landfill or undefined location) (Fig. 1-2) with a low recycling rate.

Vietnam is a developing country, so the economy grows at a high speed and the living standard has been improving year by year. Therefore, more and more infrastructure has been building to facilitate the development of economics such as the metro system, highway, high-rise building, etc. Consequently, a huge amount of excavated soft soil is produced from construction projects. For example, Ho Chi Minh City People's Committee had a plan to build Metro Rail System with six main lines. As a result, a large amount of excavated soil is disposed in the environment. According to a report by Ho Chi Minh City People's Committee Management Authority for Urban Railways, Line No.2 of this project discharged about 1.4 million m^3 excavated soil [2].

In general, soft soil and sludge are considered as a kind of waste causing environmental issues and costing a large cost for disposal. Therefore, recycling sludge and weak soil to use as a new alternative material in construction [3–6] is the best solution to deal with their discharge and related problems.

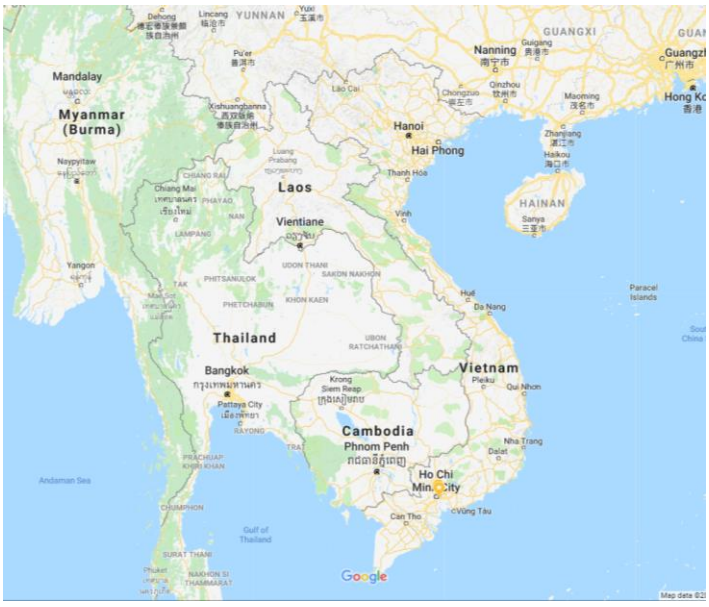

Fig. 1-1 Location of Vietnam

http://moitruong24h.vn/Data.

Fig. 1-2 Sludge disposal in Viet Nam

1.1.2 Crop residue disposal

Viet Nam is a tropical country and abundant in water which are good conditions for the development of agriculture. Therefore, Vietnam has become an agricultural country with a high yield in the top ten of the world. In agriculture, rice is the dominant crop that contributes to the development of agriculture. The area of rice counts for two-thirds of the total planting area. After rice, maize is the second crop in Vietnam and following by sweet potatoes, cassava, sugar cane, peanut, etc. The yield areas under cultivation of main crops in Viet Nam are shown in Table 1-1.

The high yield of food crops results in a huge amount of crop residue. After harvesting, a

large amount of by-product is produced such as rice straw, rice husk from rice crop, corn husk, corn silk, cob corn from maize, etc. The ratio of crop residue yield to food crop production of some main crop residue and yield of crop residue are shown in Table 1-2. The yield of the by-product is calculated from the production of agriculture and the ratio of crop residue yield to the production of the crop.

Table 1-1 Main crops in Viet Nam 2016 [7]

Name of crop	Area (Thousand ha)	Production (Thousand tons)
Rice	7,790.4	43,609.5
Maize	1,152.4	5,225.6
Sweet potatoes	119.0	1,289.1
Cassava	569.9	10,931.8
Sugar cane	274.2	17,171.3
Peanut	191.3	441.4

Table 1-2 Crop residue yield to food crop production

Residue crop	Ratio [8]	Yield of crop residue (Thousand tons)
Rice straw	1.757	76,621.892
Rice husk	0.2 - 0.33	8,721.9 - 14,391.135
Corn husk	0.2	1,045.12
Bagasse	0.1 - 0.33	1,717.13 - 5,666.529
Cassava stalks	0.167 - 2	1,825.611 - 2,186.36

In Viet Nam, the use of crop residue is limited. A small amount of the residue crop is used for mushroom production, livestock feed, utensil making, compost product, and a large amount is burnt (Fig. 1-3). However, crop residue burn causes many environmental issues. The gas (methane and nitrous oxide) emitted from residue crops will trap the heat that leads to an increase in the rate of global warming. Therefore, the mitigation of residue crop burning is necessary to reduce the rate of climate change. The statistic of greenhouse gases emitted from agricultural activities in 2005 and 2010 is shown in Table 1-3.

https://muabanrom.com/khong-nen-dot-rom-ra-sau-vu-thu-hoach.html

Fig. 1-3 Residue crop burning in Viet Nam

Table 1-3 Greenhouse gas emission from agriculture [9]

Sources (Gg-CO_2)	2005			2010		
	CH4	N2O	Total	CH4	N2O	Total
Enteric Fermentation	9,275.1	0.0	9,275.1	9,467.5	0.0	9,467.5
Manure management	2,149.6	5,906.5	8,056.2	2,319.5	6,240.5	8,560.0
Rice cultivation	42,511.6	0.0	42,511.6	44,614.2	0.0	44,614.2
Agricultural soils	0.0	22,282.9	22,282.9	0.0	23,812.0	23,812.0
Burning savanna	3.1	0.6	3.7	1.4	0.3	1.7
Burning crop residue	**1,342.6**	**348.3**	**1,690.9**	**1,506.3**	**393.0**	**1,899.3**

1.2 Objectives

Due to the negative impacts of excavated soil and canal dredging sludge discharge, this study proposes the methods to mitigate these negative effects. In geotechnical engineering, Fiber-Cement Stabilized Soil method and Liquified-Stabilized Soil method are effective method for recycling excavated soil and canal dredging sludge. Therefore, this research applies these two methods for recycling to mitigate the problems from discharging excavated soil and canal dredging sludge. The output modified soil is used as an alternative construction material. This solution contributes to the reduction of cost for sludge and soft soil discharge, transportation fee for disposal, and the investigation cost in construction due to the reuse of modified soil. This fiber-cement stabilized soils have already been used widely in Japan [10]

by using paper debris as a fiber material. However, it is hard to obtain a large amount of paper debris at a low cost when applying this method in Viet Nam. Therefore, the local fiber materials should be considered to use, and crop residues from agriculture are the good candidates. If crop residue of agriculture is used as fiber materials for soil improvement, the negative impact of crop residue burning on the environment can be solved. However, the workability of agricultural by-products and the suitable by-product for soil improvement are unclear.

The current work aims to find out the best fiber material for recycling soft soil and sludge in Viet Nam by comparing the workability of five fiber materials consisting of rice straw, rice husk, corn silk, corn husk, and paper debris in terms of Fiber-Cement Stabilized Soil method for recycling sludge. Then the best fiber is selected for studying deeply the engineering properties of the selected fiber-cement stabilized soil produce by the Fiber-Cement Stabilized Soil method and Liquified-Stabilized Soil method. The mechanical properties of selected fiber-reinforced cemented soil are evaluated in terms of a series of laboratory experiments containing flow test, bleeding test, unconfined compression test, splitting tension test, direct tension test, shear box test, and durability test. Besides, since selected fiber is the new material, tensile strength of fiber is measured to understand more clearly its properties.

1.3 Literature review

During several past decades, cemented soil is an effective soil stabilization method researched by many studies. In this method, the production of hydration reaction in the cement is responsible for the formation of the skeleton in the soil matrix. Due to the development of cementitious structure in the void of the soil matrix, failure strength, stiffness, tensile strength, etc. are significantly improved. However, the brittleness property of the cemented soil, a disadvantage property for construction, is also increased. Previous researches have used the fiber-reinforced cemented soil method to overcome the weakness of cemented soil approach (high brittleness).

S. Sasaniana et al. (2014) [11] investigated the properties of cemented clays through a series of laboratory experiments including undrained tri-axial, unconfined compression, shear vane, and oedometer tests with different types of clays treated with Portland cement. Although the hydration rate of cement decreases significantly with curing time, cemented clay still gains

remarkably strength when curing time increases.

S. H. Chew et al. (2004) [12] studied the behavior of the cementitious product in cemented soft clay and the relationship between cement development and the engineering behavior. This study showed that the failure strength and stiffness increase even if at very low cement content. As cement content less than 10%, the ductile behavior of specimens is exposed and the post-peak stress declines gradually. With higher cement content, the specimen changes from ductile to brittle behavior. Hence, after reaching peak stress, the compressive stress abruptly drops.

F. Sariosseiri et al. (2008) [13] studied consolidated-undrained tri-axial, compaction characteristics, unconfined compressive strength, Atterberg limits, and the drying rate of stabilized soil by Portland cement in the state of Washington, USA. The shear strength, unconfined compressive strength, and drying rate of soil are significantly improved when adding cement. The results showed that specimens are ductile with less than 10% cement content. With above 10% cement content, split in pore pressures rapidly rises and results in the effective pressure at failure near zero.

In many past decades, synthetic fiber is the main kind of fiber used in fiber-reinforced soil and cemented soil, such as polypropylene [14–18], polyethylene terephthalate [19], nylon fiber [20]. N. C. Consoli et al. (1998, 2009) [21, 22] investigated the mechanical properties of polypropylene fibers-cement stabilized sand under drained tri-axial loading conditions to evaluate the influence of fiber on brittleness, ultimate behavior, initial stiffness, stress–dilatancy, and peak stress of uncommented sand and sand treated with cement contents of 1%, 4%, 7%, and 10%. The results showed that stiffness and peak stress significantly increase with the addition of cement, but the sand behavior is more brittle. However, the cemented sand changes from brittle behavior to ductile behavior when adding fiber. Besides, failure strength and post-peak stress are dependent on additive fiber.

N. C. Consoli et al. (2010) [23] aimed to investigate the difference in failure strength of cemented soil and fiber-cement stabilized soil. The study depicted that fiber inclusion results in the increase of failure strength of cemented soil. As for the role of the addition of cement, the strength of fiber-reinforced or unreinforced cemented soil increases linearly with the increase of cemented content. Moreover, the increase of cement content also leads to the increase of dry density and the reduction of the porosity of compacted cemented soil and compacted fiber-cement stabilized soil.

R. F. Dean (1986) [24] studied the impact of fiber (i.e., spun nylon string, polypropylene rope fiber, and polypropylene olefin) on the strength of compacted fine-grained soil. The addition of fiber increases failure strength at a lower water content than optimum water content. Randomly distributed fiber results in more deformation of specimens which leads to the increase of toughness.

Nowadays, from the environmental and economic viewpoints, it is necessary to pay more attention to natural waste materials, specially by-production from agriculture, due to two reasons. The first reason is that crop residue disposal causes environmental issues. F.N. Tubiello et al. (2014) [25] reported that according to the report of the Food and Agriculture Organization of the United Nations, in non-Annex I countries, over two-thirds of greenhouse gas emission of agriculture is emitted from burning crop residue. In 2011, emission from maize and rice is very high about 45% and 25%, respectively. Therefore, the reuse of crop residue contributes to the reduction of the negative impact on the environment from the discharge of by-products from agriculture. The second reason is that it is reported that natural waste materials are cheap, abundant, low density, renewable, and sustainable [26–28]. In addition, biodegradable and non-hazardous properties of natural materials drive fiber-reinforced cemented soil to avoid causing environmental pollution. Nowadays, some research focus on using natural fiber to reinforce soil and cemented soil. For example, hemp [29], sisal [30, 31], jute [32], banana fiber [33], etc.

Mori et al. (2003) [34] have already developed a new recycling system for the sludge named “Fiber-Cement Stabilized Soil method”. In this method, paper debris and cement are mixed with the sludge. The modified sludge produced by this method has several features, such as high failure strength, high failure strain, and high durability for drying and wetting. Fig. 1-4 shows the concept of Fiber-Cement Stabilized Soil method. In the original construction sludge, soil particles freely move in the mixture because of high water content. After adding paper debris, water in the construction sludge is absorbed into debris paper. Therefore, the superficial water content of sludge decreases. Finally, cement is added to sludge to obtain the necessary strength.

H. Takahashi et al. (2011) [10] reported that Fiber-Cement Stabilized Soil method has already been used widely in Japan. This method successfully applied in many real constructions, such as the Hamao Basin Embankment Work, Fukushima Prefecture; Imokawa River Landslide Dam Construction Emergency Measure, Niigata Prefecture;

Sunaoshi River Channel Excavation Work, Miyagi Prefecture.

T. Satomi et al. (2014) [35] carried out unconfined compression test and permeability test to study the relationship between failure strength and permeability of modified soil in terms of Fiber-Cement Stabilized Soil method. The results showed that strength of fiber-cement stabilized soil is higher than that of cemented soil and increases with the increase of paper debris content. Moreover, the hydraulic conductivity of fiber-cement stabilized soil is almost unchangeable or decreases with the increase of additive of cement.

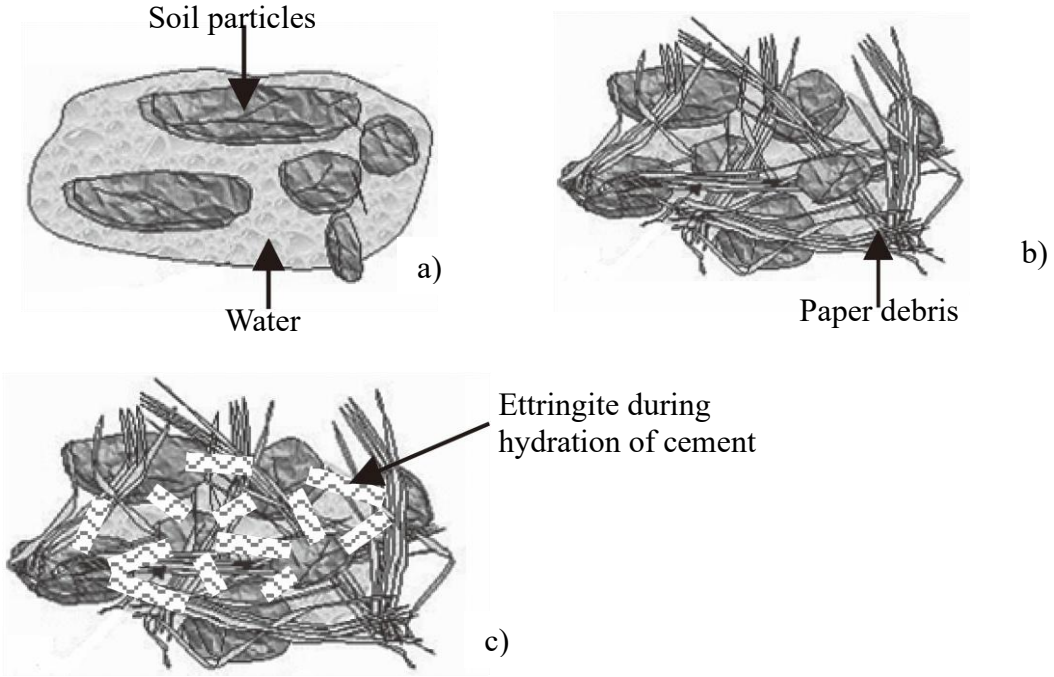

Fig. 1-4 The concept of Fiber-Cement Stabilized Soil method [34]
a) High-water-content sludge; b) Addition of paper debris; c) Addition of cement

K. Q. Tran et al. (2017) [36] used corn silk as fiber material in the Fiber-Cement Stabilized Soil method to modify sludge. The study investigated the mechanical properties (i.e., failure strength, ductility, stiffness) of corn silk-reinforced cement sludge and the relationship between the water-cement-fiber ratios and failure strength. The addition of fiber to cemented sludge causes the increase of failure strength in general. The failure strength and ductile property increase with increasing the additive amount of fiber. The study also reported that with a large amount of cement, fiber inclusion contributes to the decreasing of stiffness.

Maize is the thirst most planted food crop of the world with enormous production, so a large amount of by-product from maize is also generated after harvesting cob corn. Consequently, corn husk, a by-product of maize, is an available, abundant, and cheap material. Corn husk from the by-product of maize has been utilized in many fields. A. M. Youssef et al. (2015) [37] studied the effect of corn husk on low-density polyethylene composite when using corn husk to recycle it. The results showed that the addition of corn husk fiber improves mechanical properties, swelling property, and water absorption of the composite. C. Tachaapaikoon et al. (2006) [38] utilized many kinds of agriculture residue to purify xylanase from alkaliphilic Bacillus sp. K-8a and revealed that under controlled conditions, corn husk can purify xylanase. Although corn husk is a promising material in many areas, there is no research investigating the behavior of cemented soil with corn husk fiber inclusion in geotechnical engineering. Thus, the characteristics of corn husk-cement stabilized soil are ambiguous and need to be clearly understood.

In geotechnical engineering, when using fiber for reinforcing soil or cemented soil, the fiber properties are important. Fibers with different properties including tensile strength, Young's modulus, length, and diameter, etc. have different effects on the mechanical properties of cemented soil. M. E. A. Fidelis et al. (2013) [39] conducted a tension test to measure tensile strength of several natural fibers including curaua fiber, jute fiber, sisal fiber, piassava fiber, and coir fiber. The research reported that it is necessary to measure the cross-sectional area of fiber for analyzing tensile strength of fiber. Besides, gage length has no effect on tensile strength and Young's modulus of fiber. Curaua, sisal, and jute are in the group with high tensile strength and Young's modulus, while coir and piassava are in the group with low tensile strength and Young's modulus. The results showed that there are two developing tendencies of tensile stress-strain curve. The first tendency is linear region for hole curve (for curaua, jute, and sisal). The second tendency is the linear region at the initial phase and then followed by the non-linear region (for coir and piassava).

N. Defoirdt et al. (2010) [40] measured and analyzed tensile properties of natural fiber consisting of coir, bamboo, and jute fiber. The authors revealed that tensile strength and strain to failure of fiber decrease with the increase of tested fiber length. The study applied Weibull distribution to evaluate the variation of tensile strength of the natural fiber. The higher Weibull parameter, the lower variation of tensile strength. Weibull parameters of these fibers are in the range of natural fiber from 1 to 5. Based on the slope of the plot of tensile

strength versus gage length, it is reported that the density of the defect of bamboo and jute is highest and lowest, respectively.

In the application field of natural fiber, the degradation property of fiber in an alkaline environment is the obstacle. L. Yan et al. (2016) [28] reported that the degradation of fiber in a cementitious environment includes two kinds: mineralization and alkaline degradation. In which, the degrading order of components in fiber is lignin and part of hemicellulose, hemicellulose, cellulose, cellulose microfibrils, and finally cellulosic. The degradation results in the brittleness of fiber, so mechanical properties of fiber-cement stabilized soil decline, such as failure strength, tensile strength, and durability, etc.

According to J. Wei et al. (2016) [41], the degradation of natural fiber could be mitigated by two methods: fiber pre-treatment and modification of cement matrix. J. Wei et al. (2016) [42] analyzed the degradation mechanisms of sisal fiber-cement matrices. To study the alkali attack of natural fiber in a cement matrix, the Portland cement is partially replaced by metakaolin. In a cement mixture, the tensile strength decreases significantly and fibers degrade completely. However, in metakaolin-modified cement, sisal fiber's degradation is mitigated. The tensile strength of fibers immersed in Portland cement decreases by 86% after 30 wetting and drying cycles and decreases 66% and 38% in MK10 and MK30 in comparison with the raw fiber, respectively.

J. Wei et al. (2017) [43] investigated the effects of montmorillonite and metakaolin on the degradation of sisal fiber in Portland cement. The study reported that both metakaolin and montmorillonite contribute to the mitigation of alkaline degradation and mineralization of fiber. The tensile strength of fiber increases with the increase of replaced cement content. The 50% of replaced cement is the most effective replaced cement content to mitigate the degradation of sisal fiber.

1.4 Outline of thesis

This thesis includes 6 chapters. The content of each chapter is as follows.

Chapter 1 introduces the problem statements including the construction sludge and excavated soil discharge, and crop residue disposal problems in Viet Nam. Objectives of study and literate reviews from previous researchers are described in this section.

Chapter 2 investigates the impacts of different fiber kinds on the mechanical properties of

different cemented sludges. In this section, five kinds of fibers and two kinds of sludge are used. Four experiments including unconfined compression test, splitting tension test, permeability test, and durability test are performed to evaluate and to compare the workability of five kinds of fibers in terms of Fiber-Cement Stabilized Soil method. From the results, the fiber showing the best workability for soil improvement is selected for studying deeply in the next chapters.

Chapter 3 studies the mechanical properties of corn husk fiber-cement stabilized soil with high water content produced by Liquified-Stabilized Soil method. In this chapter, bleeding test, flow test, unconfined compression test, splitting tension test, and durability test are conducted to investigate the potential of the application of corn husk fiber to improve characteristics of cemented sludge without compaction method. Besides, tensile strength of corn husk fiber is measured.

Chapter 4 carries out a series of laboratory experiments including unconfined compression test, splitting tension test, direct tension test, and shear box test to understand the effect of corn husk fiber on cemented soil at optimum water content (low water content). In this chapter, specimens are made under the compaction method.

Chapter 5 analyzes the results obtaining from Chapters 3 and 4. In this chapter, the regression model is applied to predict output data including failure strength, splitting tensile strength, direct tensile strength, shear strength, and cohesion from input data including water content, cement content, fiber content, fiber length, and normal stress.

Chapter 6 is the conclusions of this research.

CHAPTER 2

STUDY ON EFFECT OF DIFFERENT KINDS OF FIBERS ON MECHANICAL PROPERTIES OF FIBER-CEMENT STABILIZED SOIL WITH HIGH WATER CONTENT

2.1 Introduction

The use of crop residue including rice straw, rice husk, corn husk, corn silk in Fiber-Cement Stabilized Soil method contributes to the solution of crop residue burning and sludge discharge. Besides, this is an effective method to produce an ecologically friendly material in construction. Nevertheless, the problem is which by-product is suitable for soil improvement.

In practice, the structure must withstand the impact of several factors from natural phenomena and human activities, such as external force, water, rain, wind, runoff, change of temperature, etc. In which, the effect of external force, water, change of temperature are the main factors causing common failure or destruction of the structure, for example, a decrease in strength, erosion, tensile crack, etc. Many research about rice straw, rice husk focused on only failure strength of specimens and reported that the addition of fibers leads to the increase of failure strength, failure strain, and durability. Moreover, there is no research investigating cemented soil reinforced by corn husk fiber. Until now, a limited number of researchers investigated cemented soil reinforced by rice straw, corn silk, and paper debris [35, 36, 44]. Therefore, to find out the best fiber for soil improvement, it is important to assess and parallel the mechanical properties of cemented sludge reinforced by agricultural by-products including rice straw, corn husk, corn silk, rice husk. Furthermore, it is necessary to compare these results of a mixture including by-products with that of a mixture including paper debris.

This research aims to compare the workability and effects of rice straw, corn husk, corn silk, rice husk, and paper debris on cemented sludge by carrying out unconfined compression, splitting tension, permeability, and durability tests under the same mixing conditions. Two kinds of sludge are used in this study including sludge No.1 with 80% water content by dry mass of soil, and sludge No.2 with 50% water content by dry mass of soil. For each kind of sludge, a mixing condition is used for all fiber materials: 50 kg/m^3 cement, 30 kg/m^3 fiber for sludge No.1, and 50 kg/m^3 cement, 15 kg/m^3 fiber for sludge No.2. From the results of experiments, additive materials giving good performances for reinforcing cemented sludge are obtained.

2.2 Materials

2.2.1 Sludge

To carry out the systematic experiments under constant conditions, this study uses two kinds of artificial dry sludge which are imitated real dry sludge of The Southern, Viet Nam.

- Imitated dry sludge No. 1: The main component is Kasaoka clay and silt with the ratio of 40:60 in dry mass according to research by P. Chien et al. (2017) [45]. The grain size distribution and properties of dry sludge are shown in Fig. 2-1 and Table 2-1, respectively.
- Imitated dry sludge No. 2: The main component is Kasaoka clay and sand No. 9 with the ratio of 60:40 in dry mass according to previous report [46], respectively. The gain size distribution and properties of dry sludge are shown in Fig. 2-2 and Table 2-2, respectively.

2.2.2 Cement

Geoset 200 cement used in the present study is supplied by Taiheiyo Cement Corporation, Japan. This binder is widely applied to problematic soil and can minimize the leaching process of hexavalent chromium from itself into the environment. The chemical and physical properties of cement are summarized in Table 2-3.

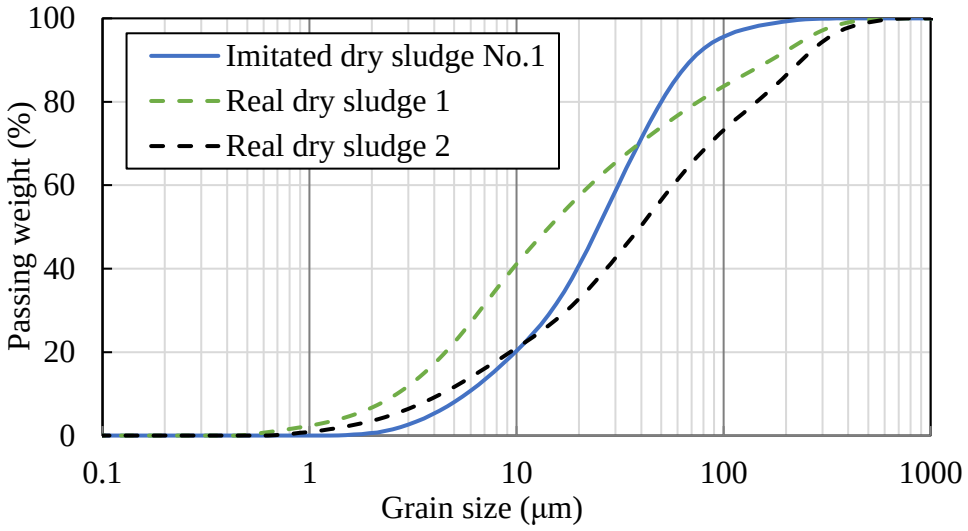

Fig. 2-1 Grain size distribution curve of imitated and real dry sludge No. 1 [45]

Table 2-1 Properties of imitation dry sludge No. 1 [45]

Properties	Value
Specific Gravity	2.47
Sand (%)	8.10
Silt (%)	83.4
Clay (%)	8.50
Chemical compound	
SiO_2 (%)	74.31
Al_2O_3 (%)	15.80
Fe_2O_3 (%)	3.40
K_2O (%)	2.50
Na_2O (%)	1.71
CaO (%)	1.49
MgO (%)	0.43
TiO_2 (%)	0.31
MnO (%)	0.05

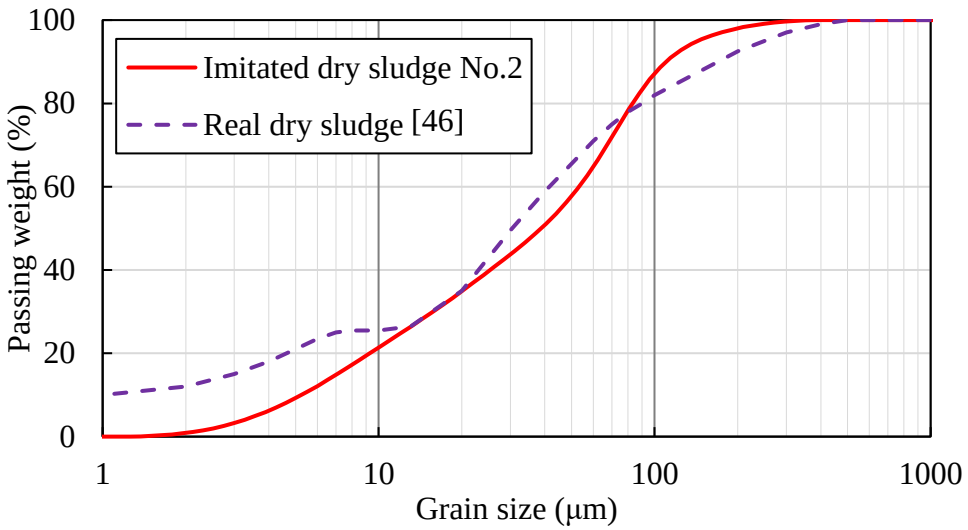

Fig. 2-2 Grain size distribution curve of imitated and real dry sludge No. 2

Table 2-2 Properties of imitation dry sludge No. 2

Properties	Value
Specific Gravity	2.73
Sand (%)	24.0
Silt (%)	66.7
Clay (%)	9.30
Chemical compound	
SiO_2 (%)	78.32
Al_2O_3 (%)	13.49
Fe_2O_3 (%)	3.33
K_2O (%)	2.30
Na_2O (%)	1.13
CaO (%)	0.57
MgO (%)	0.48
TiO_2 (%)	0.31
MnO (%)	0.05

Table 2-3. Properties of Geoset 200 cement

Properties	Values
Chemical compound	
SiO_2 (%)	23.6
Al_2O_3 (%)	7.76
Fe_2O_3 (%)	1.83
CaO (%)	53.9
MgO (%)	3.35
SO_3 (%)	6.53
Physical properties	
Specific surface (cm^2/g)	3.68
Specific gravity	3.01

2.2.3 Fiber materials

2.2.3.1 Corn husk

Corn husk is a by-product of corn crop collected from corn-dealer in Viet Nam. Corn husk which is the cover of the corn kernel is obtained after separating the husk part and kernel part. To blend raw corn husk into fibrous form easier, the dry raw corn husk is cut into segments of 30 mm in length. Then, the segments are immersed in water and milled by a blender until obtaining the fibrous form. Finally, corn husk fibers are dried until a constant mass is obtained (Fig. 2-3). The size of corn husk fibers is 0.35 mm in average longest diameter (Fig. 2-3c) and 23.4 mm in average length. Water absorption of corn husk fiber is 4.8 cc/g. The longest diameter distribution, length distribution, and compositions of corn husk are shown in Fig. 2-4, Fig. 2-5, and Table 2-4, respectively.

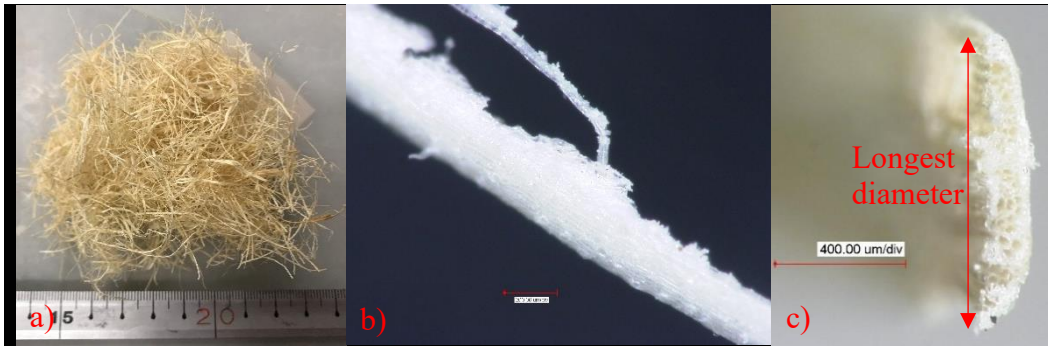

Fig. 2-3 Corn husk

a) Dry corn husk fibers; b) Microscope image of corn husk fiber;

c) Microscope image of cross-section

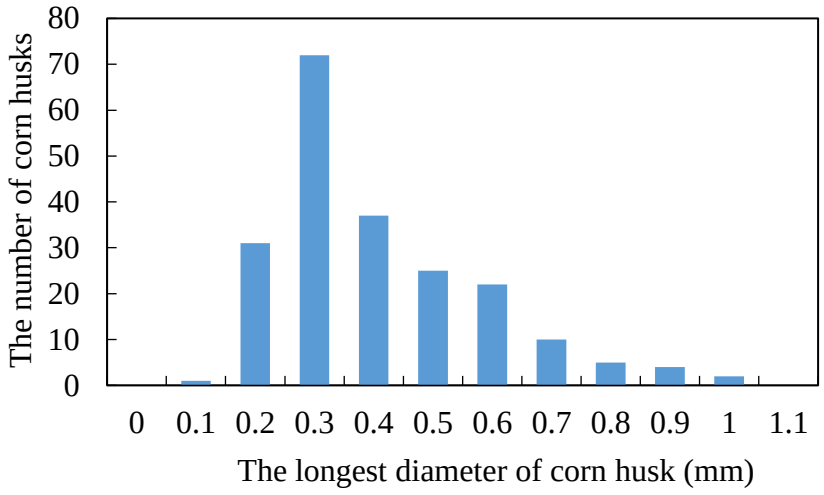

Fig. 2-4 The longest diameter distribution of corn husk

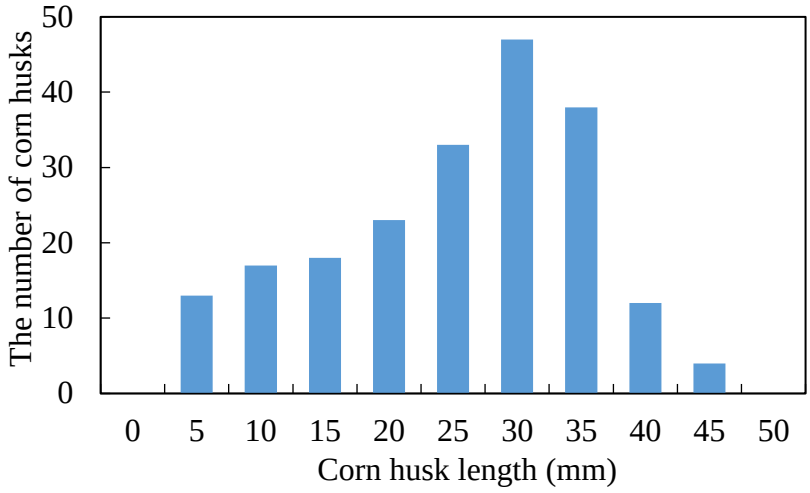

Fig. 2-5 Length distribution of corn husk

Table 2-4 Constituent in corn husk [47]

Property	Value
Density (kg/m^3)	1254.0
Ash content (wt%)	5.0
Holocellulose (wt%)	73.1
Hemicellulose (wt%)	37.5
Cellulose (wt%)	35.3
Lignin (wt%)	7.9

2.2.3.2 Corn silk

Corn silk is from Thanh Binh Company, Ho Chi Minh City, Viet Nam. Corn silk is silk in the top of the corn ear. Raw corn silk including corn leaves and dust is cleaned in water. Raw corn silk is long, soft, and twists together, so to mix fiber with soil easily, raw corn silk is straightened in water by hand and cut into segments of 10 mm in length. Although raw corn silk is straightened, some fibers are still curve. Hence, the cut fiber is still longer than 10 mm. After cutting, wet corn silk is dried under 40 ± 3^{0}C to constant weight. The average length and the average longest diameter of corn silk are approximately 9.8 and 0.29 mm, respectively. Mature corn silk includes 5.5% ash, 29.7% carbohydrate, and 51.3 g/100 g dietary fiber [48]. The used corn silk, longest diameter distribution, and length distribution of corn silk are shown in Fig. 2-6, Fig. 2-7, and Fig. 2-8, respectively.

Fig. 2-6 Corn silk

a) Dry corn silk fiber; b) Microscope image of corn silk fiber

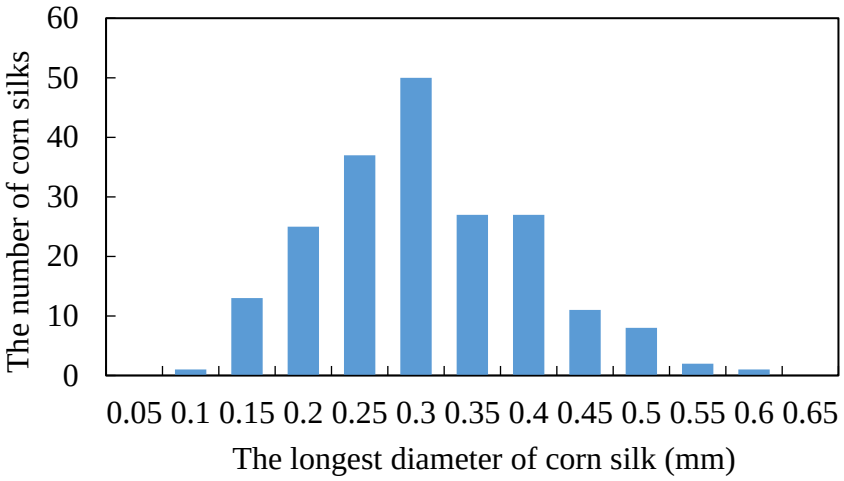

Fig. 2-7 The longest diameter distribution of corn silk

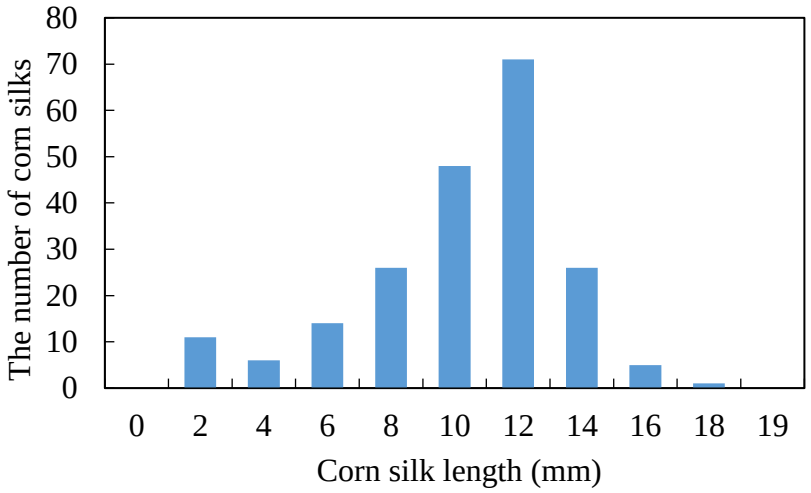

Fig. 2-8 Length distribution of 10 mm cut corn silk

2.2.3.3 Rice husk

Rice husk is obtained from Miyagi Prefecture, Japan. The rice husk in hull form is a cover layer of rice which is a by-product produced after obtaining rice (Fig. 2-9). The used rice husk is about 5.5 mm in average length and 1.9 mm in average longest diameter. The longest diameter distribution, length distribution, and organic constituent of rice husk are shown in Fig. 2-10, Fig. 2-11, and Table 2-5.

Fig. 2-9 Rice husk

a) Dry rice husk; b) Microscope image of rice husk

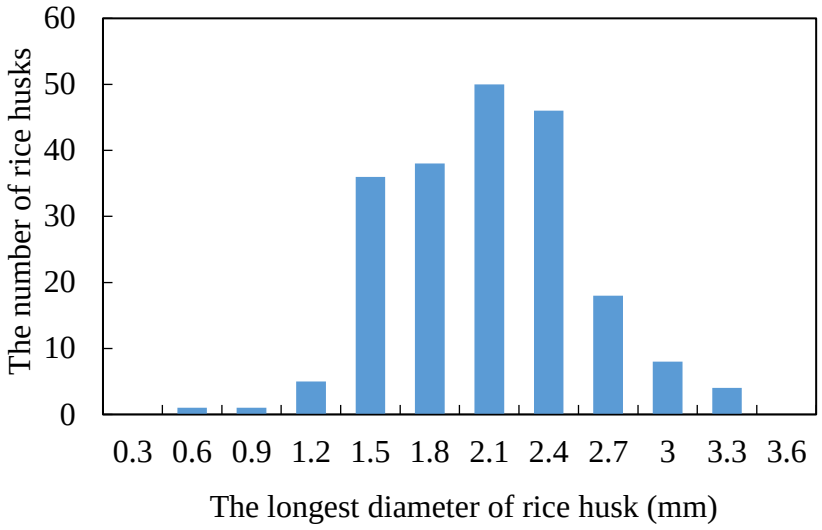

Fig. 2-10 The longest diameter distribution of rice husk

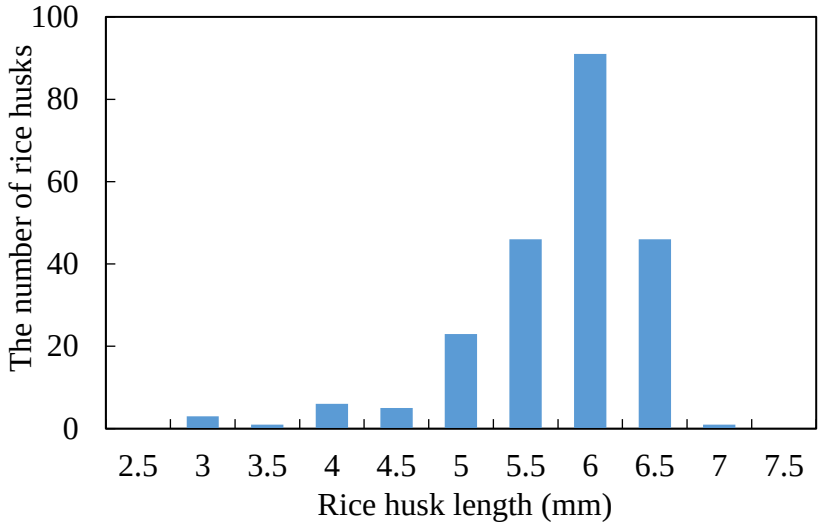

Fig. 2-11 Rice husk length distribution

Table 2-5 Organic constituent in rice husk [49]

Constituent	Value (wt%)
Cellulose	43.3
Lignin	22.0
D-xylose	17.5
I-arabinose	6.5
Methyl glucuronic acid	3.3
D-galactose	2.7

2.2.3.4 Rice straw

Rice straw is a by-product of rice crop after harvesting. It includes the stem and the leaf of rice. The used dry rice straw is obtained from Japan. Raw rice straw is long and hard, so to mix fiber with soil easily, the raw rice straw is cut into segments of 30 mm in length. Then, the segments are immersed in water and milled until obtaining a fibrous form. Finally, wet rice straw fibers are dried until a constant mass is obtained. The average longest diameter and the average length of rice straw fibers are 0.17 and 15.4 mm, respectively. The components of rice straw are 18% ash, 36% cellulose, 24% hemicellulose, and 15.6% lignin [50]. The used rice straw, longest diameter distribution, and length distribution of rice straw are shown in Fig. 2-12, Fig. 2-13, and Fig. 2-14, respectively.

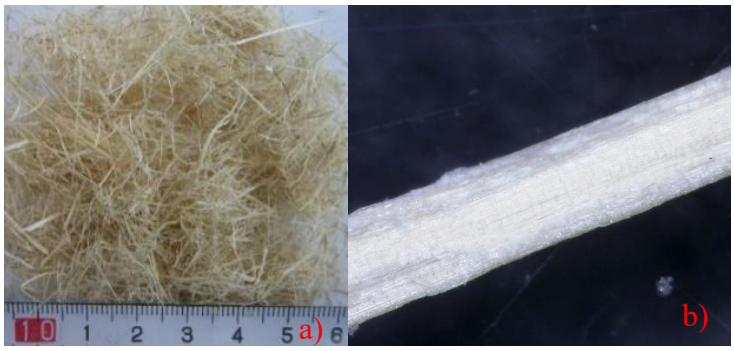

Fig. 2-12 Rice straw

a) Dry rice straw fibers; b) Microscope image of rice straw fiber

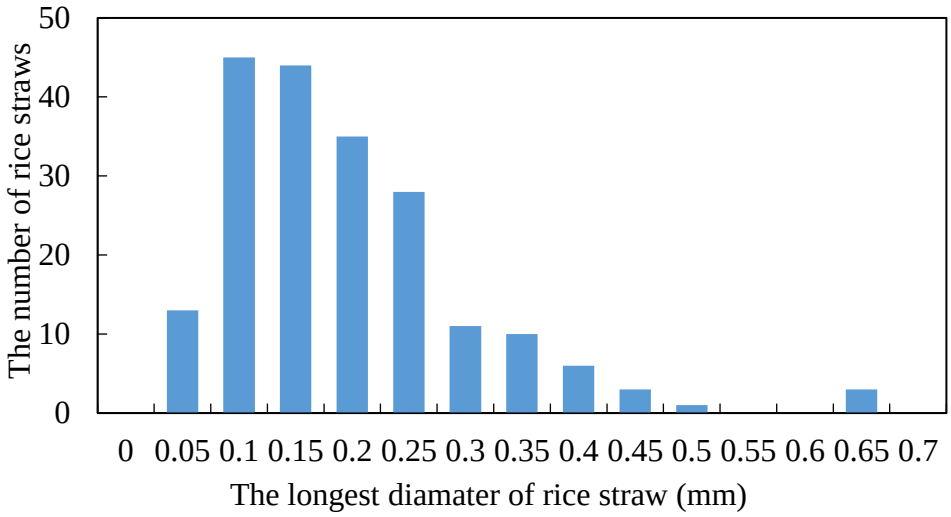

Fig. 2-13 Longest diameter distribution of rice straw

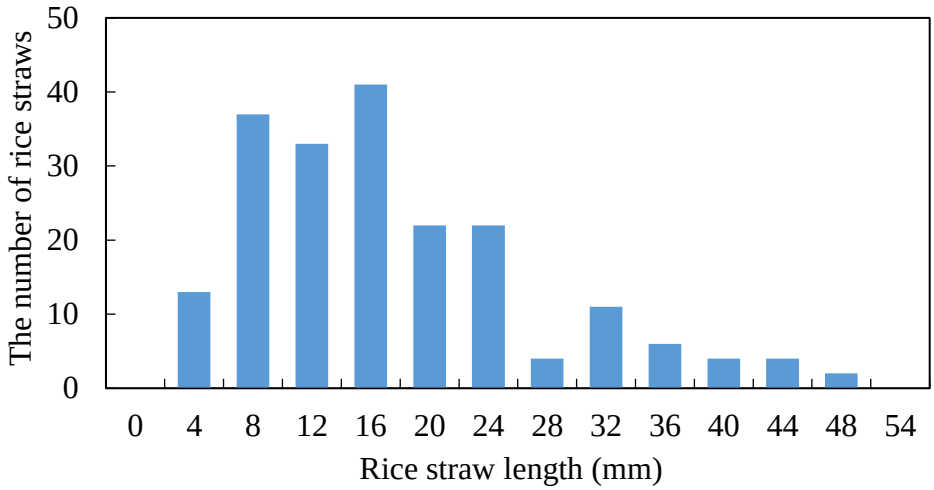

Fig. 2-14 Length distribution of 30 mm cut rice straw

2.2.3.5 Paper debris

Paper debris is obtained from Miyagi Prefecture, Japan. Paper debris which is obtained after cutting old newspapers is a grid of cellulose fibers with about 1-3 mm in length and 0.02-0.03 mm in diameter [51]. The used paper debris is shown in Fig. 2-15.

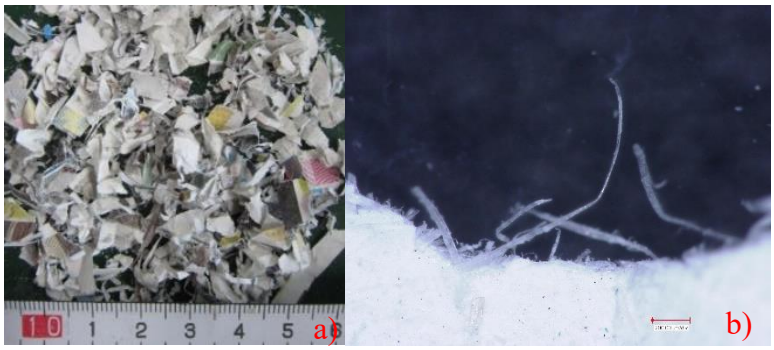

Fig. 2-15 Paper debris

a) Paper debris; b) Microscope image of paper debris

2.3 Specimen preparations

2.3.1 Specimen preparation apparatus

- Mixing machine

The mixing machine is used to mix dry artificial sludge, water, fiber, and cement to produce a homogeneous admixture. The used mixing machine is Shinohara Seisakusjo type ss-s-338 (Fig. 2-16).

Fig. 2-16 Mixing machine

- Mold and rammer

Two kinds of mold with different size are used. A size with 100 mm in height and 50 mm in inside diameter is used to make specimens for unconfined compression test, splitting tension test, and durability test. Another mold size with 51 mm in height and 50 mm in inside diameter is used to make specimens for permeability tests (Fig. 2-17). Rammer for compacting specimens includes a weight of 1.5 kg and a falling height of 200 mm. Rammer set and 100 mm high mold are shown in Fig. 2-18.

Fig. 2-17 Mold for permeability test

Fig. 2-18 Rammer and mold with 100 mm in height

- Dry oven

Two kinds of oven are used in this study. An oven that is used for curing admixtures and specimens for 3 days, 7 days, and 28 days is set at 20 ± 3^0C (Fig. 2-19). Another oven that is used for cycles of durability test is set at 40 ± 3^0C (Fig. 2-20).

Fig. 2-19 Yamato IN 804 Program Incubator

Fig. 2-20 Yamato DVS 604 Dry Oven

2.3.2 Preparation process

Two sizes of specimen are used in this study. The specimens with the size of 50 mm in diameter and 100 mm in height are used for unconfined compression, splitting tension, and durability tests. The specimens with the size of 50 mm in diameter and 51 mm in height are used for permeability tests.

The procedures for mixing admixture and making specimens are as follows.

1. According to the mixing condition, water is added into artificial dry sludge and mixed by a mixing machine until admixture is homogenous. The mixing is carried out two times with 1 min/time.

2. The fiber material is added to the artificial sludge and agitated until the mixture is homogenous by the mixing machine. The mixing is carried out three times with 1 min/time.

3. Addition and agitation of cement in admixture. The mixing performs three times with 1 min/time.

4. Because sludge with high water content exposes the behavior like water and particles could freely move in sludge, the admixture is cured in a closed box under 20^0C for three days before compaction to reduce the water content of admixture due to the hydration reaction of cement and the water absorption of fiber.

5. After three days, the specimens are made by compaction using rammer and sample mold. Specimens are made with four layers of compaction for unconfined compression test, splitting tension test, durability test, and three layers for permeability test. Rammer for compacting specimens includes a weight of 1.5 kg and a falling height of 200 mm. The falling time of rammer for specimens of unconfined compression test, splitting tension test, durability test is 5, 10, 10, 20 times, and for specimens of permeability test is 4, 9, 9 times.

6. The specimens are wrapped in a plastic sheet and cured under 20 ± 3^0C for 7 or 28 days.

The 7-day cured specimens are used for unconfined compression, splitting tension, and permeability tests. The 28-day cured specimens are used for durability tests. Besides, for permeability test, after curing 7 days, specimens are saturated by sinking in water for 1 day. This process for mixing sludge has been reported by many researchers and applied in practice in Japan [10, 34–36].

2.4 Testing programs

2.4.1 Unconfined compression test

Unconfined compression test is conducted by a compression test machine with the maximum load capacity of 2 kN. The rate of displacement is 1 mm/min. The compression test machine is presented in Fig. 2-21. Data are continuously recorded by a computer until reaching peak stress or 15% of failure strain in accordance with ASTM D2166 [52]. The deviation of the failure strength value is within 10% of the average value. In unconfined compression test, the failure strain (strain to failure) and failure strength are defined as strain and stress at either the maximum stress or 15% of strain as shown in Fig. 2-22.

Fig. 2-21 Unconfined compression test machine

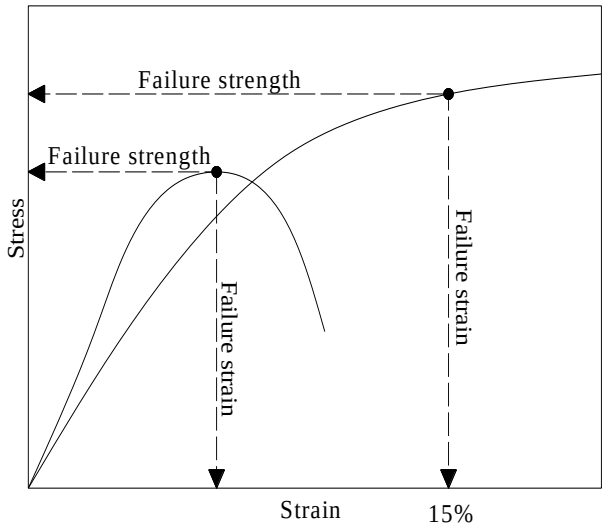

Fig. 2-22 Definition of failure strain and failure strength

2.4.2 Splitting tension test

The splitting tension test is conducted in accordance with ASTM C496 [53]. The testing machine is modified from the compression test machine of unconfined compression test by adding a couple of strips with the length of 120 mm, the width of 10 mm, and the height of 5 mm. The modified compression test machine is shown in Fig. 2-23. The experiment stops when peak tensile stress or 15% of failure strain is obtained. The deviation of the tensile strength value is within 10% of the average value. The splitting tensile strength is calculated as follows.

$$T=2P/\pi ld \quad (2\text{-}1)$$

where T is the splitting tensile strength (kPa), P is the applied load (kN), l is the length of the specimen (m), d is the diameter of the specimen (m).

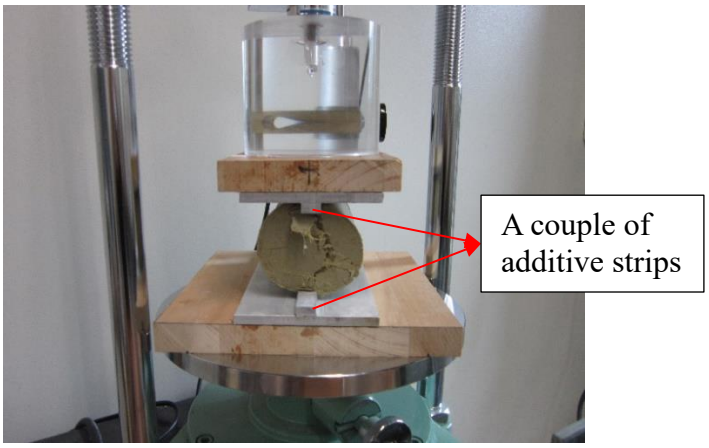

Fig. 2-23 Splitting tension testing machine

2.4.3 Permeability test

Permeability test is carried out according to a falling head method. This method is used to find out the hydraulic conductivity of intermediate and low seepage soil in the laboratory. The test is carried out a couple of times for each mixture. Time and hydraulic conductivity deviation are within 10% of the average time and the average hydraulic conductivity, respectively. The permeability test equipment is shown in Fig. 2-24. The hydraulic conductivity is calculated by the formula as follows.

$$K = \frac{2.3 \times a \times L}{A \times t} \log_{10}\left(\frac{h_1}{h_2}\right) \quad (2\text{-}2)$$

where K is the hydraulic conductivity of specimen (m/sec), a is the cross-sectional area of scale tube, a = 50.3 mm^2; A is the cross-sectional area of the specimen, A = 1690 mm^2; L is the length of the specimen, L= 51 mm; t is the measurement time (sec); h_1 is the height from the upper line of scale tube to the water level of the bottom of sampling tube, h_1 = 170 mm; h_2 is the height from the lower water level of scale tube to the water level of the bottom of sampling tube (cm).

Fig. 2-24 Permeability test equipment

2.4.4 Durability test

The durability test consists of 10 cycles for wetting and drying. In each cycle, the specimens experience 2 days for drying under 40 ± 3^0C, 1 hour for cooling at 20 ± 3^0C room temperature, and 1 day for wetting (submerging specimens in a water tank which is put at 20^0C room temperature). The soundness evaluations of specimens after each drying and wetting cycle are shown in Table 2-6. To understand the effect of weather on the behavior of cemented sludge reinforced by rice straw, corn silk, corn husk, paper debris, and rice husk, the failure strength and failure strain of specimens after 0, 2nd, 6th, and 10th cycle are obtained.

Table 2-6 Classification of soundness evaluation [34]

	Appearance of crack	Appearance of breakage
A	Remain the same	
B	Micro-crack appearance, Partly crack appearance	Surface delamination
C	Appearance of obvious crack, partly	Appearance of exfoliation, partly
D	Appearance of obvious crack, totally	Appearance of exfoliation, totally
E	Specimen deterioration, partly or totally	
F	Specimen deterioration, maintain the shape of specimen	
G	Specimen deterioration, massive form	
H	Specimen deterioration, grain refining	

2.5 Experiment results

2.5.1 Unconfined compression test

2.5.1.1 Failure strength and failure strain

Fig. 2-25 and Fig. 2-26 show the effect of fiber on failure strength of cemented sludge. The figures show that fiber inclusion significantly improves failure strength of cemented sludge except for rice husk inclusion. The specimens reinforced by paper debris, rice straw, corn silk, and corn husk expose better performance in comparison with unreinforced cemented specimens in terms of unconfined compression test. The additions of corn silk, rice straw, and corn husk increase failure strength of unreinforced cemented sludge by about 157%, 224%, and 384% for sludge No.1 (Fig. 2-25), and about 66%, 107%, and 91% for sludge No. 2 (Fig. 2-26), respectively. The improvement of failure strength is attributed to the water absorption capacity of fiber, interlocking force of fiber to hold soil-cement particles, and the interfacial interaction between fiber and soil-cement particles in specimens [54]. Fig. 2-27a, c, and e show that rice straw, corn husk, and corn silk form the network to interlock soil-cement particles. Fig. 2-27b, d, and f display interfacial interaction between fiber and soil-cement particles with a large number of soil-cement particles attaching to the surface of fiber after 7 days. These interlocking forces and interface interaction limit the movement of soil-cement particles and fiber under loading to improve failure strength.

Failure strength of cemented sludge added paper debris increases about 123% in the case of sludge No.1 and 37% in the case of sludge No.2 in comparison with that of unreinforced cemented sludge. The improvement of failure strength of specimens reinforced by paper debris may happen due to water absorption capacity and the presence of a large amount of paper fiber. The fibrous form of paper debris is produced in specimens after paper debris is disintegrated in sludge. Therefore, paper fibers play the same role as corn silk, corn husk, and rice straw in the specimen. Fig. 2-27g and h show the paper fiber network in cemented sludge and the attachment of soil-cement particles on paper fiber to improve failure strength. The difference in failure strength of specimens including corn husk, rice straw, corn silk, and paper debris may happen due to the difference in fiber length. The longer fiber may make a contribution to the increase of the friction between fiber and soil-cement particles and the increase of the grain interlocking effectiveness of fiber.

Failure strength of rice husk-reinforced specimens is unchanged and slightly higher than that

of unreinforced specimens for sludge No.1 or sludge No.2, respectively. The lower failure strength of rice husk-cement specimens in comparison with specimens including other fiber can be explained by low attachment between rice husk surface and soil-cement particles (Fig. 2-27j) and no interlocking force in specimens. The absence of interlocking force is due to a non-fiber form of rice husk, so there is no network of rice husk like other additives in the specimen as shown in Fig. 2-27i.

As for failure strain of specimens from sludge No.1 (Fig. 2-25), failure strength of specimens reinforced by corn silk, rice straw, and corn husk increases until failure strain obtains 15% even further. Meanwhile, failure strains of rice husk and paper debris are 6.9%, 4.6% and higher than that of fiber-unreinforced specimens, respectively. For sludge No.2 (Fig. 2-26), failure strain of unreinforced specimens slightly decreases when including paper debris and rice husk. In contrast, failure strain increases from 2.9% for cemented specimens to 3.7%, 4.5%, and 4.7% for specimens reinforced by corn silk, rice straw, and corn husk, respectively. The results indicate that fiber materials divide into two groups: the first group consists of specimens including corn husk, corn silk, rice straw with high failure strain, and another group consists of specimens including paper debris and rice husk with low failure strain.

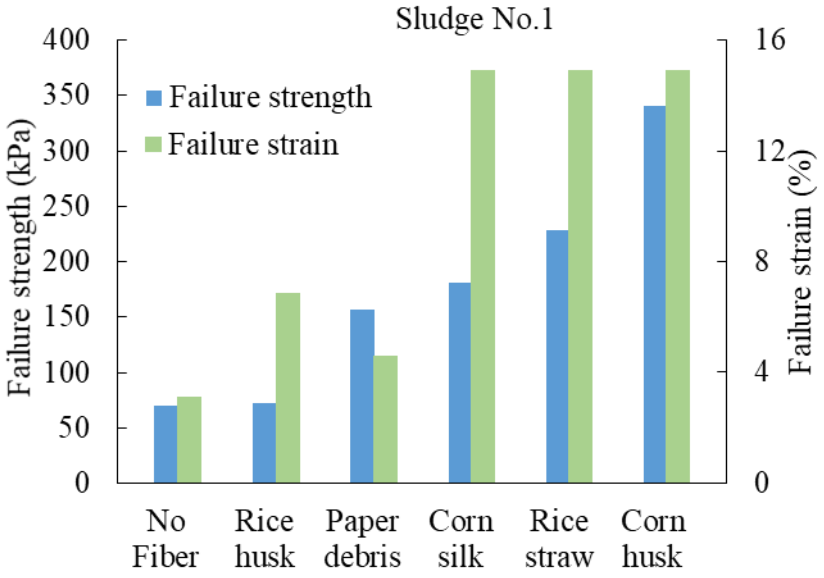

Fig. 2-25 Effect of fiber on cemented sludge from sludge No. 1

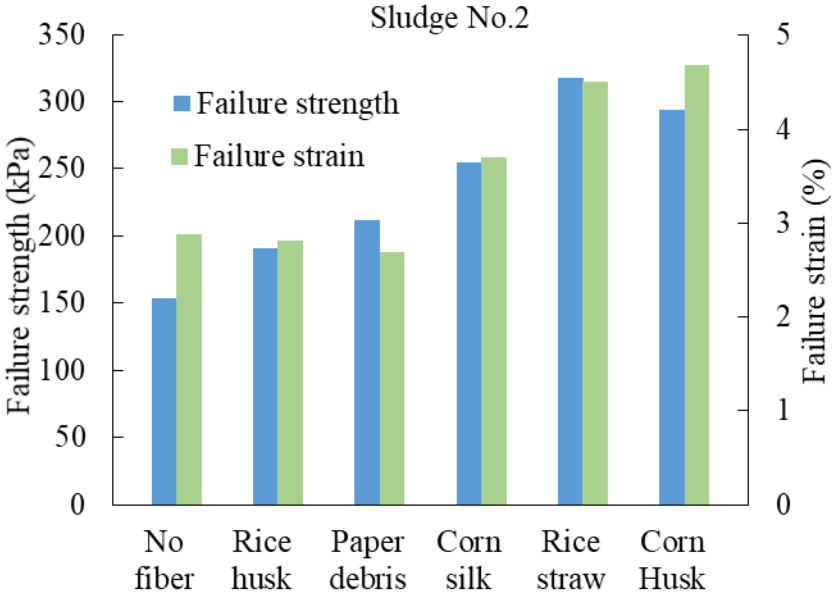

Fig. 2-26 Effect of fiber on cemented sludge from sludge No. 2

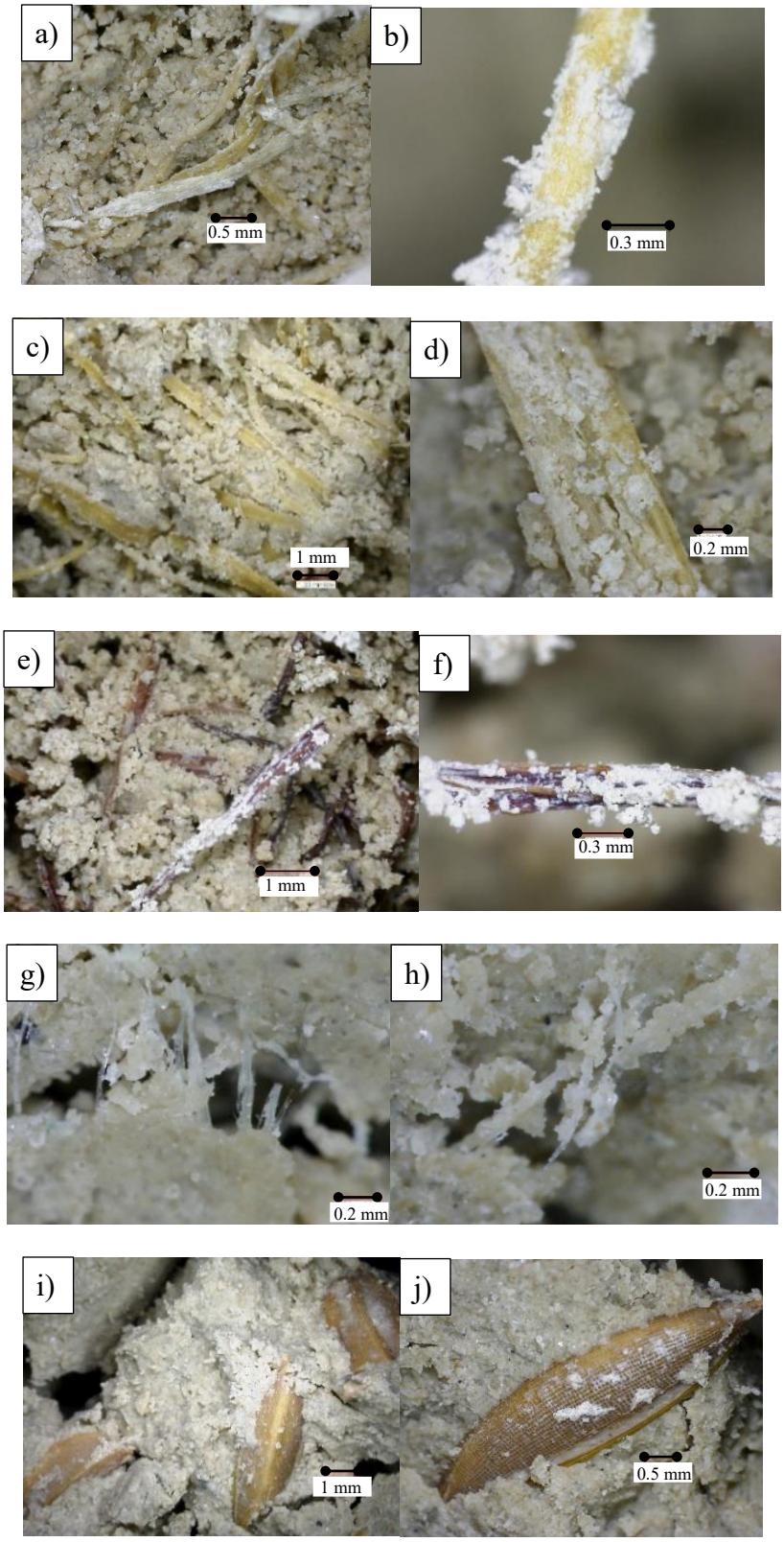

Fig. 2-27 Particle interlock and particle attachment of additive materials

a and b) Corn husk; c and d) Rice straw; e and f) Corn silk;

g and h) Paper debris; i and j) Rice husk

2.5.1.2 Secant modulus

Secant modulus plays a key property in terms of failure strength. Secant modulus gradually decreases when failure strength and failure strain increase. In this study, secant modulus value is derived from the ratio of compressive stress at strain of 2% to 2% strain value as shown in Fig. 2-28 . Fig. 2-29 and Fig. 2-30 show secant modulus of specimen with several fibers. The figure depicts that the secant modulus of specimens from sludge No.1 is highest when added paper debris with 4478 kPa. Paper debris, corn husk, and rice straw inclusion result in a higher secant modulus as compared to that of no fiber inclusion. As for sludge No.2, fiber inclusion contributes to the improvement of the secant modulus of cemented specimens. In which, specimen reinforced by rice straw performs the highest secant modulus with 11423 kPa and followed by corn husk, corn silk, paper debris, and rice husk (Fig. 2-30), respectively.

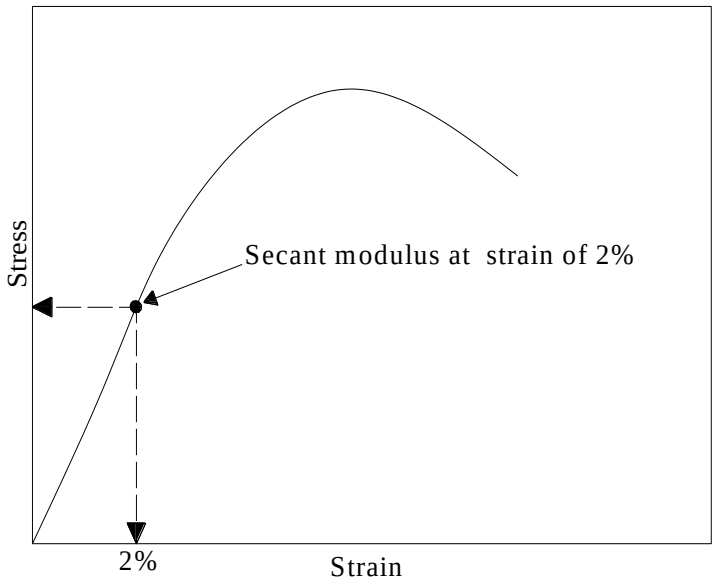

Fig. 2-28 Definition of secant modulus

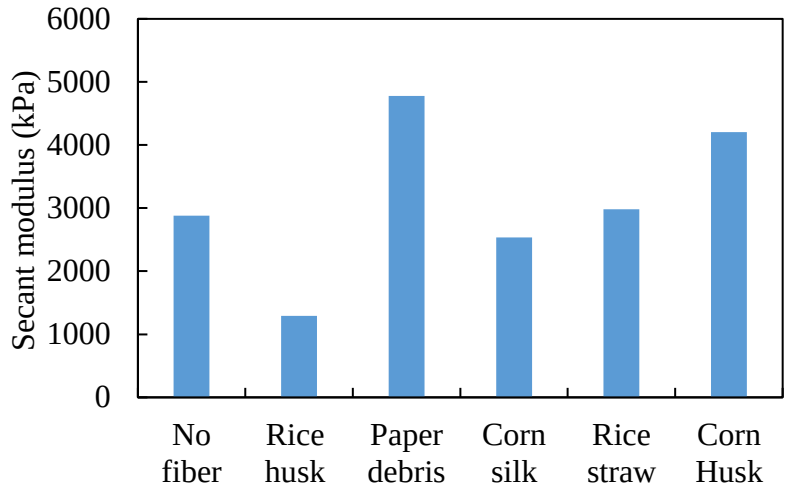

Fig. 2-29 Secant modulus of cemented sludge No.1 reinforced by several fibers

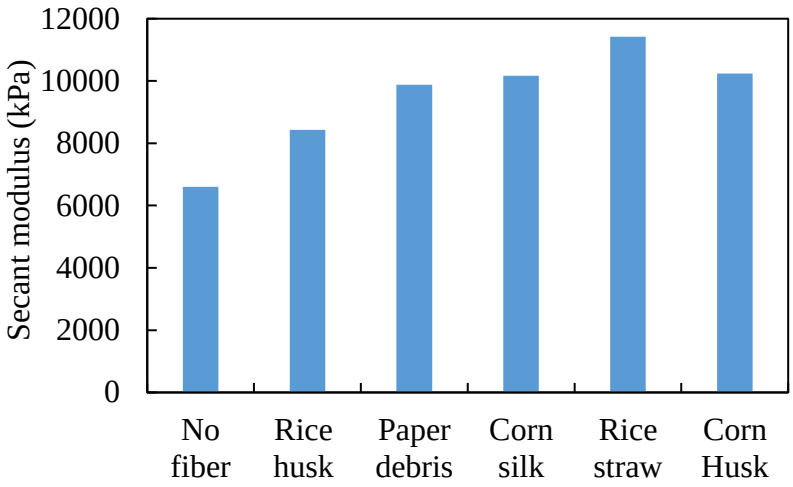

Fig. 2-30 Secant modulus of cemented sludge No.2 reinforced by several fibers

2.5.2 Splitting tension test

In terms of splitting tensile strength, the addition of fiber makes an important role in the enhancement of splitting tensile strength. Fig. 2-31 and Fig. 2-32 show the effect of fiber on splitting tensile strength. The figures show that with sludge No.1, fiber inclusions including paper debris, corn silk, rice straw, and corn husk increase tensile strength of cemented specimens from 9.7 kPa to 13.7 kPa, 37.5 kPa, 38.2 kPa, and 55.6 kPa, respectively. With rice husk inclusion, tensile strength slightly changes in comparison with cemented specimens. In the case of sludge No.2 from Fig. 2-32, rice husk, paper debris, corn silk, rice straw, and corn husk inclusions increase tensile strength of cemented specimens from 29.5 kPa to 34.1 kPa, 38.3 kPa, 45.6 kPa, 56.3 kPa, and 59.0 kPa, respectively.

Like unconfined compression test, splitting tensile stress of specimens reinforced by corn

silk, rice straw, and corn husk increases until failure strain reaches 15% even further for sludge No.1. However, failure strain of the specimen mixed with rice husk or paper pieces do not increase significantly compared to failure strain of the specimen mixed with other fiber materials (Fig. 2-31). With sludge No.2, failure strain of corn husk is highest (5.8%) and followed by corn silk and rice straw with the same strain value (4.9%). Cemented specimens and specimens reinforced by rice husk and paper debris perform equal failure strain (2.5%).

The improvement of tensile strength of cemented sludge with the inclusion of corn husk, rice straw, and corn silk may be attributed to bonding strength between fiber and soil-cement particles which leads to the restraint of displacement and the pull-out of fiber in soil-cement matrix, and the share of load in fiber-soil-cement matrix [55]. The insignificant enhancement of tensile strength of cemented sludge reinforced by paper debris can be explained by the presence of very weak and slender paper fiber. Although the tensile strength of specimens could be shared with paper fiber due to the formation of a network of paper fiber and particle attachment on fiber, the weaker and slender paper fibers in specimens result in the decrease of displacement restraint effect of fiber under loading. With rice husk, due to the low bond between fiber and soil-cement particles, it is easy to break the bond between soil-cement particles and rice husk at the potential crack plane under loading. Thus, tensile strength of specimens reinforced by rice husk is lower or almost equal to that of cemented specimens. The difference in the tensile strength between specimens reinforced by rice husk, rice straw, and corn silk may be explained by the difference in fiber length as mentioned in the previous section. The greater presence probability of the long fiber at the crack plane results in the increase of tensile strength [56].

It can be observed from Fig. 2-33 that the crack pattern of specimens with and without additive material is different. After the load is applied, the crack of unreinforced cemented specimens appears in a quite smooth plane at the vertical diameter plane and along specimen length in the horizontal axis. However, the crack of specimens with the additive materials appears in the multiple-crack form. With rice straw, corn husk, and corn silk inclusion, the crack appears in form of a zigzag plane. The zigzag form is due to the random distribution of fiber which leads to the appearance of cracks at the low fiber distribution plane. Meanwhile, the crack pattern concerning specimens with rice husk and paper debris inclusion consists of a clear main crack and many small cracks. The change of crack

morphology of specimens as adding five kinds of material is attributed to the potential weakness plane limitation capacity at the vertical diameter plane of additive fibers [55].

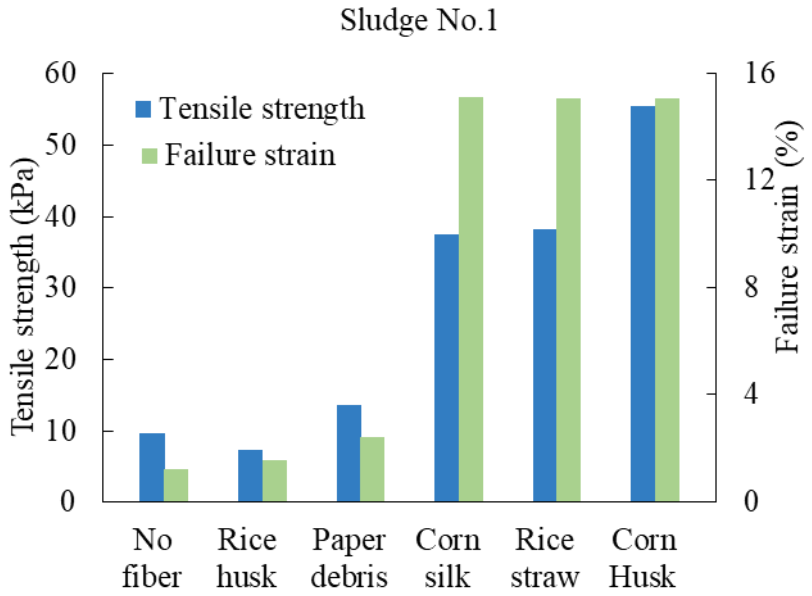

Fig. 2-31 Tensile strength of cemented sludge No.1 reinforced by several fibers

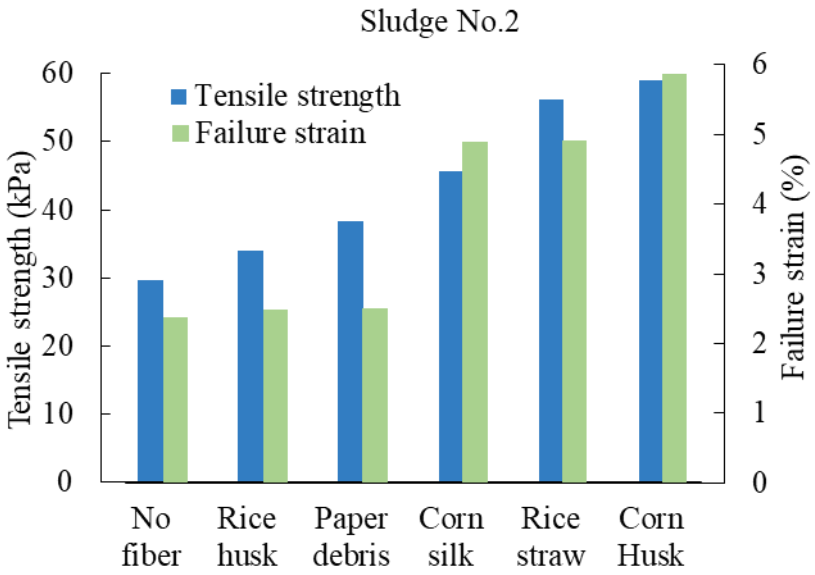

Fig. 2-32 Tensile strength of cemented sludge No.2 reinforced by several fibers

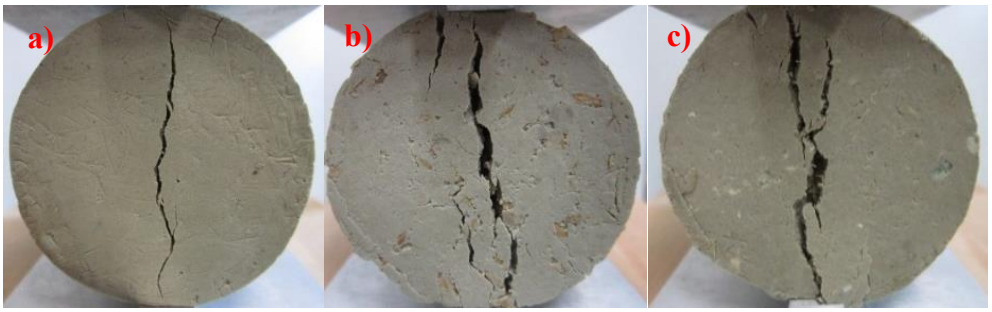

No additive Rice husk Paper debris

Corn silk Rice straw Corn husk

Fig. 2-33 Tensile crack shape under loading

2.5.3 Permeability test

Fig. 2-34 and Fig. 2-35 illustrate the effect of fiber on the hydraulic conductivity of cemented sludge. The plots indicate that the additive materials result in a decrease of hydraulic conductivity as compared with cemented specimens except for rice husk inclusion in sludge No.2. Rice straw, corn silk, corn husk inclusions result in the lowest hydraulic conductivity and followed by paper debris and rice husk, respectively. When adding paper debris, corn silk, corn husk, and rice straw, the hydraulic conductivity of cemented specimens from sludge No.1 decreases from 7.0×10^{-8} m/sec to 3.8×10^{-8} m/sec, 2.4×10^{-8} m/sec, 2.1×10^{-8} m/sec, 1.9×10^{-8} m/sec, and the hydraulic conductivity of cemented specimens from sludge No.2 decreases from 6.8×10^{-9} m/sec to 5.9×10^{-9} m/sec, 4.1×10^{-9} m/sec, 3.7×10^{-9} m/sec, and 3.9×10^{-9} m/sec, respectively. The decline of seepage capacity of specimens due to the presence of additives agrees with the previous study [57]. The lower hydraulic conductivity as adding fiber into cemented sludge may happen due to the increase of solid ingredients and decrease of initial water in specimens.

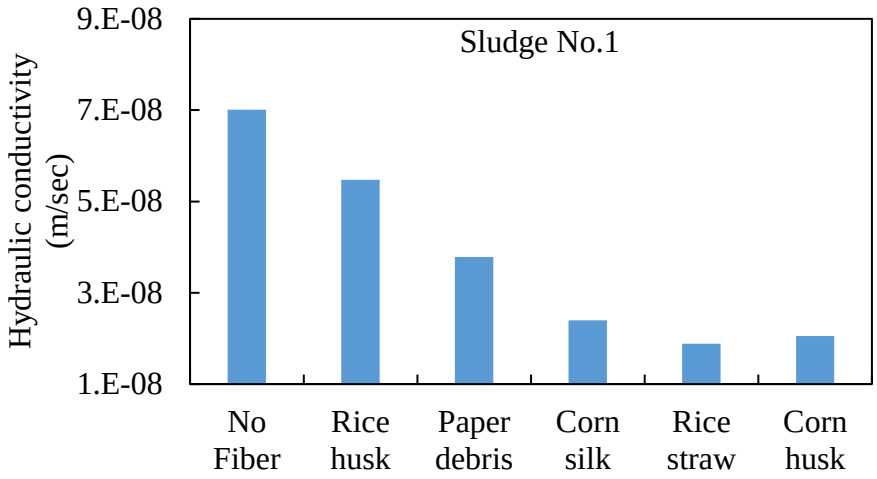

Fig. 2-34 Hydraulic conductivity of cemented sludge No.1 reinforced by several fibers

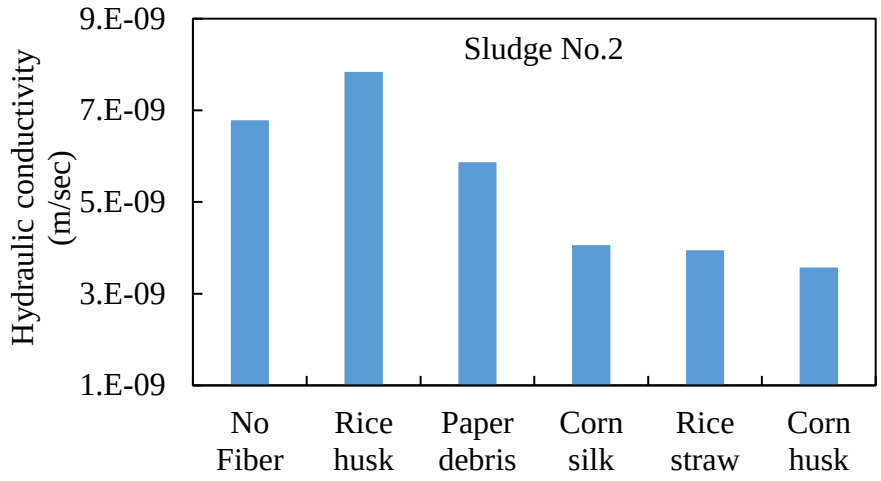

Fig. 2-35 Hydraulic conductivity of cemented sludge No.2 reinforced by several fibers

2.5.4 Durability test

Fig. 2-36 shows the soundness evaluation of specimens from sludge No. 1 during durability test. It is seen that specimens with paper debris, rice straw, corn husk, and corn silk inclusion survive after 10^{th} cycle of drying and wetting, cemented specimens are destroyed as immersed in water at the first cycle, and specimens including rice husk are destroyed after 4^{th} cycle. The failure process of specimens during 10 cycles is as follows.

1. The specimens reinforced by corn silk and rice straw start to degrade after 8^{th} and 9^{th} cycle with unclear indication, respectively. After 10^{th} cycle, few micro-cracks and little delamination appear, but specimens seem to be undamaged as shown in Fig. 2-37a and b.

2. Specimens including paper debris start to degrade after 3^{th} cycle and after 10^{th} cycle, little

exfoliation occurs (Fig. 2-37c).

3. After 2nd cycle, specimens reinforced by corn husk appear micro-crack and surface delamination, then until the 4th cycle, obvious cracks and exfoliation appear and these statuses occur from 4th to 10th cycle (Fig. 2-37d).

4. With rice husk-reinforced specimens, after the first cycle, the degradation starts and develops quickly in the next cycle. After 2nd cycle, the cracks and the exfoliation clearly occur then the big cracks appear after 3rd cycle. Finally, specimens are completely declined after 4th cycle under the massive form.

The improvement of durability of fiber-cement stabilized specimens in comparison with cemented specimens is attributed to the presence of additives which leads to the limitation of the appearance and extension of the crack in each cycle.

Failure strength and failure strain of specimens from sludge No.1 after 0, 2nd, 6th, and 10th cycle are displayed in Fig. 2-38. The plot presents that failure strength decreases according to the increase of cycle number (Fig. 2-38a). The declining percentage of failure strength of specimens including rice straw, corn silk, paper debris, and corn husk after 10th cycle in comparison with that before 10 cycles is 8.5%, 8.5%, 31.4%, and 44%, respectively. As for rice husk inclusion, compared with before 2 cycles, 15.3% of failure strength is decreased after 2nd cycle. The rapid decline of failure strength after 2nd cycle is considered as an indicator of the quick destruction of rice husk-reinforced cemented sludge (destroyed after 4th cycle). As for strain, Fig. 2-38b shows that the failure strain values of specimens reinforced by rice straw, corn silk, corn husk, paper debris, and rice husk insignificantly change during durability test.

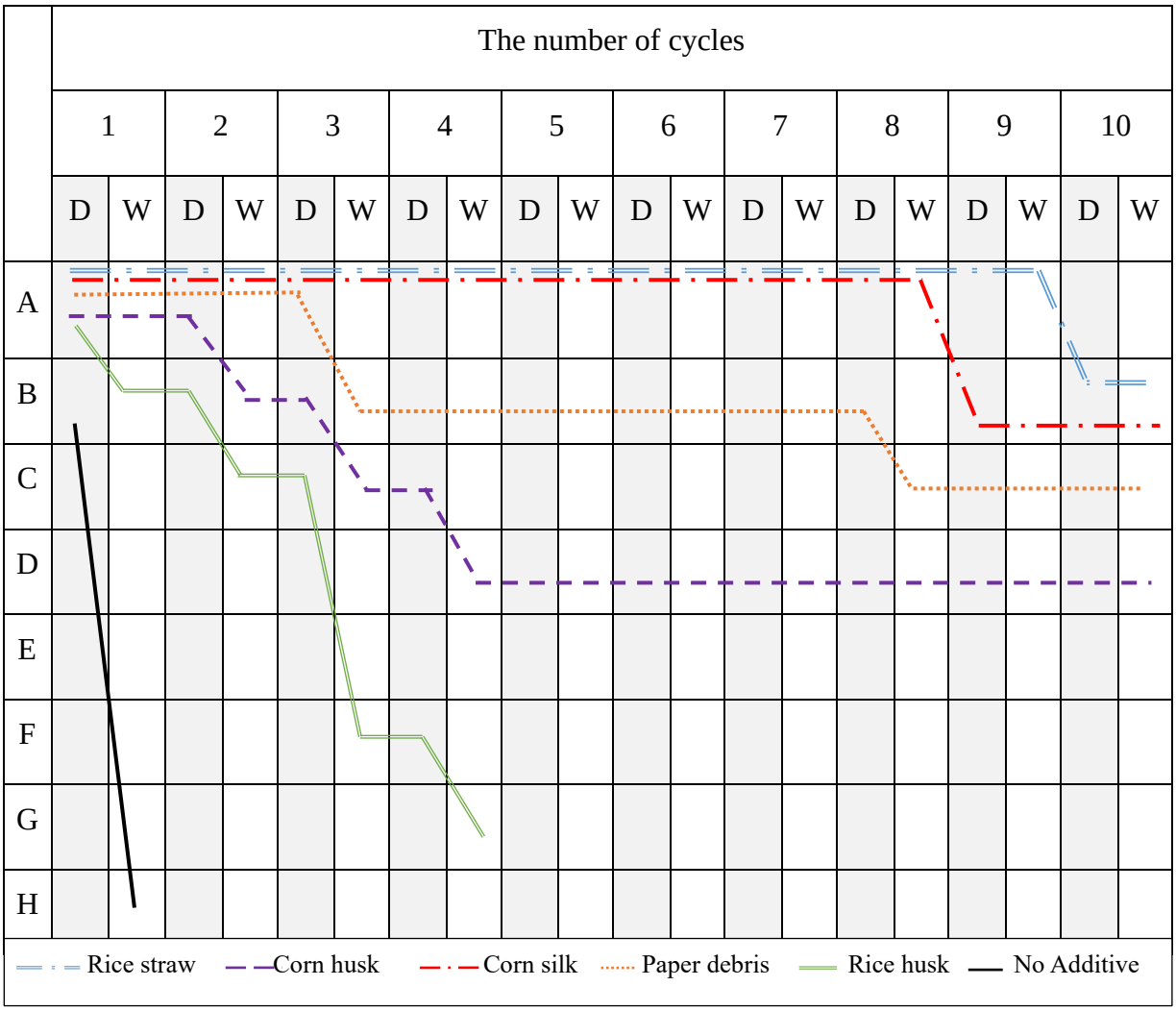

Fig. 2-36 Soundness evaluation of cemented sludge No.1 reinforced by several fibers

Rice straw Corn silk Paper debris Corn husk

Fig. 2-37 State of cemented sludge No.1 reinforced by fibers after 10th cycle

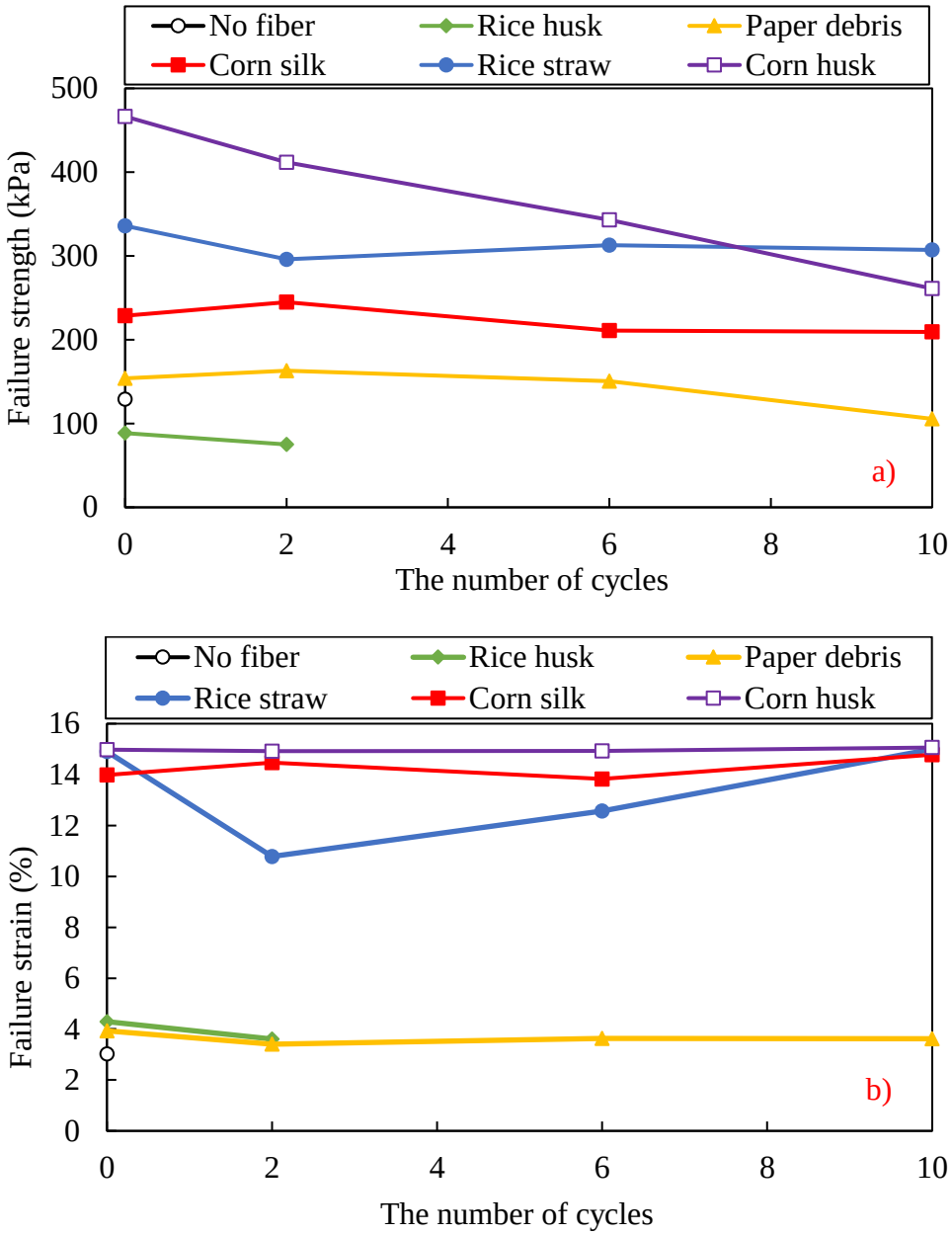

Fig. 2-38 Failure strength of cemented sludge No.1 reinforced by several fibers

a) Failure strength; b) Failure strain

Fig. 2-39 shows the soundness evaluation of specimens from sludge No. 2 during durability test. It is seen that specimens with rice straw, corn husk, and corn silk inclusion survive after 10^{th} cycle, cemented specimens and specimens including rice husk and paper debris are destroyed after 3^{rd}, 8^{th}, and 9^{th} cycle, respectively. The failure process of specimens during 10 cycles is as follows.

1. The specimens reinforced by rice straw, corn husk, and corn silk start to degrade after 4^{th}, 2^{nd}, and 3^{rd} cycle with clear indications, such as crack appearance and surface delamination,

respectively. After each cycle, the specimens gradually destroy. Then after 10^{th} cycle rice straw-reinforced cemented soil is totally exfoliated and specimens with corn husk and corn silk inclusion partly deteriorate as shown in Fig. 2-40.

2. Specimens including paper debris start to degrade after the first cycle with partly crack and surface delamination. From the 4^{th} cycle, specimens quickly destroy, and after 9^{th} cycle specimens are destroyed in the massive form.

3. Specimens reinforced by rice husk start to degrade after the first cycle. Then specimens gradually degrade until destroy under massive form after 8^{th} cycle.

4. Without fiber inclusion, specimens are rapidly degraded from the first cycle and completely declined after 3^{th} cycle under the massive form.

Failure strength and failure strain of specimens from sludge No.2 after 0, 2^{nd}, 6^{th}, and 10^{th} cycle are displayed in Fig. 2-41. The plot presents that failure strength tends to quickly decrease according to the increase of the number of cycles (Fig. 2-41a). The declining percentage of failure strength of specimens including rice straw, corn silk, and corn husk after 10^{th} cycle in comparison with that before 10 cycles is 55.3%, 66.0%, and 74.2%, respectively. As for rice husk and paper debris inclusion, failure strength decreases 85.2% and 76.4 after 6^{th} cycle. With cemented specimens, failure strength decreases 79.9% after 2^{nd} cycle. As for failure strain, failure strains of specimens reinforced by corn silk, corn husk, and rice straw decrease from 0 to 6^{th} cycle, then increase again from 6^{th} to 10^{th} cycle (Fig. 2-41b). With rice husk inclusion, strain decreases more rapidly (from 2.3% at 0 cycle to 0.8% at 6^{th} cycle) than that of paper debris-reinforced cemented soil (from 3.5% at 0 cycle to 2.5% at 6^{th} cycle).

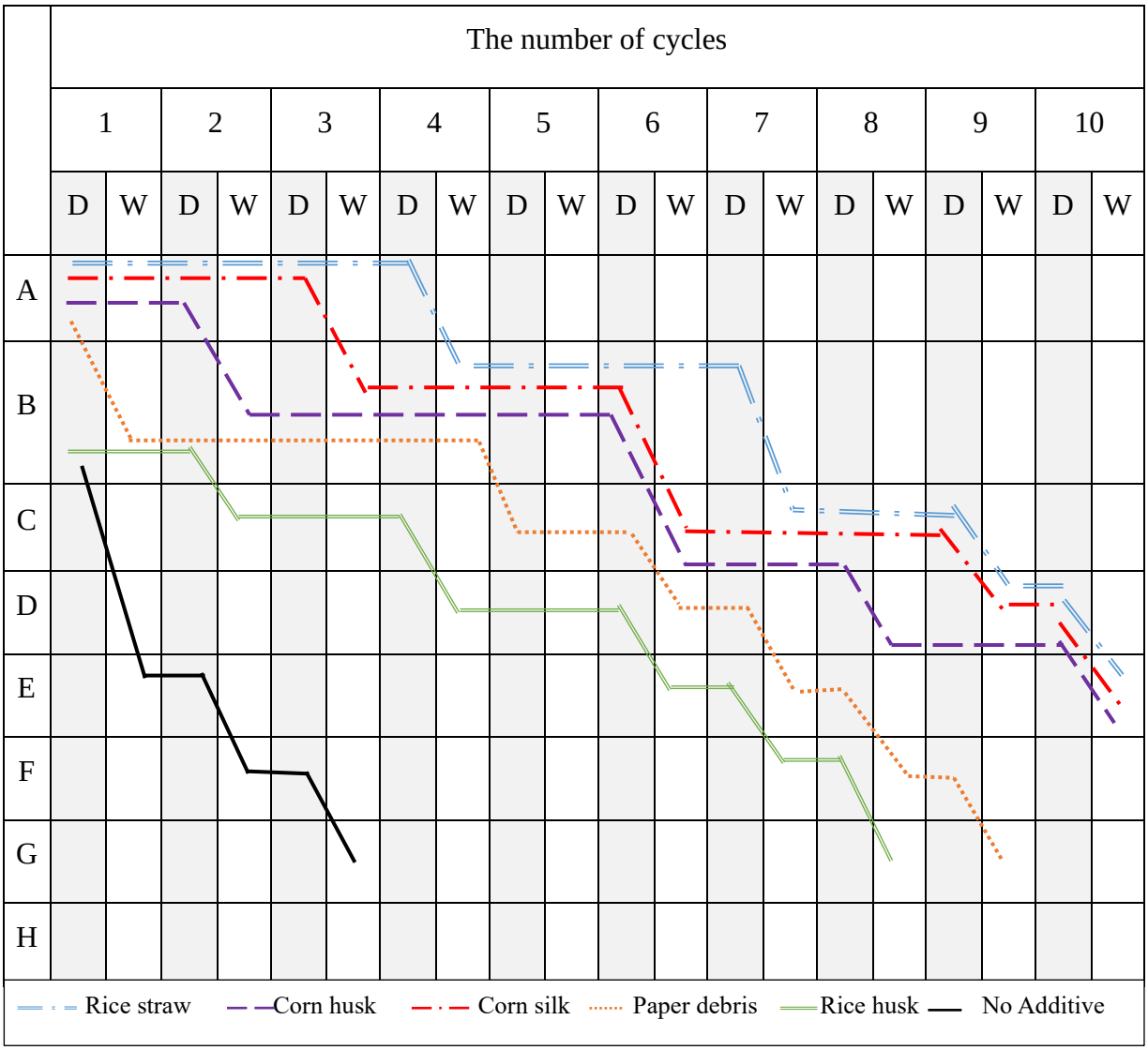

Fig. 2-39 Soundness evaluation of cemented sludge No.2 reinforced by several fibers

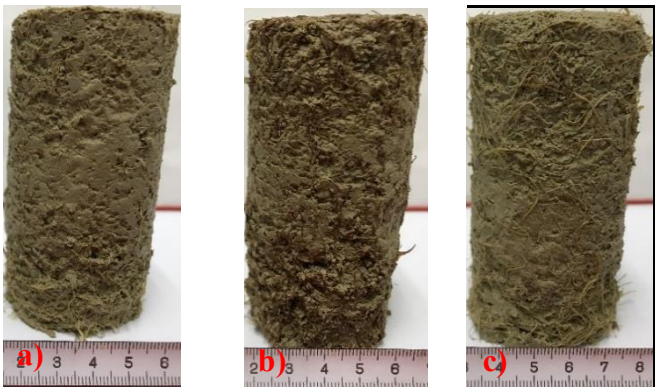

Rice straw Corn silk Corn husk

Fig. 2-40 State of cemented sludge No.2 reinforced by fibers after 10th cycle

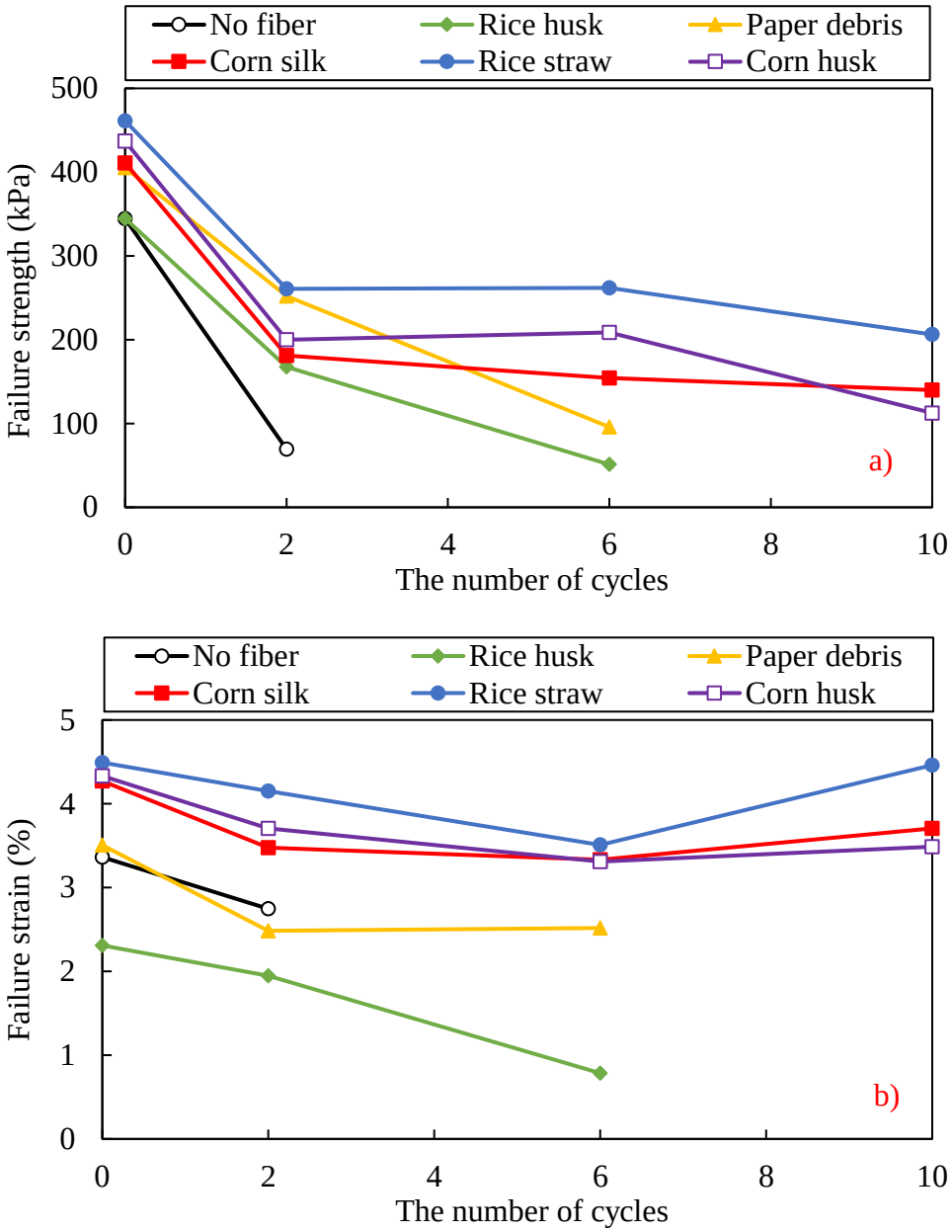

Fig. 2-41 Failure strength of cemented sludge No.2 reinforced by several fibers

a) Failure strength; b) Failure strain

2.5.5 Relationship between failure strength and tensile strength

The relationship between failure strength and tensile strength for fiber-cement stabilized soil and cemented soil of two kinds of sludge and five kinds of fiber material is shown in Fig. 2-42. As can be seen from the plot, the relationship between failure strength and tensile strength shows a strong linearity with a correlation coefficient of 0.9. The relationship coefficient between failure strength and tensile strength is 0.16 which is quietly parallel to the relationship coefficient reported by many previous researchers. Xiao et al. (2016) [58]

reported that the relationship coefficient between failure strength and tensile strength is 0.09-0.15 for cemented soil, 0.14 for fiber-cement stabilized soil. Tran et al. (2018) [59] reported that the relationship coefficient is 0.162 and 0.145 for cemented soil and fiber-cement stabilized soil, respectively.

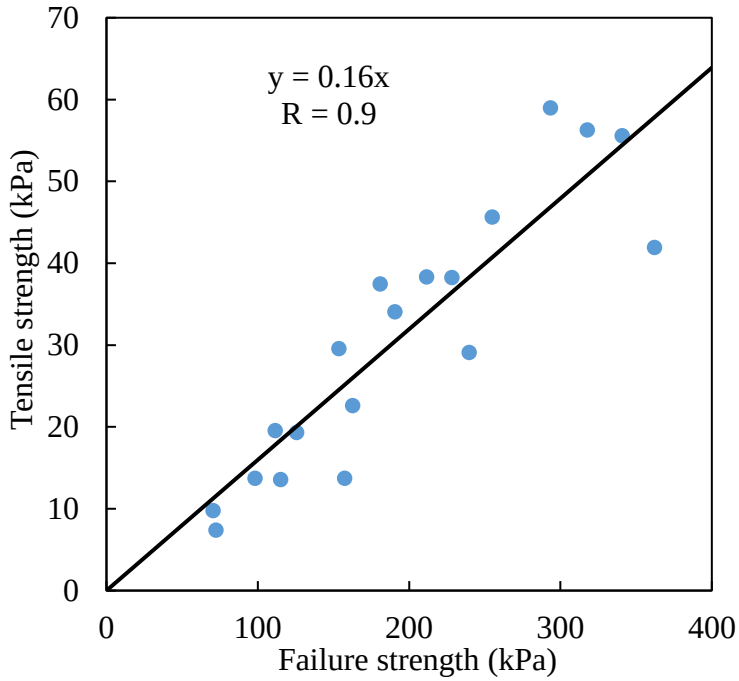

Fig. 2-42 Relationship between failure strength and tensile strength

2.6 Conclusions

A series of unconfined compression, splitting tension, permeability, and durability tests are performed to evaluate and compare the workability of five kinds of fiber (i.e., corn husk, corn silk, rice straw, rice husk, and paper debris). In this chapter, two kinds of sludge (sludge No.1 including 40% Kasaoka clay and 60% silk, sludge No.2 including 40% sand and 60% Kasaoka clay) are used. The results obtained from the experiments could be summarized as follows.

- Failure strength of specimens from sludge No.1 and sludge No.2 with corn husk and rice straw inclusion increase highest with 384% and 106% when compared with that of specimens without fiber inclusion, respectively. For sludge No.1, failure strain of specimens with corn silk, rice straw, and corn husk inclusion is highest with 15%. However, failure strain of specimens from sludge No.2 is highest with 4.7% when adding corn husk.

- Tensile strength of specimens without fiber inclusion from sludge No.1 and sludge No.2 increases highest (469% and 100%, respectively) when adding corn husk fiber. Failure strain of specimens from sludge No.1 with corn silk, rice straw, and corn husk inclusion is highest with 15%. Failure strain of specimens from sludge No.2 with corn husk inclusion is highest with 5.9%. Moreover, the morphology of tensile crack changes from a smooth crack plane to a multiple crack plane due to the additive materials in specimens.

- Hydraulic conductivity of cemented sludge generally decreases when adding fiber materials. The order of fiber according to descending order of hydraulic conductivity is rice husk, paper debris, corn silk, corn husk, and rice straw for specimens from sludge No.1 and rice husk, paper debris, corn silk, rice straw, and corn husk for specimens from sludge No.2.

- After 10^{th} cycle, specimens from sludge No.1 with rice straw, corn husk, corn silk, and paper debris inclusion survive and decrease failure strength about 8.5%, 44%, 8.5%, and 31.5% in comparison with that after 28 days, respectively. For specimens from sludge No.2, rice straw, corn silk, and corn husk inclusions result in the survival of specimens after 10^{th} cycle. Failure strength decreases quickly according to the increase of the number of cycles, namely, failure strength of specimens reinforced by rice straw, corn silk, and corn husk decrease 55.3%, 66%, and 74.2% in comparison with that before the durability test.

In general, specimens with corn husk inclusions give the best performances in terms of Fiber-Cement Stabilized Soil method. Hence, corn husk is selected to study deeply in the next chapters.

CHAPTER 3

STUDY ON MECHANICAL PROPERTIES OF CORN HUSK FIBER-CEMENT STABILIZED SOIL WITH HIGH WATER CONTENT PRODUCED BY LIQUIFIED-STABILIZED SOIL METHOD

3.1 Introduction

Nowadays, high-water-content soil is produced more and more from construction activities and dredging operations. There are significant challenges to the disposal of this kind of soil due to economic and environmental problems. To deal with the problems relating to soil discharge, soil stabilization is a suitable solution to recycle them for reusing as a backfilling material for land reclamation. Therefore, many previous researchers have studied high-water-content soil stabilization by adding some additives such as fly ash, cement, etc. [60–70]. Over recent decades, Liquefied-Stabilized Soil is an effective method to stabilize high-water-content soil. In this method, cement is added to high-water-content soil, the homogenous admixture of soil and cement is directly injected from transportation vehicles to construction sites. The admixture flows like mortar before hardening and there is no compaction afford in this method. Hence, it is possible to apply the treated soil at a narrow space underground or between constructions where it is impossible to conduct compaction of treated soil. After adding cement, the products of the hydration reaction of cement are responsible for the formation of the cement skeleton in the soil matrix. Owing to the development of cementitious structure, the properties of treated soil (i.e., tensile strength, stiffness, failure strength, etc.) are significantly improved. On the other hand, brittleness property of cemented soil also enlarges with the increase in cement content. Many studies have reported that the addition of fiber to excavated soil or cemented excavated soil contributes to the improvement of composite properties. Fiber inclusion not only increases failure strength, shear strength, tensile strength, energy absorption but also changes the cemented soil property from brittle to ductile, etc. [16, 19, 44, 55, 71–76]. Due to the advantages of excavated soil reinforced by fiber, it seems that the application of fiber to Liquefied-Stabilized Soil method can enhance the mechanical characteristics of cemented soil, especially change from brittle behavior to ductile behavior. Nevertheless, until now, the use of fiber in Liquefied-Stabilized Soil method to improve cemented soil properties with high water content is limited. As a result, the effect of fiber on the mechanical properties of cemented soil in terms of Liquefied-Stabilized Soil method is not fully understood.

The current study aims to utilize waste corn husk fiber in Liquefied-Stabilized Soil method to recycle high-water-content soil. The effect of corn husk fiber on the cemented soil properties is investigated. A series of mixing conditions changing water, cement, and fiber content are subjected to laboratory experiments to compare the behavior of fiber-cement

stabilized soil with that of cemented soil in terms of splitting tension, unconfined compression, and durability tests. In Liquified-Stabilized Soil method, not only durability and failure strength but also bleeding ratio and flow value are important parameters. It is important to make sure that flow value and bleeding ratio satisfy target values. Target values of flow value and bleeding ratio are larger than 100 mm and less than 1%, respectively. Therefore, in this chapter, flow test and bleeding test are also carried out to investigate the effect of corn husk fiber on flow value and bleeding ratio, respectively. Besides, tension test of corn husk fiber is conducted to measure its tensile strength.

3.1.1 Sludge

This chapter uses imitated dry sludge No. 1 including 40% Kasaoka clay and 60% silt. The grain size distribution, properties of dry sludge are shown in Section 2.2.1.

3.1.2 Cement

This chapter uses Geoset 200 cement for soil stabilization. The chemical and physical properties of cement are summarized in Section 2.2.2.

3.1.3 Fiber materials

Corn husk fiber is used in this chapter. The dry raw corn husk is cut to short segments of 20 mm in length. Then, the cut segments are immersed in water and milled into a fibrous form. Finally, wet corn husk fibers are dried until obtaining a constant mass (Fig. 3-1). The size of corn husk fibers is 0.26 mm in average longest diameter and 14.8 mm in average length. The chemical composition and other properties of corn husk fiber are listed in Section 2.2.3.

Fig. 3-1 Corn husk fiber

3.2 Specimen preparations

3.2.1 Specimen preparation apparatus

- Mixing machine

The mixing machine used to prepare mixture is shown in Section 2.3.1

- Tools of flow test

Flow test requires several tools including a plate with smooth surface, cylindrical mold without cover at top and bottom of the mold, and a ruler. The dimension of cylindrical mold is 80 mm in length and 80 mm in inside diameter. Fig. 3-2 displays all tools of flow test.

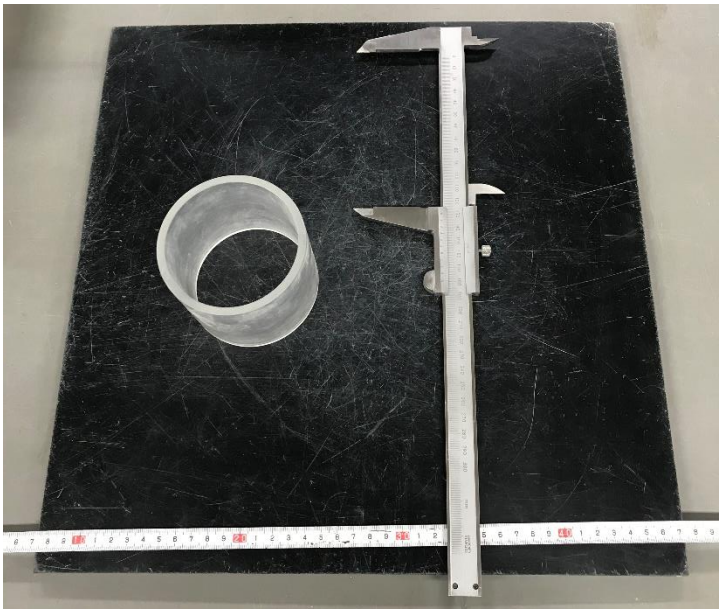

Fig. 3-2 Tools of flow test

- Tools of bleeding test

The tools for conducting bleeding test include a plastic bag of 50 mm in diameter, a funnel, a volumetric glass cylinder. All tools of bleeding test are given in Fig. 3-3.

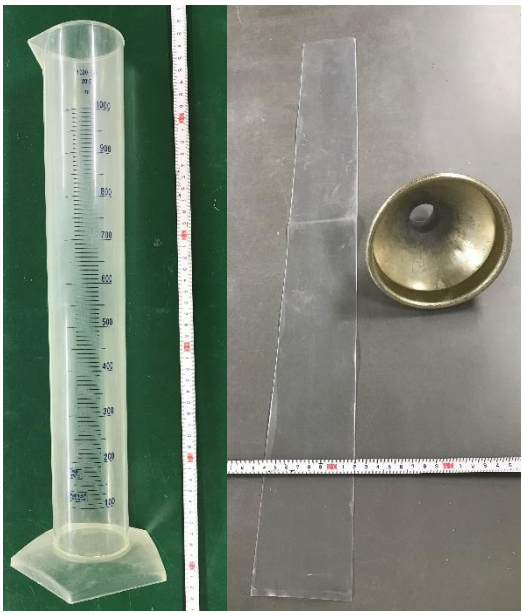

Fig. 3-3 Tools of bleeding test

- Mold

The plastic mold is used for preparing specimens of unconfined compression test, splitting tension test, and durability test. The dimension of cylindrical mold is 100 mm in length and 50 mm in inside diameter (Fig. 3-4).

Fig. 3-4 Cylindrical plastic mold

- Dry oven

Two kinds of oven are used in this chapter, which are shown in Section 2.3.1

3.2.2 Preparation process

- Tensile test of single corn husk fiber

120 randomly selected fibers are subjected to the test with different gage lengths including

10, 20, and 30 mm. The average diameter of fiber is 0.29 mm. To set up the samples, setting boards are prepared as illustrated in Fig. 3-5a and b. After completing installing and before applying load to fiber, the paper board is cut as presented in Fig. 3-5c.

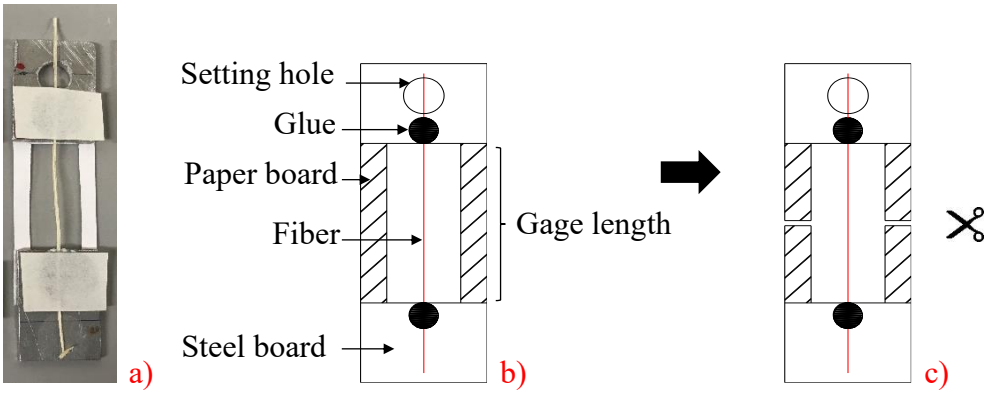

Fig. 3-5 Preparation of fiber

a) Setting board; b) Detail of setting board;
c) Cutting paper board before applying load

- Other tests

With the different water contents of sludge (80% and 100%), cement contents (40, 60, 80, and 100 kg/m^3), and fiber contents (0, 3, 6, 9, 12, and 15 kg/m^3), all mixing conditions used for experiments are detailed in Table 3-1. The cement and fiber content in each mixing condition is the weight of cement and fiber in 1m^3 of dry soil and water.

The procedures for mixing admixture and making specimens are as follows.

1. According to the mixing condition, water is added to artificial dry sludge and mixed by mixing machine until admixture is homogenous. The mixing is carried out two times with 1 min/time.

2. The fiber material is added to the artificial sludge and agitated until the mixture is homogenous by the mixing machine. The mixing is carried out three times with 1min/time.

3. Addition and agitation of cement in admixture. The mixing is carried out three times with 1 min/time.

4. After obtaining a homogenous admixture, the admixture is directly applied to flow and bleeding tests. To make specimens for splitting tension, unconfined compression, and durability test, the admixture is poured into cylinder plastic mold with 100 mm in height and 50 mm in inside diameter after mixing.

5. The plastic sheet is used to closely cover the specimens. The specimens are cured under 20 ± 3^0C for either 7 days (for unconfined compression and splitting tension test) or 28 days (for durability test).

6. After 7 and 28 days, specimens are extruded from the plastic mold with the surface polished before being subjected to unconfined compression test, splitting tension test, and durability test.

Table 3-1 Mixing conditions for experiments

No.	W (%)	C (kg/m^3)	F (kg/m^3)	Name	Experiments
1	80	40	0	W80C40F0	UCT, STT, BT, FT
2	80	40	3	W80C40F3	UCT, STT, BT, FT
3	80	40	6	W80C40F6	UCT, STT,
4	80	40	9	W80C40F9	UCT, STT,
5	80	40	15	W80C40F15	UCT, STT, BT, FT
6	80	60	0	W80C60F0	UCT, STT, BT, FT, DT
7	80	60	3	W80C60F3	UCT, STT, BT, FT
8	80	60	6	W80C60F6	UCT, STT,
9	80	60	9	W80C60F9	UCT, STT,
10	80	60	12	W80C60F12	UCT, STT, BT, FT, DT
11	80	80	0	W80C80F0	UCT, STT, BT, FT
12	80	80	3	W80C80F3	UCT, STT, BT, FT
13	80	80	6	W80C80F6	UCT, STT,
14	80	80	9	W80C80F9	UCT, STT, BT, FT
15	80	100	0	W80C100F0	UCT, STT, BT, FT
16	80	100	3	W80C100F3	UCT, STT, BT, FT
17	80	100	6	W80C100F6	UCT, STT, BT, FT
18	80	100	9	W80C100F9	UCT, STT, BT, FT
19	100	80	0	W100C80F0	UCT, STT, BT, FT, DT
10	100	80	3	W100C80F3	UCT, STT, BT, FT
21	100	80	6	W100C80F6	UCT, STT, BT, FT
22	100	80	9	W100C80F9	UCT, STT, BT, FT
23	100	80	15	W100C80F15	UCT, STT, BT, FT, DT
24	100	100	0	W100C100F0	UCT, STT, BT, FT
25	100	100	3	W100C100F3	UCT, STT, BT, FT
26	100	100	6	W100C100F6	UCT, STT, BT, FT
27	100	100	9	W100C100F9	UCT, STT, BT, FT
28	100	100	15	W100C100F15	UCT, STT, BT, FT

Note: W = water content; C = cement content; F = fiber content; UCT = unconfined compression test; STT = splitting tension test; BT = bleeding test; FT = flow test; DT = durability test

3.3 Testing programs

3.3.1 Tension test of fiber

The tension test for measuring tensile strength of fiber is performed by using the testing machine as shown in Fig. 3-6. The 2 kN load cell and strain gauge displacement sensor are used to measure stress and displacement. The displacement rate of the load is 1 mm/min. A computer is used to collect both stress and displacement data. Fibers are loaded until they are fractured. Tension tests of fiber are carried out at room temperature (~21^{0}C). Eq. (3-1) performs the formula for calculating tensile strength of each fiber.

$$T=F/A \tag{3-1}$$

where F is the applied load (kN), A is the cross-sectional area of fiber at the fracture position (m^2), and T is the tensile strength of each fiber (kPa). The cross-sectional area of fiber is investigated by an optical microscope. The cross-section images with the magnification of 200X obtained from an optical microscope are processed by using the ImageJ software. The contour line is drawn, and the cross-sectional area is measured (Fig. 3-7). The previous study assumed that the cross-section of fiber is round and cross-sectional area is calculated from the diameter of fiber [77]. This calculation method is correct for synthetic fibers because they are perfectly round for all fibers. However, the cross-section of natural fiber is the non-round shape. Hence, collecting the cross-sectional area data of fiber at fracture section by the optical microscope contributes to the rise in the precision of tensile strength value.

Since the elongation of fiber is indirectly measured, the real elongation of fiber is not determined. The record elongation is cross-head displacement including the real elongation of fiber and the movement of the loading system and clamp system. The displacement of the load and clamp system is associated with system compliance. Hence, determination of the system compliance value is necessary. The system compliance value of the tests is obtained from the plot of the ratio of displacements to forces at three different gage lengths according to ASTM C1557-03 [78]. This plot performs a straight line with the intercept of system compliance. The system compliance of all tests and real elongation of fiber are calculated from Eq. (3-2) and (3-3), respectively.

$$\frac{\Delta L}{F} = \frac{1}{EA} L + C \tag{3-2}$$

$$\Delta l = \Delta L - F \times C \tag{3-3}$$

where ΔL is the recording elongation (mm), Δl is the real elongation of fiber (mm), L is the gage length (mm), F is the applied load (N), A is the cross-sectional area of fiber at a fractured session (mm^2), E is Young's modulus of the fiber (N/mm^2), and C is the system compliance (mm/N).

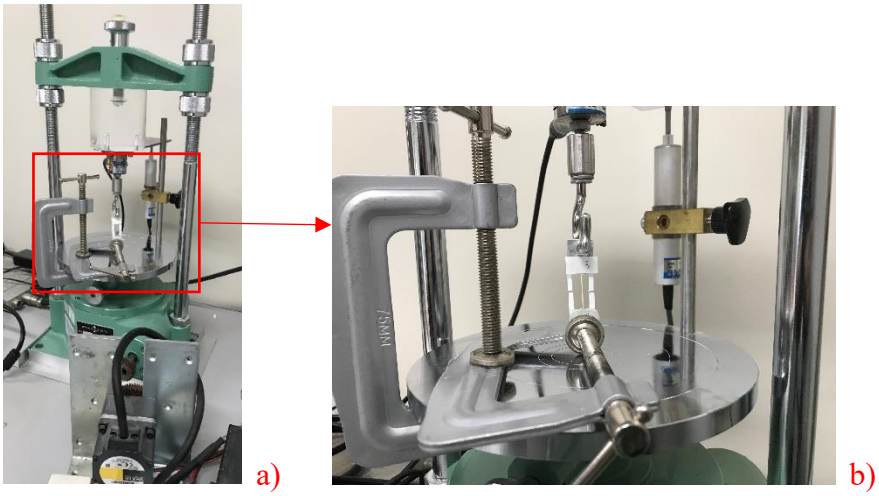

Fig. 3-6 Testing machine of tension test of fiber

a) Testing machine; b) Detail of setting

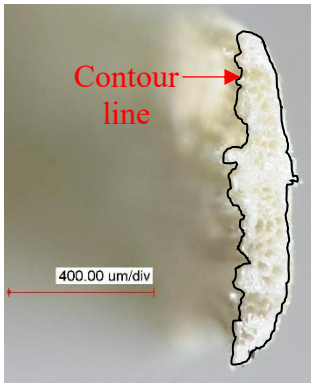

Fig. 3-7 The cross-sectional area of fiber

3.3.2 Flow test

Flow test is the experiment to investigate fluidity of admixture. This is the important parameter of mixture to make sure that the mixture can be pumped out. Fluidity is assessed based on flow value. In this study, target value of flow test is higher than 100 mm [79]. To

determine flow value, the testing procedure includes the following steps:

1. The homogenous mixture is fully poured into a cylindrical mold with 80 mm in height and 80 mm in inside diameter which is put on the flat plate.

2. The surface of the admixture at the edge of the mold is smoothed.

3. The cylindrical mold is gradually raised and removed in the vertical direction. After removing the mold, admixture spread out on the flat plate. The longest diameter of the spread admixture and the spread diameter perpendicular to the longest spread diameter are measured (Fig. 3-8). The flow value is calculated by using Eq. (3-4).

$$F=(D_x+D_y)/2 \tag{3-4}$$

where F is the flow value (mm), D_x is the longest spread diameter (mm), D_y is the spread diameter perpendicular to the longest spread diameter (mm).

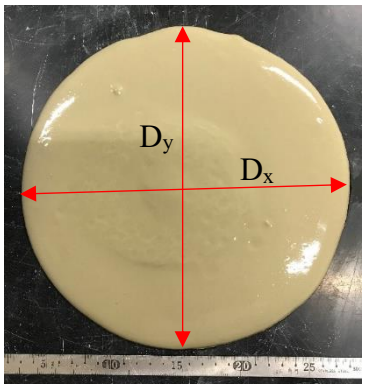

Fig. 3-8 Spread admixture on the flat plate

3.3.3 Bleeding test

Bleeding test aims to measure the bleeding value of admixture after 3 hours according to Standard Specification of Japan Society of Civil Engineering [80]. Bleeding is a segregation form of material in the composite. In this phenomenon, water rises to the fresh surface and solid compounds settle down. Bleeding occurs since water is the lighter ingredient in composite, and it is impossible for the composite to keep all water. In this study, target value of bleeding test is less than 1%. The testing procedure includes the following steps.

1. After mixing, the admixture is poured into a plastic bag of 50 mm in diameter.

2. The admixture bag is sunk into a given water volume contained in a volumetric glass cylinder until the surface of the admixture in the bag and the surface of the water in the

cylinder are of equal height. The rising water volume comparing with the given water volume in the glass cylinder is the volume of the mixture.

3. The bag with the admixture inside is placed for 3 hours.

4. The depth of water at the surface of the admixture is measured (Fig. 3-9). The bleeding rate is calculated as Eq. (3-5).

$$B=100h(\pi D^2/4)/V \tag{3-5}$$

where B is the bleeding ratio (%), D is the plastic bag diameter (mm), h is the depth of water layer on the surface of admixture (mm), V is the volume of admixture (mm^3).

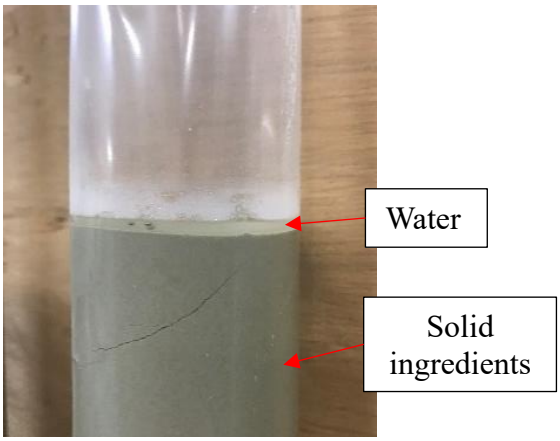

Fig. 3-9 Segregation phenomenon of mixture

3.3.4 Unconfined compression test

The testing machine and testing procedure of unconfined compression test are shown in Section 2.4.1.

3.3.5 Splitting tension test

The testing machine and testing procedure of splitting tension test are shown in Section 2.4.2.

3.3.6 Durability test

The testing machine and testing procedure of durability test are shown in Section 2.4.4.

3.4 Experimental results

3.4.1 Tension test of fiber

3.4.1.1 Tensile behavior

Typical tensile stress-strain curves of corn husk are plotted in Fig. 3-10. The figure indicates that the stress-strain curves perform two phases including linear phase and non-linear phase. Linear phase is from origin to around 7-10 MPa, and non-linear phase is from around 7-10 MPa to the peak point. It was reported that banana, coir, piassava, and sisal perform the same tensile stress-strain behavior as corn husk fiber [39, 81–83]. However, the behavior of some fibers embracing curaua and jute are unlike, namely, their curves are linear from origin to failure point [39]. The appearance of the non-linear region is attributed to the failure of the weak primary cell wall of fiber and the decohesion of the cell under tensile load [81].

Table 3-2 summarizes the results from the experiment and their standard deviation. Initial modulus is determined from the initial phase of the tensile stress-strain curve (linear region). Both initial modulus and strain values are corrected for the system compliance determined from Fig. 3-11. The results from the table present that tensile strength diminishes from 51.99 to 42 MPa, and initial modulus increases from 0.8 to 1.14 GPa when increasing gage length from 10 to 30 mm. The decrease of tensile strength and enlargement of initial modulus with increasing gage length are in good agreement with previous research [81]. In contrast, gage length has an insignificant effect on strain to failure. As can be seen from the results, tensile strength, failure strain, and initial modulus are independent of the cross-sectional area of fiber. Besides, the standard derivations of the results are high. The high derivation and the independence of tensile strength, failure strain, and initial modulus from the cross-sectional area can be explained by the fact that corn husk fiber is a natural fiber, as a result, its properties are influenced strongly by maturity and the number of defects on fiber. The age of corn husk covering cob corn gradually increases from the inside layer to the outside layer. The difference in age of corn husk leads to the variation of cellulose content in fiber which is responsible for tension load. Furthermore, random damages in fiber and on the surface of fiber either presenting intrinsically or during the fiber extraction process from raw corn husk remarkably affect fiber characteristics [84].

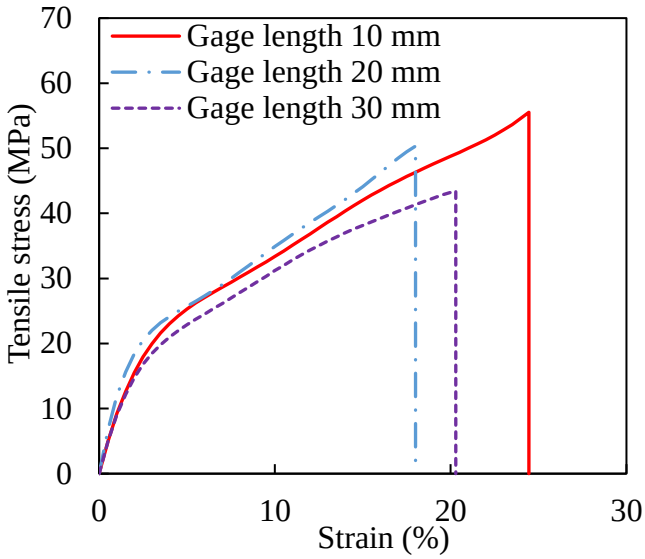

Fig. 3-10 Typical tensile stress-strain curves of corn husk fiber

Table 3-2 Experimental results of corn husk fiber from tension test

Length gage (mm)	Area (mm^2)		Tensile strength (MPa)		Strain (%)		Initial modulus (GPa)		Weibull modulus
	Mean area	SD	Mean strength	SD	Mean strain	SD	Mean modulus	SD	
10	0.06	0.02	51.99	17.87	22.77	7.20	0.80	0.29	3.43
20	0.07	0.03	45.72	16.05	15.62	6.79	1.05	0.40	3.33
30	0.07	0.03	42.00	12.96	16.56	6.18	1.14	0.53	3.62

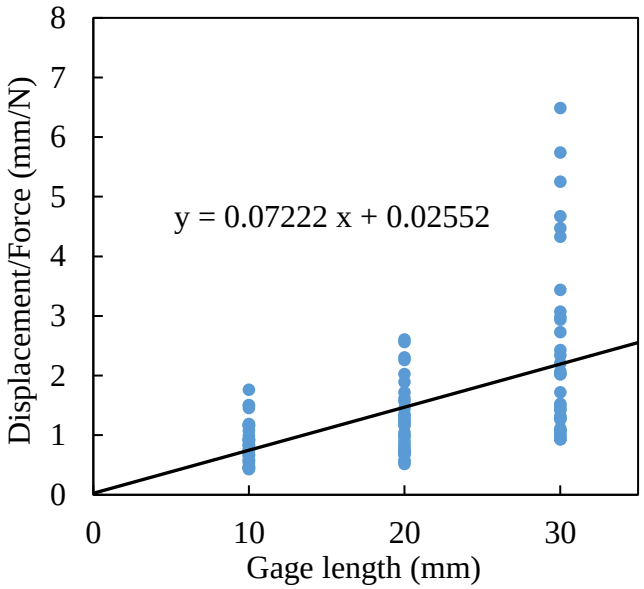

Fig. 3-11 Ratio of displacement to force versus gage length

3.4.1.2 Weibull distribution

As mentioned in the previous section, the standard derivation of tensile strength value is high, so it is necessary to evaluate the variation of strength value. In this study, Weibull modulus (Weibull parameter) from Weibull distribution is used for the evaluation. The bigger value of the Weibull parameter means the smaller variation of fiber tensile strength value.

According to the 2-parameter Weibull distribution, the cumulative probability of the failure of the ith fiber is given by Eq. (3-6).

$$P = 1 - \exp\left[-\left(\frac{\delta}{\alpha}\right)^{t}\right] \tag{3-6}$$

where t is the Weibull modulus or shape parameter, α is the scale parameter, and δ is the strength of the ith fiber.

J. C. Fothergrill (1990) [85] reported the median rank of the ith fiber with excellent approximation as seen in Eq. (3-7).

$$P_{\delta_i} = \frac{i - 0.3}{N + 0.4} \tag{3-7}$$

where $P_{\delta i}$ is the cumulative probability of the failure of the i^{th} fiber and N is the number of the tested fibers for each gage length. Substituting Eq. (3-7) into Eq. (3-6) yields Eq. (3-8).

$$\ln\ln\left(\frac{N + 0.4}{N - i + 0.7}\right) = t \times \ln(\delta) - t \times \ln(\alpha) \tag{3-8}$$

The shape parameter or Weibull modulus t is determined from the plot of ln(ln((*N*+0.4)/(*N*-*i*+0.7))) versus ln(δ) as the slope of the straight line (Fig. 3-12). Weibull modulus value of each gage length is listed in Table 3-2. It is seen that the Weibull modulus of corn husk fiber is from 3.33 to 3.62 with respect to gage length from 10 to 30 mm. There is a trivial variation of shape parameter value among different gage lengths. According to research by N. Defoirdt et al. (2010) [40], the Weibull modulus of synthetic fiber is from 5 to 15, meanwhile, natural fiber shows a great variation of tensile strength with the Weibull modulus in the range of 1 to 6. In the current study, Weibull modulus values of corn husk fiber are situated in this range of natural fiber.

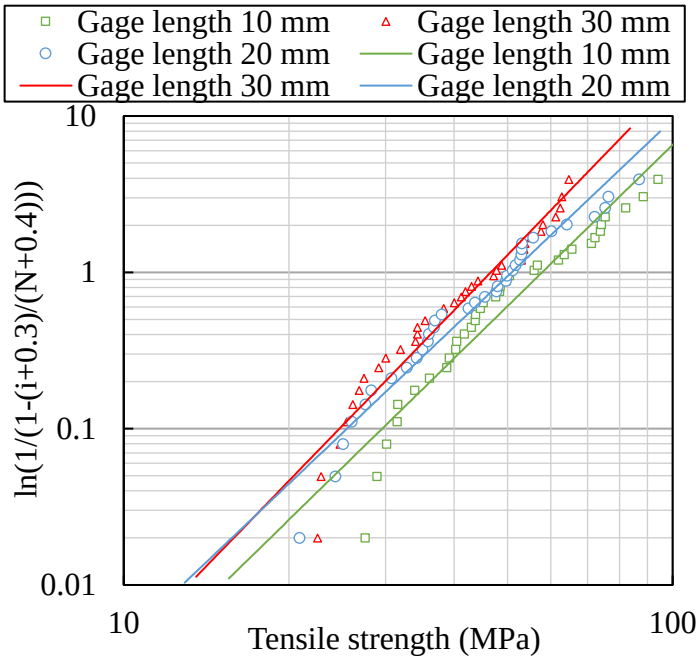

Fig. 3-12 Weibull distribution of fiber

3.4.2 Bleeding test and flow test

3.4.2.1 Bleeding ratio and flow value

Fig. 3-13 and Fig. 3-14 illustrate the effect of fiber and cement on bleeding ratio and flow value, respectively. These figures display that fluidity and bleeding ratio of admixture drop with the increase in fiber content. For bleeding test, all mixtures with 80% water content satisfy the target value of bleeding ratio (less than 1%). With mixtures of 100% water content, bleeding rate of admixture with 80 and 100 kg/m^3 cement is less than 1% when fiber content is from 9 and 6 kg/m^3, respectively. For flow test, all mixing conditions reach the target value (larger than 100 mm). The diminution of flow value and bleeding rate when adding fiber happens since the water absorption capacity of fiber contributes to the reduction of free water and fiber inclusion increases solid volume in admixture. As can be seen from these figures, cement is also a parameter affecting bleeding ratio and flow value. These two values are inversely proportional to cement content. The decrease in bleeding ratio and flow value with increasing cement content is attributed to the free water use of the hydration reaction of cement.

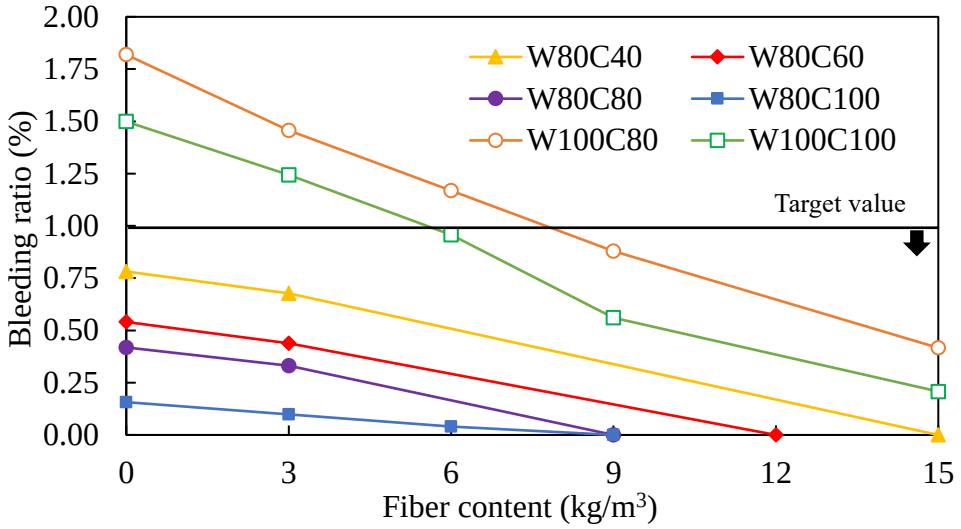

Fig. 3-13 Effect of fiber content on bleeding ratio of admixture

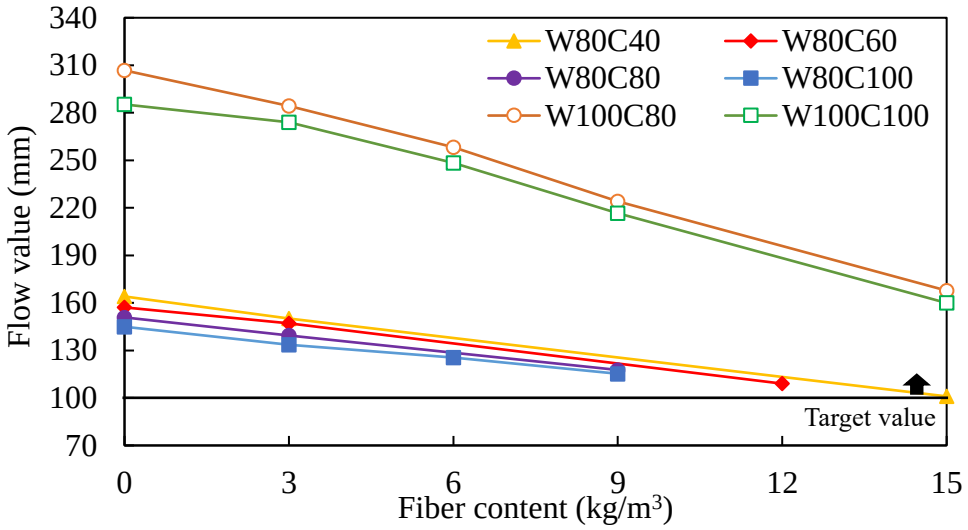

Fig. 3-14 Effect of fiber content on flow value of admixture

3.4.2.2 Superficial water content

Superficial water content of sludge significantly changes due to the inclusion of cement and fiber. With the addition of paper debris and cement, the superficial water content of the admixture is calculated by Eq. (3-9) [86].

$$W_S = \left(1 - \frac{9P + 0.25C}{\rho_w}\right) W_I - \frac{900P + 25C}{\rho_s} \tag{3-9}$$

where W_S is the superficial water content (%), P is the added paper content (kg/m^3), C is the added cement content (kg/m^3), ρ_w is the water density (1000 kg/m^3), W_I is the initial water content of admixture (%), ρ_s is the dry soil density (kg/m^3).

In this study, corn husk is used for replacing paper debris. However, corn husk and paper debris have different water absorption capacities. The water absorption capacity of paper debris in the original equation is 900%, and the water absorption capacity of corn husk is 480%. Therefore, to apply Eq. (3-9) for calculating superficial water content in this study, this equation needs to be modified. The modified equation for calculating superficial water content is as follows.

$$W_S = \left(1 - \frac{4.8CH + 0.25C}{\rho_w}\right) W_I - \frac{480CH + 25C}{\rho_s} \tag{3-10}$$

where W_S is the superficial water content (%), CH is the added corn husk content (kg/m^3), C is the added cement content (kg/m^3), ρ_w is the water density (1000 kg/m^3), W_I is the initial water content of admixture (%), ρ_s is the dry soil density (2485 kg/m^3).

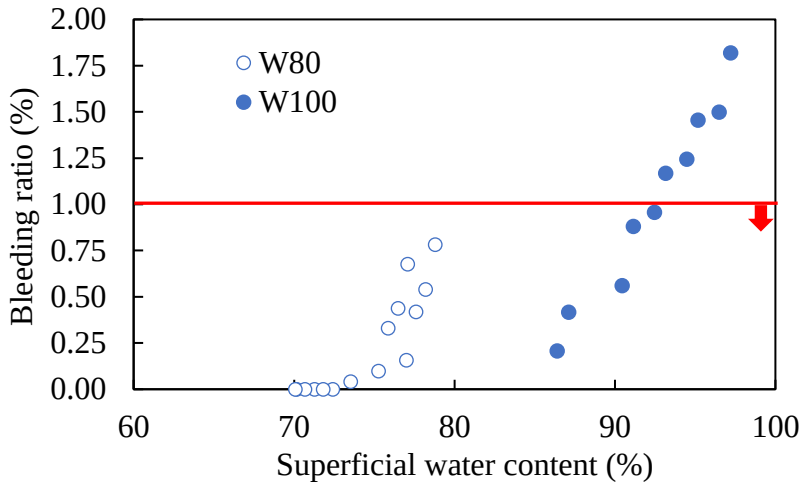

Fig. 3-15 Relationship between superficial water content and bleeding ratio

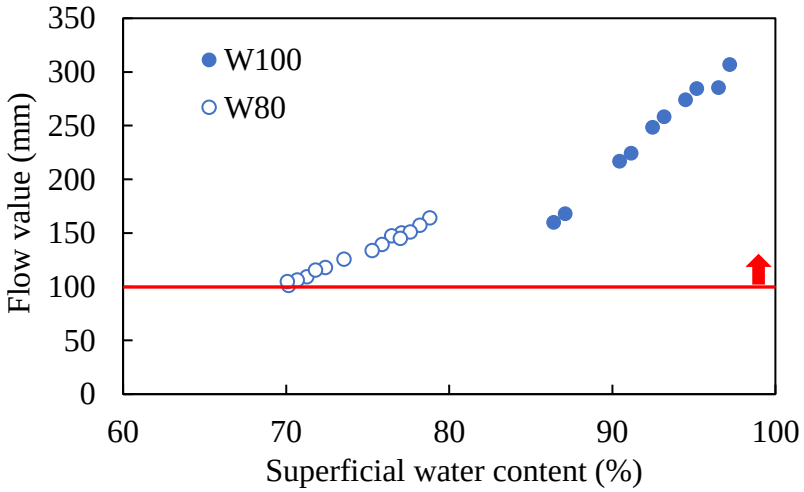

Fig. 3-16 Relationship between superficial water content and flow value

Fig. 3-15 and Fig. 3-16 show the relationship between superficial water content with bleeding ratio and flow value, respectively. It is observed that both flow value and bleeding ratio increase with the increase in superficial water content. For bleeding test, the admixtures with superficial water content less than 92.5% satisfy the target value (less than 1%). For flow test, the admixtures with the superficial water content larger than 70.1% satisfy the target value (less than 100 mm). Therefore, the mixing conditions resulting in the superficial water content of admixture less than 92.5% and higher than 70.1% obtain target value of both bleeding test and flow test. S. Tachihana et al. (2016) [87] reported that flow value and bleeding ratio are affected by the liquid limit. In this study, the liquid limit of used soil with 40% Kasaoka clay and 60% silt is 46.4%. Based on the liquid limit value, it is concluded that admixtures with the superficial water content in the range of "liquid limit +(24~46.4)" satisfy the target value of bleeding test and flow test.

3.4.3 Unconfined compression test

3.4.3.1 Stress-strain curves

Fig. 3-17 shows the stress-strain curves of specimens with and without fiber inclusion of unconfined compression test. The plot presents that fiber inclusion contributes to the improvement of stress-strain curves. After reaching the peak point, compressive stress of cemented specimens dramatically declines (excepting W80C40). Nevertheless, with fiber inclusion, the declining speed of compressive stress (loss of post-peak stress) reduces. Moreover, the more fiber is added, the more loss of post-peak stress decreases. The decrease in loss of post-peak stress indicates that the addition of fiber changes the behavior of the specimens from brittle to ductile [54].

Fig. 3-18 simulates the failure characteristics of specimens in the case of W80C40 with fiber content from 0 to 15 kg/m^3. Without fiber inclusion, the cracks appear with a small number and large width (Fig. 3-18a). With fiber inclusion, the crack is in the form of multiple cracks (Fig. 3-18b, c, d, and e). Moreover, the more fiber is added, the more, the smaller, and the shorter the cracks are. These indications translate for the change of specimen property from brittle (specimens without fiber inclusion) to ductile (specimens with fiber inclusion) as well as translate for more and more ductile with increasing fiber content.

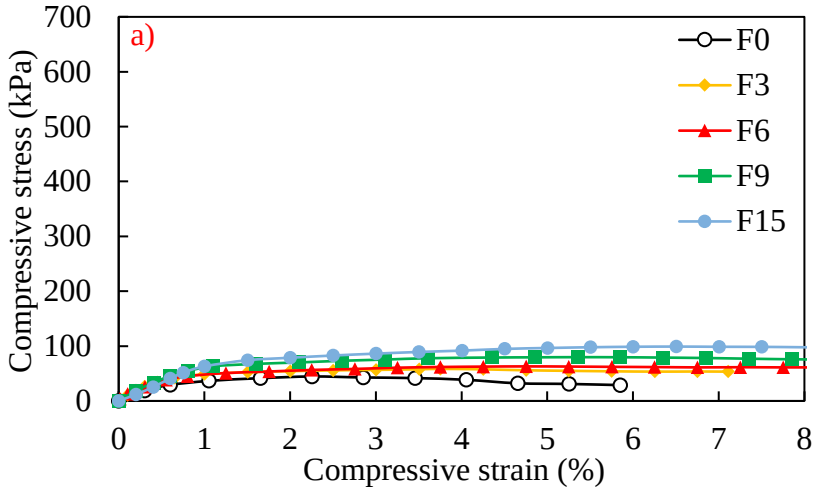
a)
F0
F3
F6
F9
F15
Compressive stress (kPa)
Compressive strain (%)
0
100
200
300
400
500
600
700
0
1
2
3
4
5
6
7
8

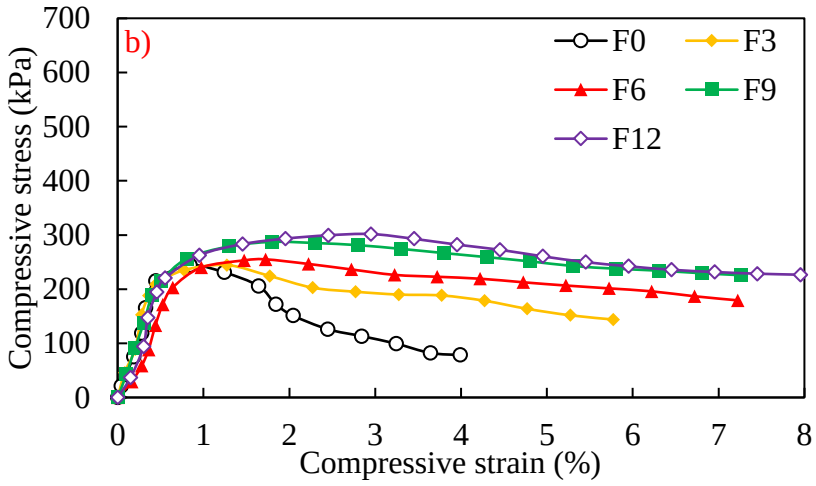
b)
F0
F3
F6
F9
F12
Compressive stress (kPa)
Compressive strain (%)
0
100
200
300
400
500
600
700
0
1
2
3
4
5
6
7
8

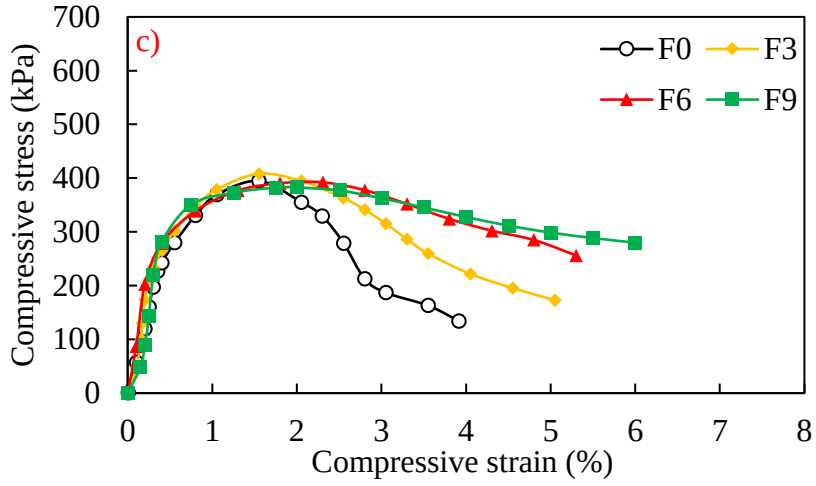
c)
F0
F3
F6
F9
Compressive stress (kPa)
Compressive strain (%)
0
100
200
300
400
500
600
700
0
1
2
3
4
5
6
7
8

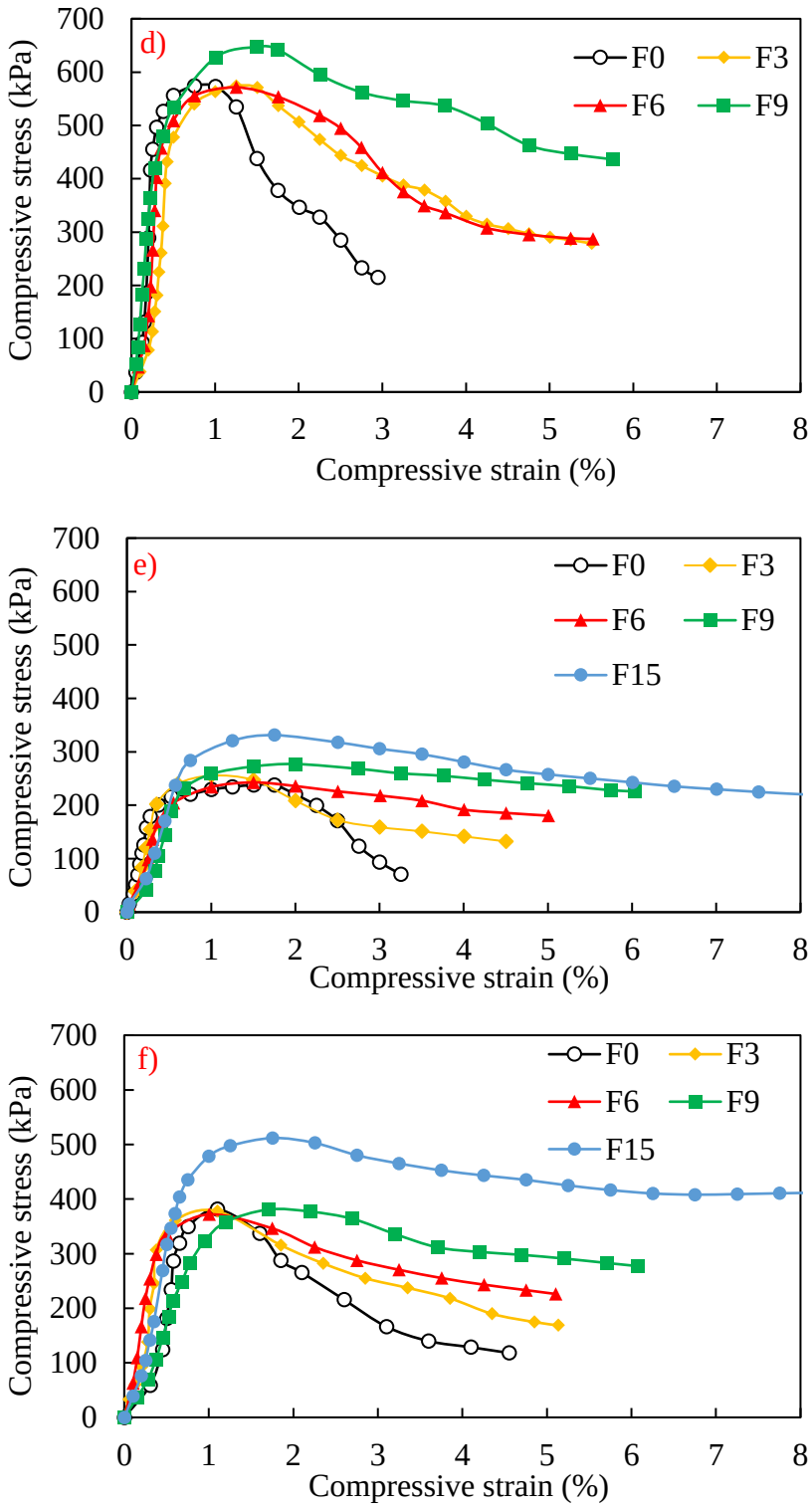

Fig. 3-17 Typical stress-strain curves of unconfined compression test

a) W80C40; b) W80C60; c) W80C80; d) W80C100; e) W100C80; f) W100C100

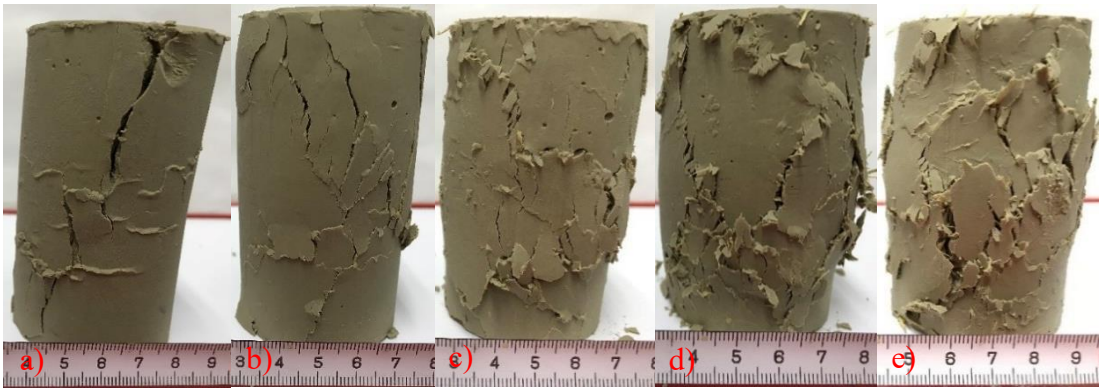

Fig. 3-18 Crack patterns of specimens from unconfined compression test

a) W80C40F0; b) W80C40F3; c) W80C40F6; d) W80C40F9; e) W80C40F15

3.4.3.2 Failure strength

The effects of fiber content on cemented soil in unconfined compression test are presented in Fig. 3-19. As can be observed in this figure, fiber inclusion improves failure strength of cemented soil in some cases. For specimens of W80C40, failure strength significantly increases with increasing fiber content. Compared with cemented specimens, the most increase in failure strength of fiber-reinforced cemented specimens is 119% at 15 kg/m^3 fiber. The improvement of failure strength owing to fiber inclusion is in good agreement with many studies using the compaction method to produce specimens [23, 59, 88]. In the cases of W80C60 and W100C80, the increase in fiber content from 0 to 6 kg/m^3 insignificantly affects failure strength. However, with further fiber inclusion (9 to 12 kg/m^3 for W80C60, and 9 to 15 kg/m^3 for W100C80), failure strength is improved. Namely, compared with cemented specimens, the most improvement of failure strength is 16% and 44% concerning W80C60F12 and W100C80F15. In the cases of W80C80, W80C100, and W100C100, the addition of fiber from 0 to 9 kg/m^3 slightly changes failure strength. Further fiber inclusion (15 kg/m^3) to W100C100, failure strength of cemented specimens increases 38%.

The enhancement of failure strength due to the inclusion of fiber could be explained by interlocking force and interfacial interaction between fibers and soil-cement particles[54]. Fig. 3-20 shows the difference between the surface of raw fiber (Fig. 3-20a and b) and the surface of fiber in specimens after a 7-day cure (Fig. 3-20c, d, and e). It could be seen that when adding fiber to cemented soil, soil-cement particles attach to the surface of fibers. This interfacial interaction produces bonding strength between fibers and soil-cement particles for improving the resistance of specimens to the applied load. Moreover, the random

distribution of fiber in the specimen creates a fiber network to interlock soil-cement particles as can be seen in Fig. 3-21. As a result, the interlocking force limits the movement of fibers and soil-cement particles in the specimen under loading. Besides, in this study, failure strength of fiber-cement stabilized soil is enhanced with the increase in fiber content. It may happen due to the increase of fiber density in the fiber network and the contact area between fibers and soil-cement particles. These lead to the enlargement of interlocking force and bonding strength to improve strength. However, the effect of fiber on failure strength of cemented soil at high cement content is insignificant. It could be explained by the fact that when increasing the volume of cement, cement products become predominant in quantity and quality as compared with fiber in the sample [23, 59].

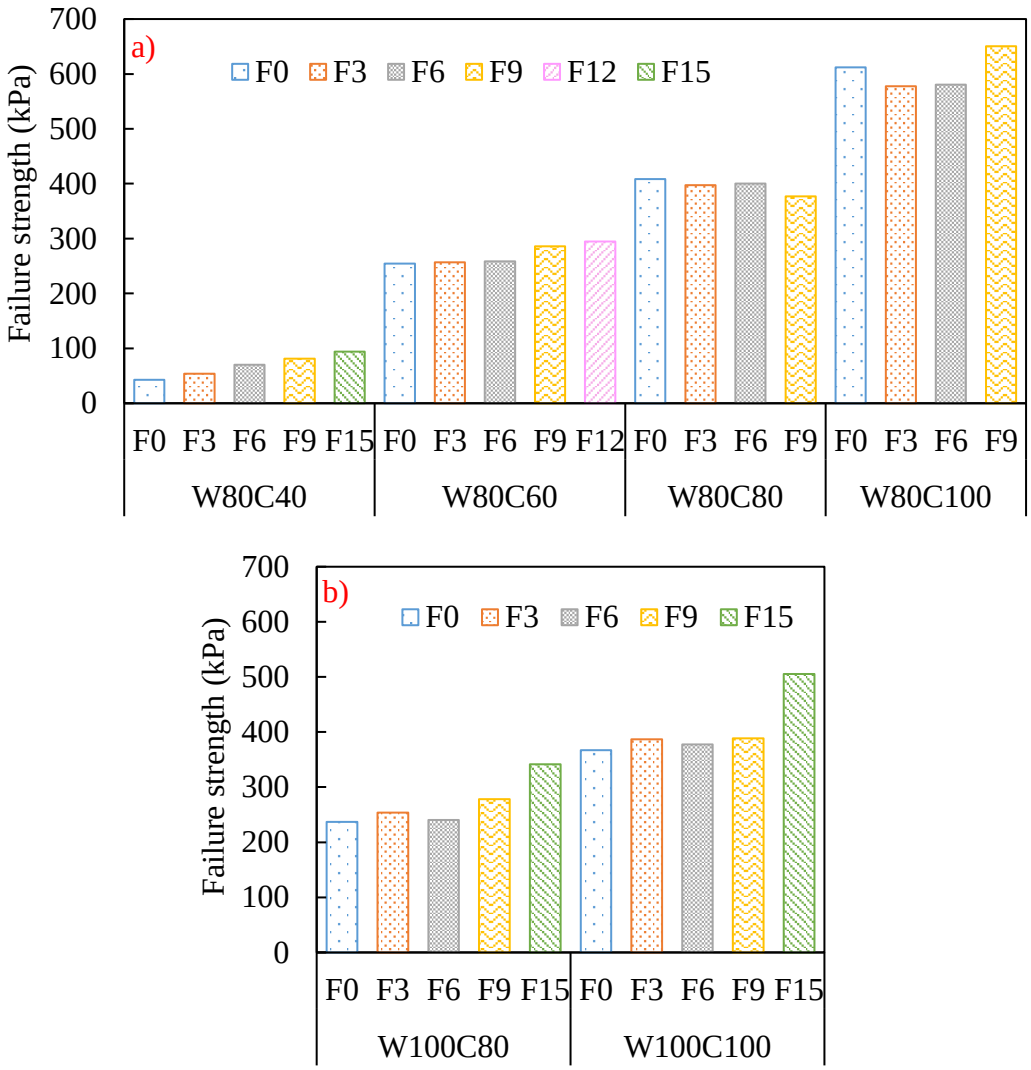

Fig. 3-19 Failure strength according to cement content and fiber content

a) Water content 80%; b) Water content 100%

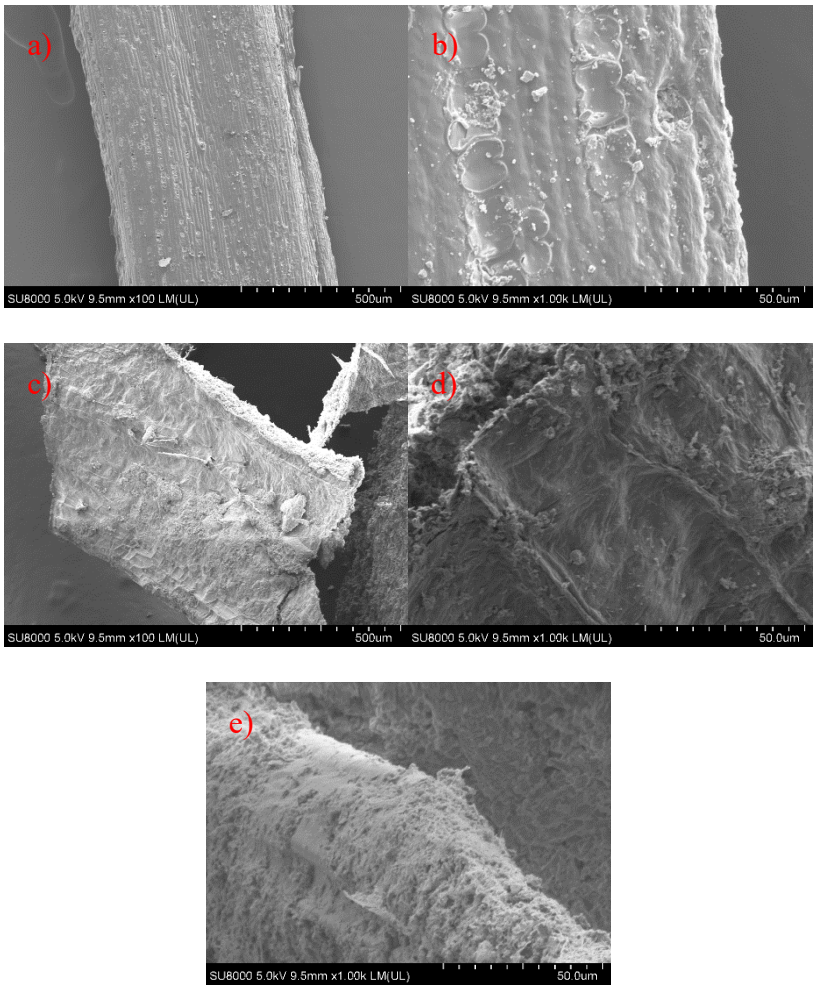

Fig. 3-20 SEM images of fiber-reinforced cemented soil

a and b) Surface of raw fiber;

c, d and e) The attachment of soil-cement particles to the surface of fiber

Fig. 3-21 Microscope image of fiber-reinforced cemented soil

3.4.3.3 Stiffness

Stiffness indicates the resistance of specimens to bending. In this study, stiffness value is derived from the ratio of compressive stress value to corresponding strain value. Fig. 3-22 indicates that the stiffness value tends to diminish according to the increase in strain. Hence, peak stiffness occurs at an initial phase when the load is applied to the specimen. This result has been shown in the previous study [89]. Besides, stiffness value decreases quickly at the early phase and gradually declines at the final phase. In the cases of 80% water content and 40 kg/m^3 cement content in Fig. 3-22a, stiffness is enhanced with the increase in fiber content at the same strain value. For the other cases of W80 (Fig. 3-22b, c, and d), at the same cement content, there is an insignificant difference in stiffness at the early phase when adding different fiber content, fiber inclusion affects stiffness at the final phase. For 100% water content (Fig. 3-22e and f), the improvement effect of fiber on stiffness-strain curve is shown in all phases and stiffness value increases with the increase in fiber content for a given strain.

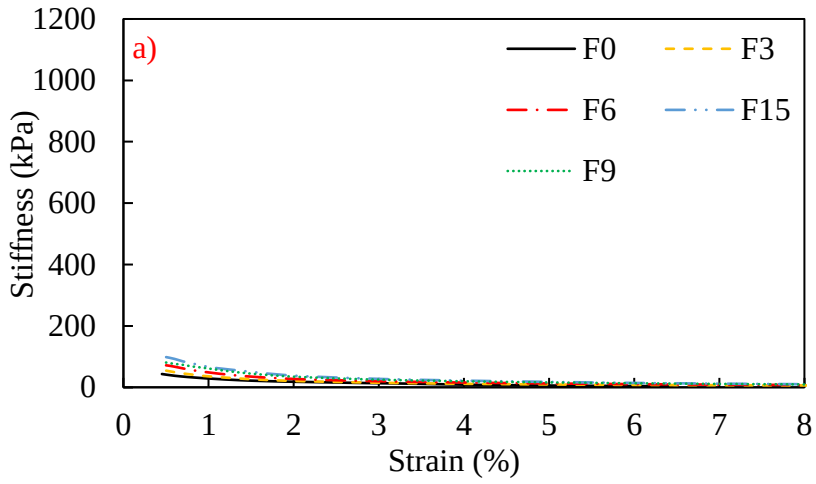
a)
F0
F3
F6
F15
F9
Stiffness (kPa)
Strain (%)

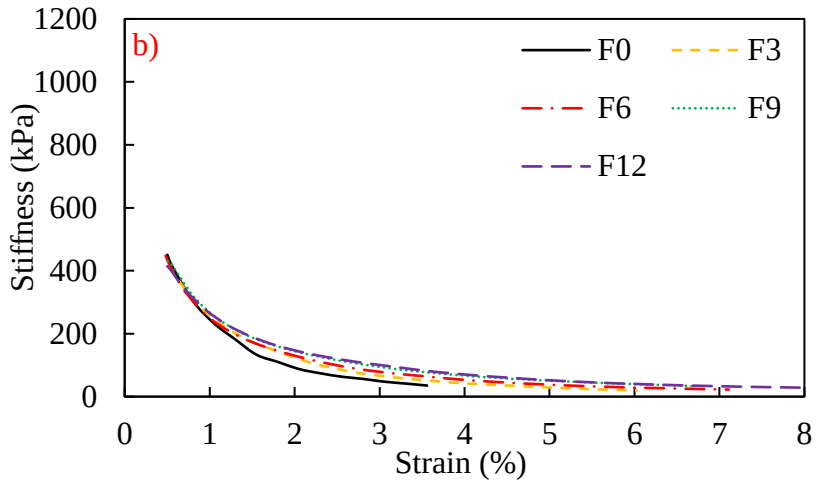
b)
F0
F3
F6
F9
F12
Stiffness (kPa)
Strain (%)

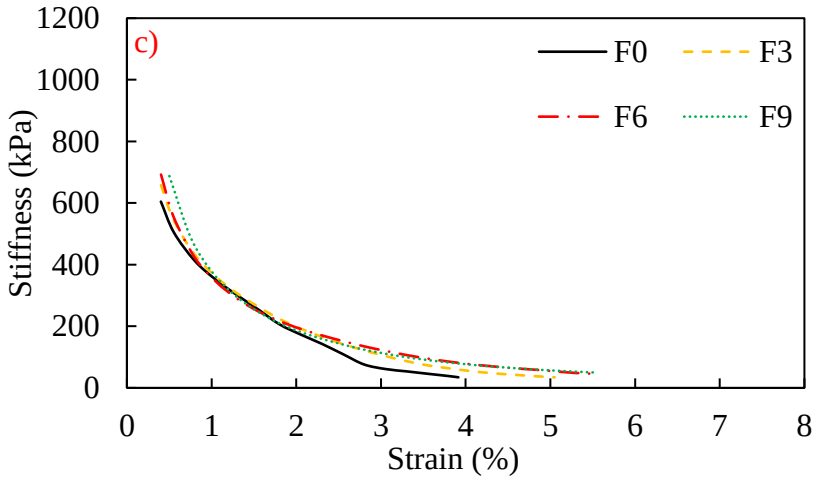
c)
F0
F3
F6
F9
Stiffness (kPa)
Strain (%)

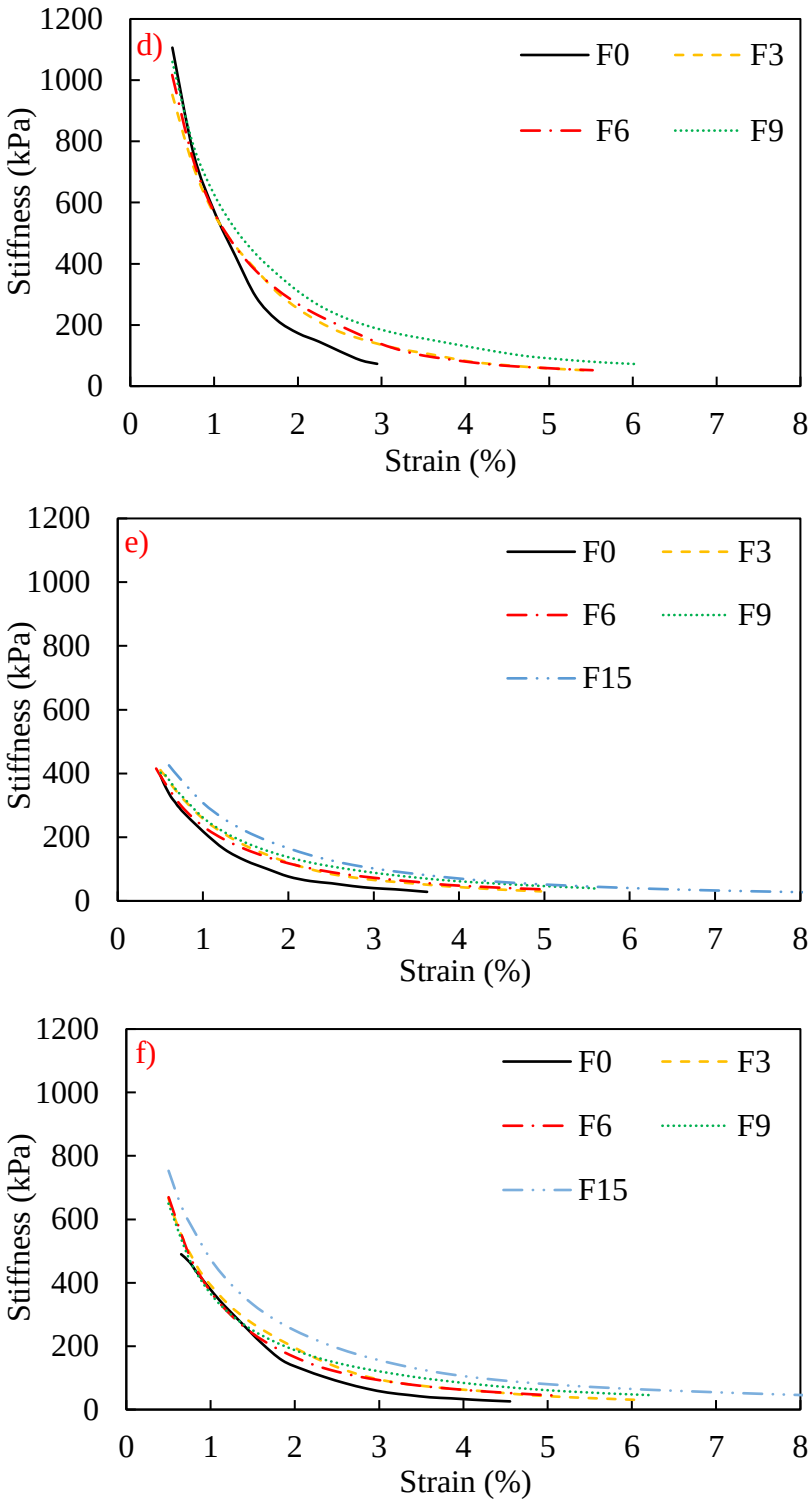

Fig. 3-22 Typical stiffness-strain curves

a) W80C40; b) W80C60; c) W80C80; d) W80C100; e) W100C80; f) W100C100

3.4.3.4 Energy absorption

Energy absorption represents the energy specimen absorbed to destroy itself. In this study, energy absorption equals the total area under the stress-strain curve from origin to given strain values as display in Fig. 3-23. Fig. 3-24 shows the development of energy absorption according to strain. It is seen that energy absorption increases with the development of strain. Besides, the improvement effect of fiber on energy absorption is gradually clear according to the increase in strain. At the same strain, energy absorption is improved with the increase of fiber content.

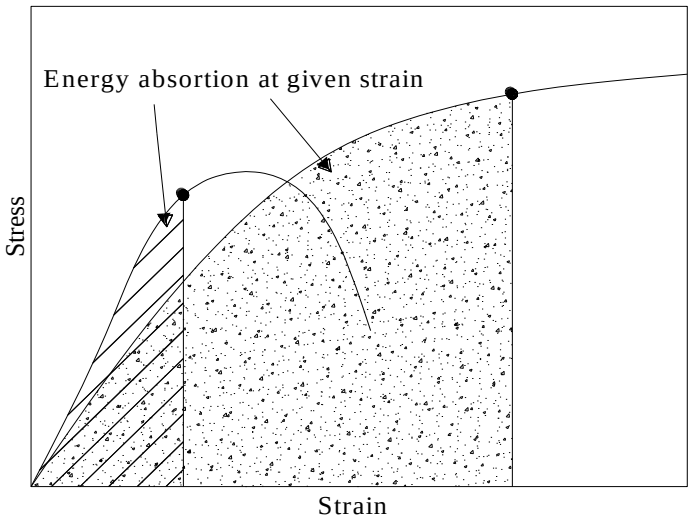

Fig. 3-23 Definition of energy absorption

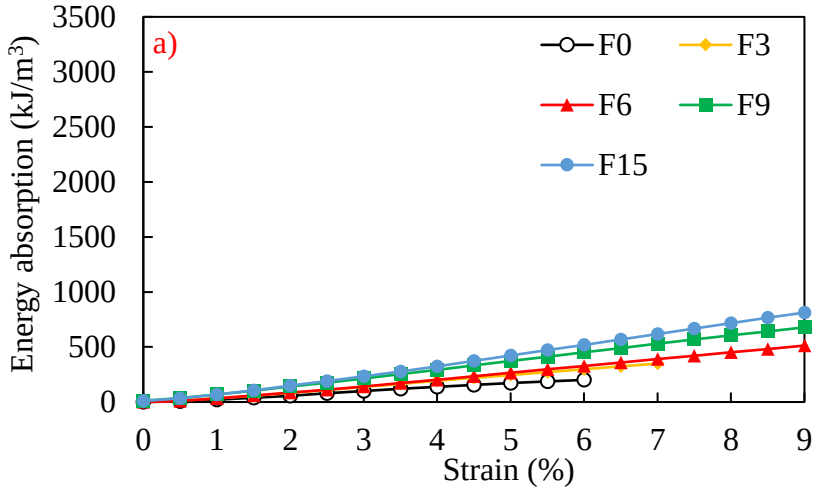
a)
F0
F3
F6
F9
F15
Energy absorption (kJ/m3)
Strain (%)
0
500
1000
1500
2000
2500
3000
3500
0
1
2
3
4
5
6
7
8
9

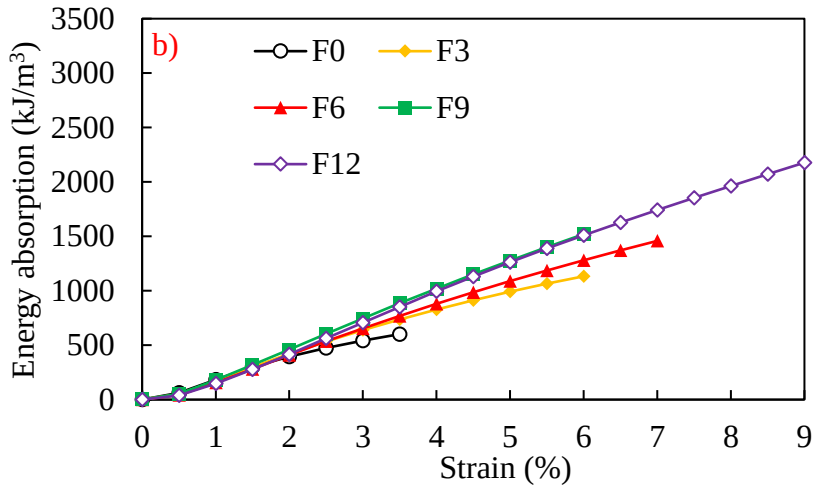
b)
F0
F3
F6
F9
F12
Energy absorption (kJ/m3)
Strain (%)
0
500
1000
1500
2000
2500
3000
3500
0
1
2
3
4
5
6
7
8
9

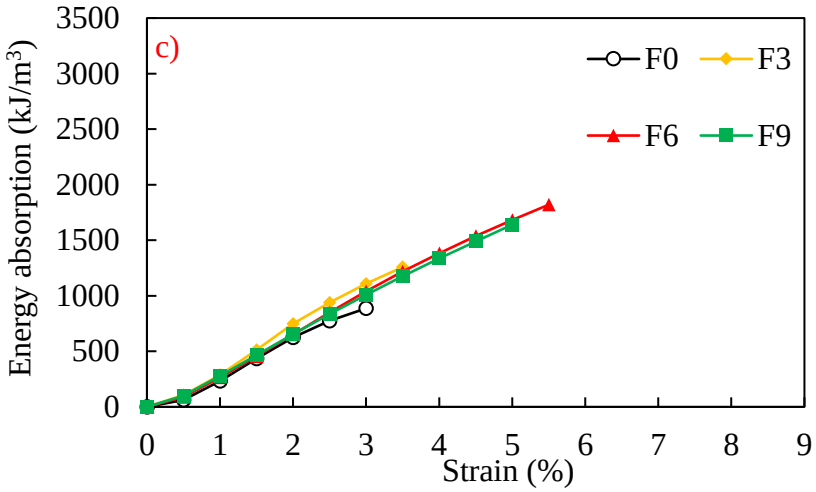
c)
F0
F3
F6
F9
Energy absorption (kJ/m3)
Strain (%)
0
500
1000
1500
2000
2500
3000
3500
0
1
2
3
4
5
6
7
8
9

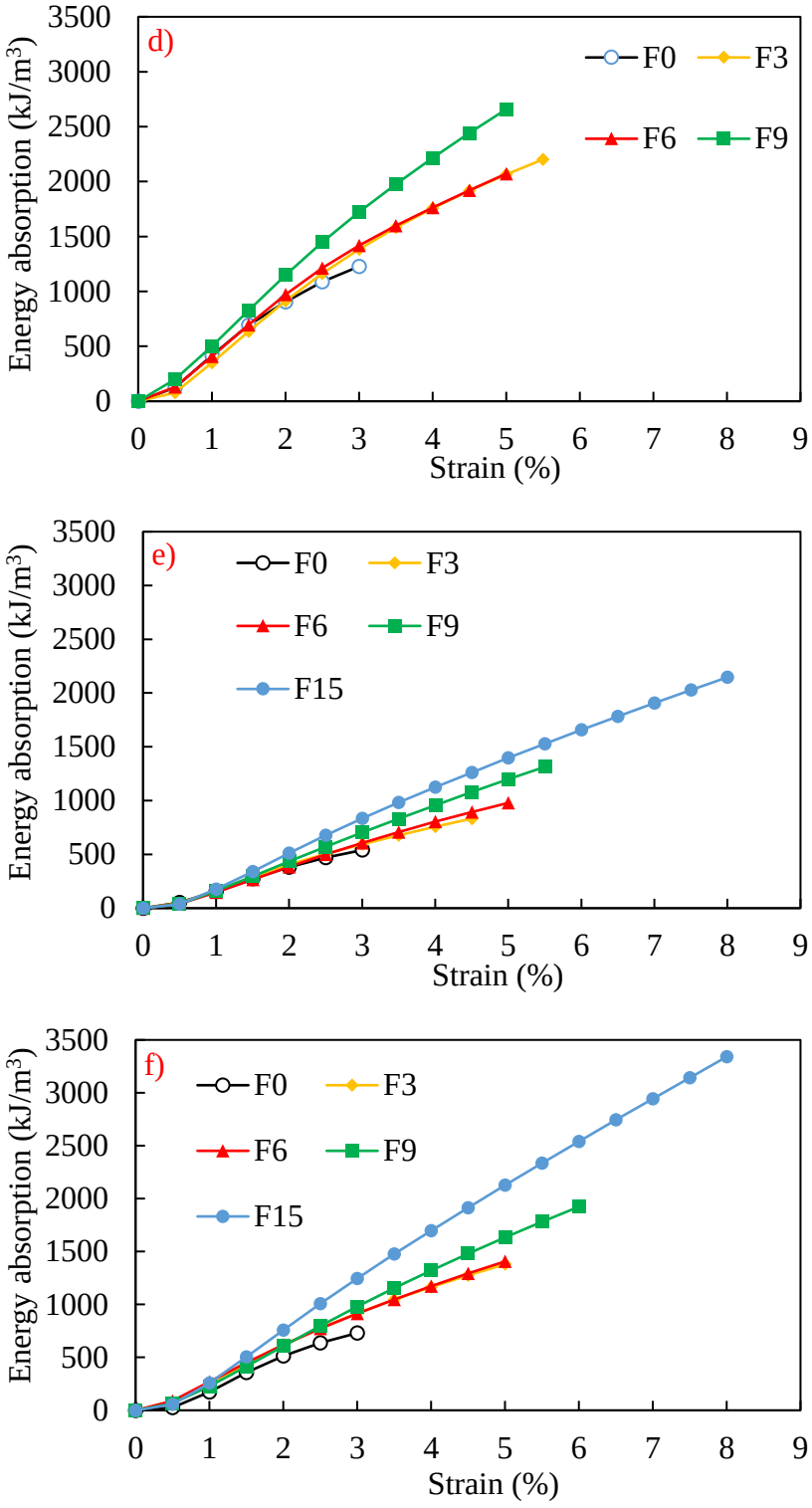

Fig. 3-24 Typical energy absorption-strain curves

a) W80C40; b) W80C60; c) W80C80; d) W80C100; e) W100C80; f) W100C100

3.4.4 Splitting tension test

3.4.4.1 Splitting tensile stress-strain curves

Typical tensile stress-strain curves of splitting tension test are displayed in Fig. 3-25. The plot depicts that from the origin to the peak point, the curve is linear up. The increase in tensile stress is proportional to the increase in diametric strain. After the peak point, tensile stress of cemented specimens abruptly drops (excepting W80C40). Meanwhile, with fiber inclusion, loss of post-peak tensile stress decreases gradually. Especially, in the mixing conditions of fiber content from 6 kg/m^3, the second peak point (second tensile strength) appears after the first peak point (excepting W80C40) and increases with increasing fiber content. In some cases, such as W80C60F6, W80C60F9, W80C60F12, W80C80F9, W100C80F6, W100C80F9, W100C80F15, and W100C100F15, second tensile strength is higher than the strength at the first peak point. The appearance of second tensile strength could be interpreted that stress transfers across the crack by the presence of fibers. These fibers play a role as bridges to connect two parts of the specimen which are split by the main crack as can be seen in Fig. 3-26 [90, 91]. Therefore, after the first cracks, fibers carry the load and prevent the crack's extension. The improvement of second tensile strength relates to the number of fibers presenting at the potential crack plane (the vertical plane from the upper strip to the lower strip). The greater fiber inclusion leads to a higher presence probability of fiber at the crack area. Hence, the increase in fiber content results in the enhancement of second tensile strength.

The crack morphology of specimens with 100% water content, 80 kg/m^3 cement, and fiber from 0 to 9 kg/m^3 is displayed in Fig. 3-27. The addition of fiber makes a contribution to the change of crack pattern form from the quite smooth crack form of the specimen without fiber (Fig. 3-27a) to the zigzag pattern form of the specimen with fiber inclusion (Fig. 3-27b, c, and d). Moreover, the increase in fiber content leads to a smaller width and a more zigzag form of crack.

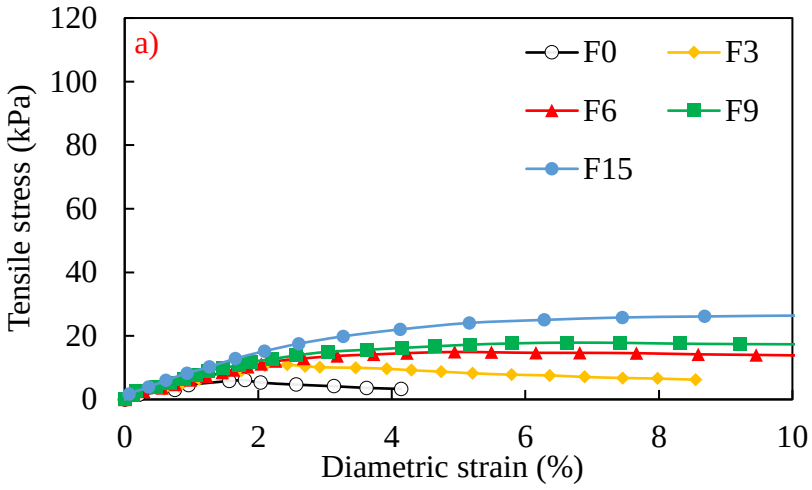
a)
F0
F3
F6
F9
F15
Tensile stress (kPa)
Diametric strain (%)
0
20
40
60
80
100
120
0
2
4
6
8
10

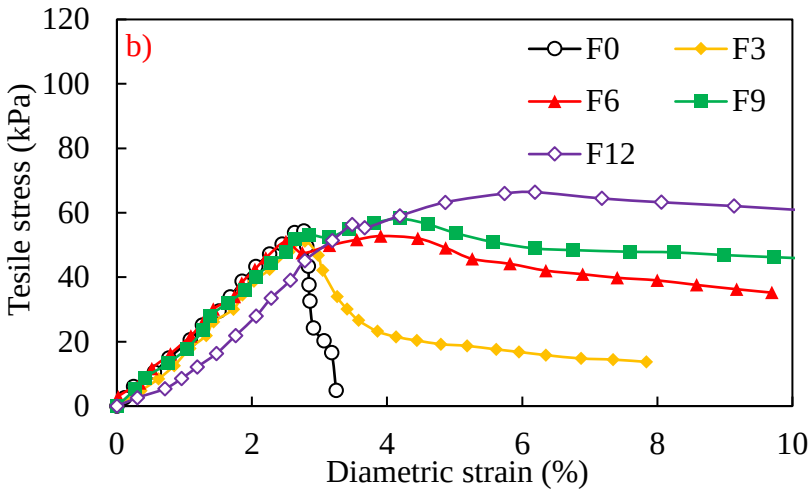
b)
F0
F3
F6
F9
F12
Tesile stress (kPa)
Diametric strain (%)
0
20
40
60
80
100
120
0
2
4
6
8
10

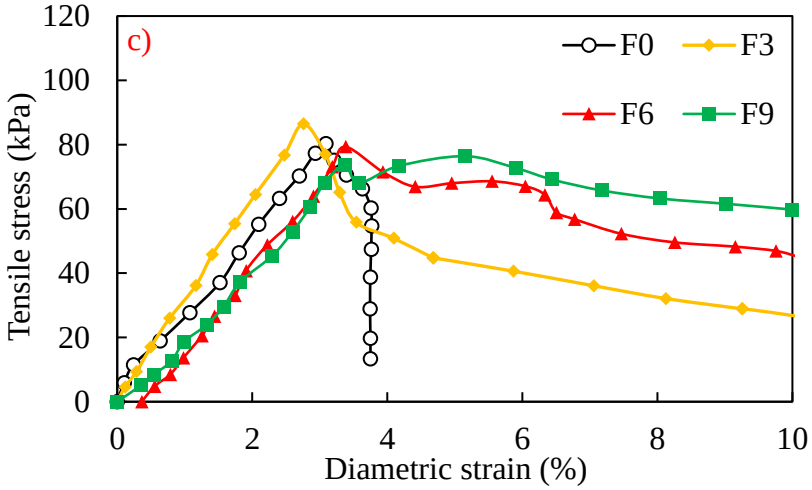
c)
F0
F3
F6
F9
Tensile stress (kPa)
Diametric strain (%)
0
20
40
60
80
100
120
0
2
4
6
8
10

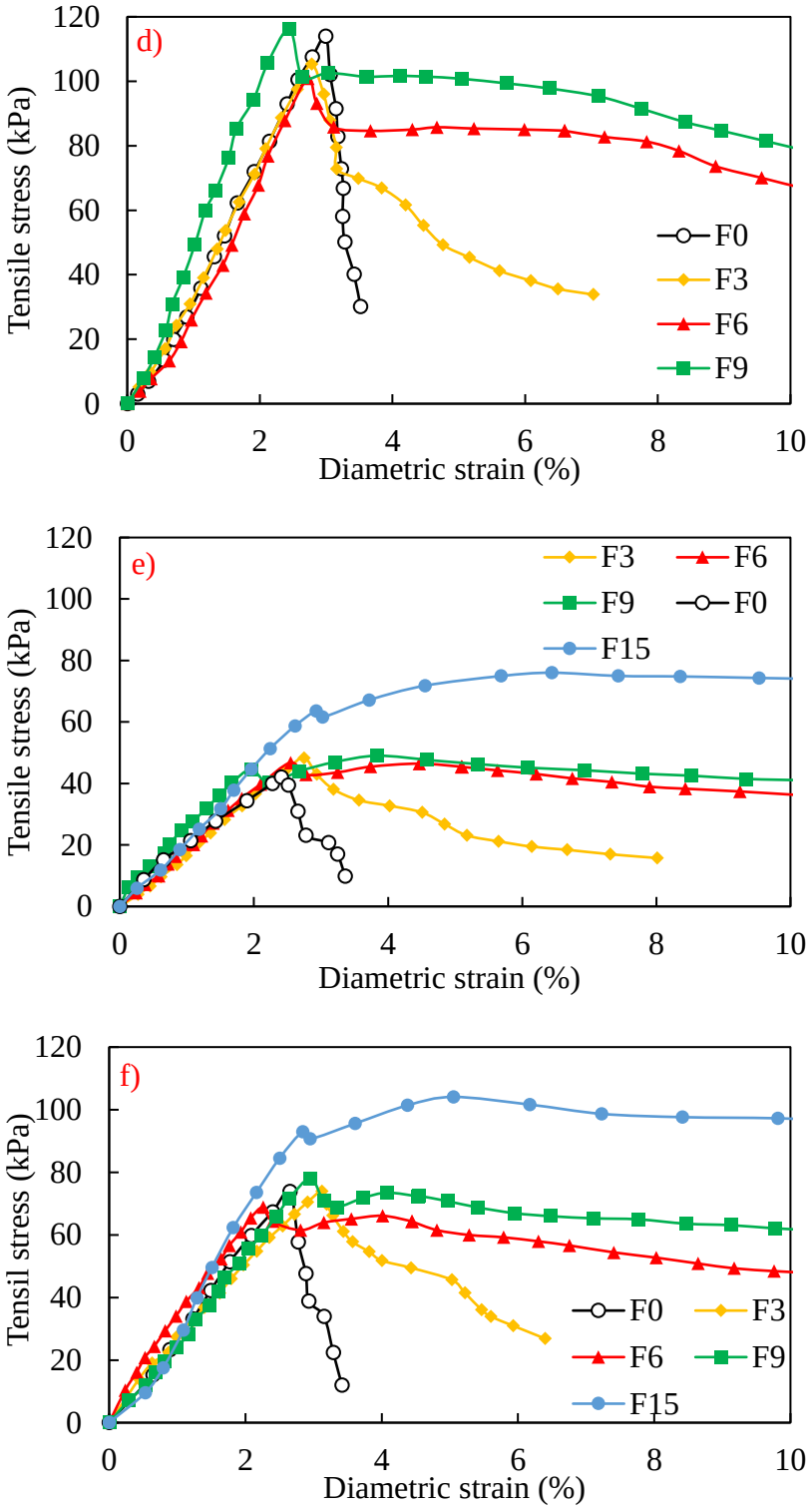

Fig. 3-25 Typical tensile stress-strain curves from splitting tension test

a) W80C40; b) W80C60; c) W80C80; d) W80C100; e) W100C80; f) W100C100

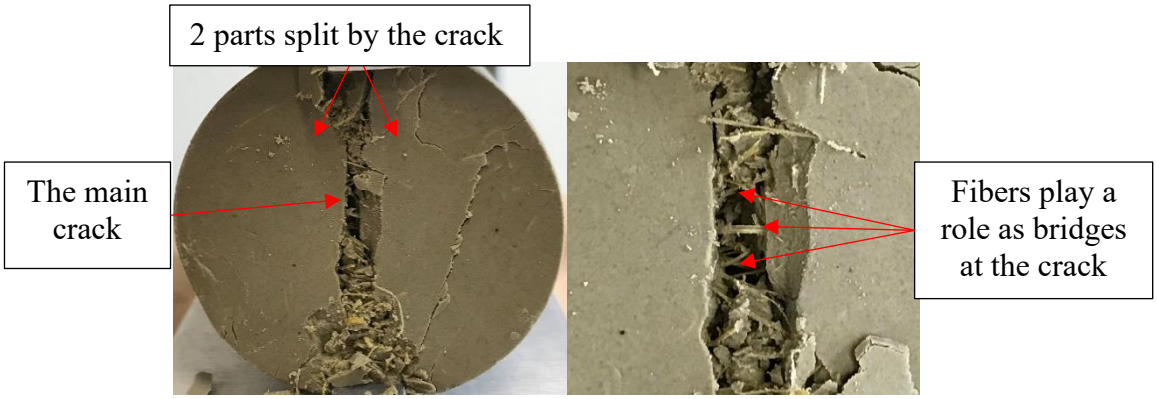

Fig. 3-26. The presence of fibers at the crack

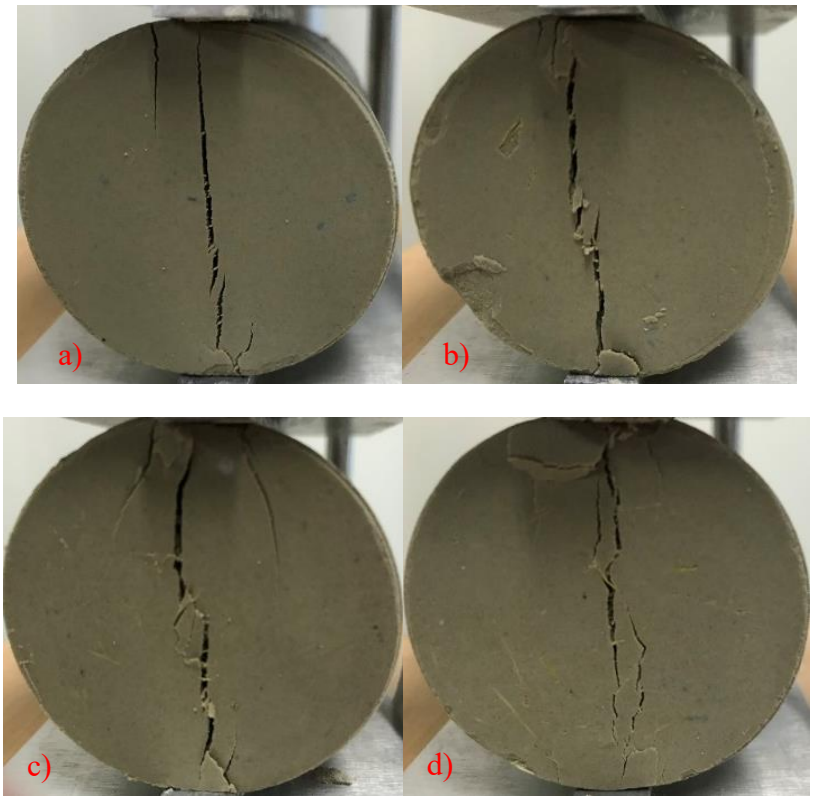

Fig. 3-27 Crack patterns of specimens from splitting tension test

a) W100C80F0; b) W100C80F3; c) W100C80F6; d) W100C80F9

3.4.4.2 Splitting tensile strength

Fig. 3-28 plots the relationship between fiber content and tensile strength (first tensile strength). The results depict that for specimens of W80C40, the effect of fiber on failure strength and tensile strength is the same. The use of fiber improves tensile strength of cemented soil. The increase in fiber from 3 to 15 kg/m^3 leads to the increase in tensile strength of cemented specimens from 79% to 330%. By contrast, with higher cement content, the inclusion of fiber from 0 to 12 kg/m^3 for W80C60 and from 0 to 9 kg/m^3 for other cases

insignificantly affects tensile strength. When adding more fibers (15 kg/m^3) to W100C80 and W100C100, tensile strength increases 49% and 24% in comparison with that of specimens without fiber, respectively.

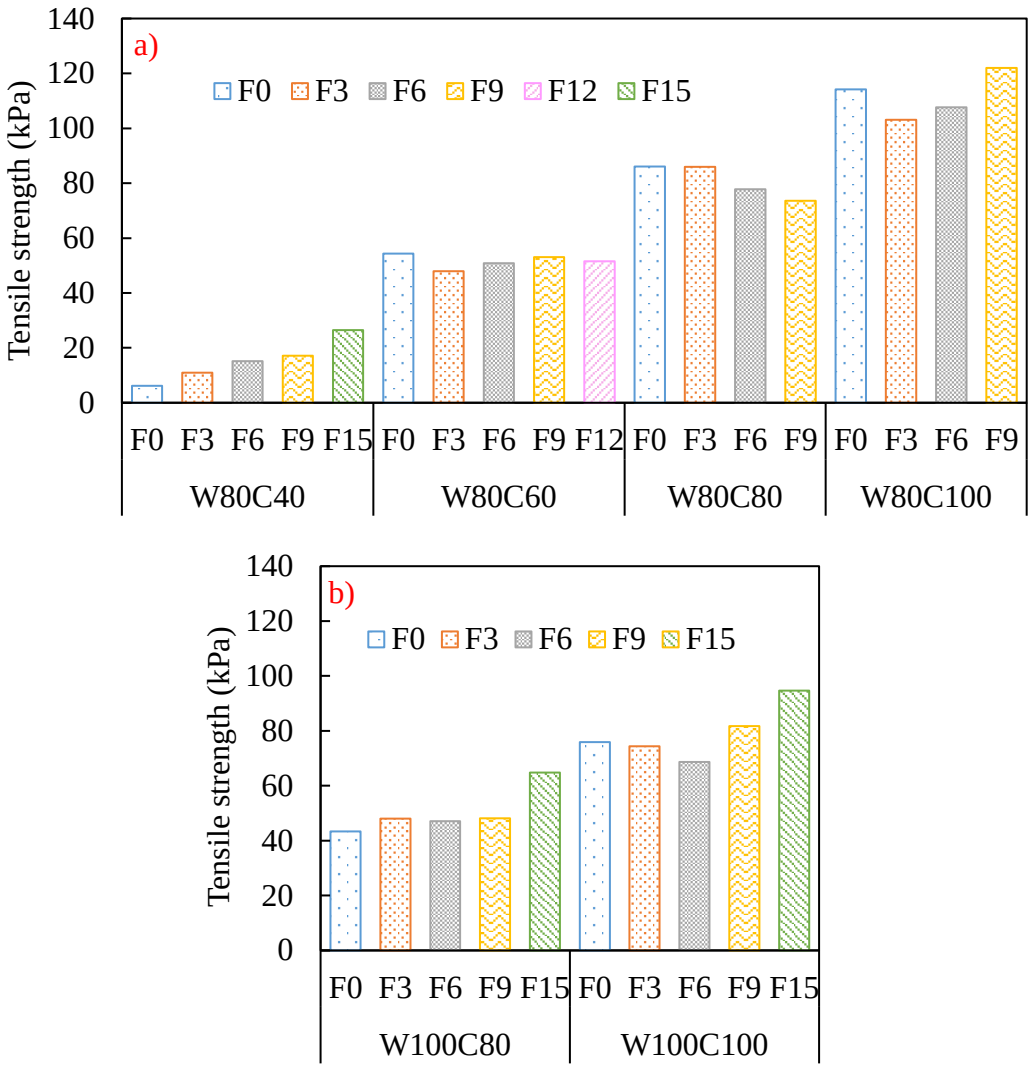

Fig. 3-28 Tensile strength according to cement content and fiber content

a) Water content 80%; b) Water content 100%

3.4.5 Durability

The soundness evaluation of specimens after 0, 2nd, 6th, and 10th cycle of drying and wetting is presented in Fig. 3-29. From the figure, it is clear that there is a significant difference in durability between specimens with and without fiber inclusion. Cemented specimens in cases of W80C60F0 and W100C80F0 gradually appear and extend the cracks from the first cycle. They are completely broken after 9th and 10th cycle, respectively. The cracks and

destruction strongly take place in the upper part of specimens (Fig. 3-30a and c). It may happen due to the segregation phenomenon of material. Fig. 3-9 shows the segregation phenomenon of the mixture after 3 hours. Due to high water content in the soil, the solid ingredients go down to the lower part, and water goes up to the upper part. Therefore, it is easier for shrinkage cracks to appear and develop in the upper part under drying and wetting cycle. However, for the case of W80C60F12 and W100C80F15, specimens experience 10 cycles of drying and wetting without significant damage (Fig. 3-30b and d). The presence of fiber leads to the limitation of crack appearance and propagation in these cases.

Fig. 3-31 shows the change of failure strength versus drying and wetting cycle number. It is observed that with 100% water content, failure strength of specimens decreases slightly under drying and wetting cycle. Failure strength declines 21% after 10^{th} cycle and 5% after 6^{th} cycle concerning specimens with and without fiber inclusion. For the case of 80% water content, failure strength decreases 29% after 10^{th} cycle and 22% after 6^{th} cycle for specimens with and without fiber inclusion, respectively.

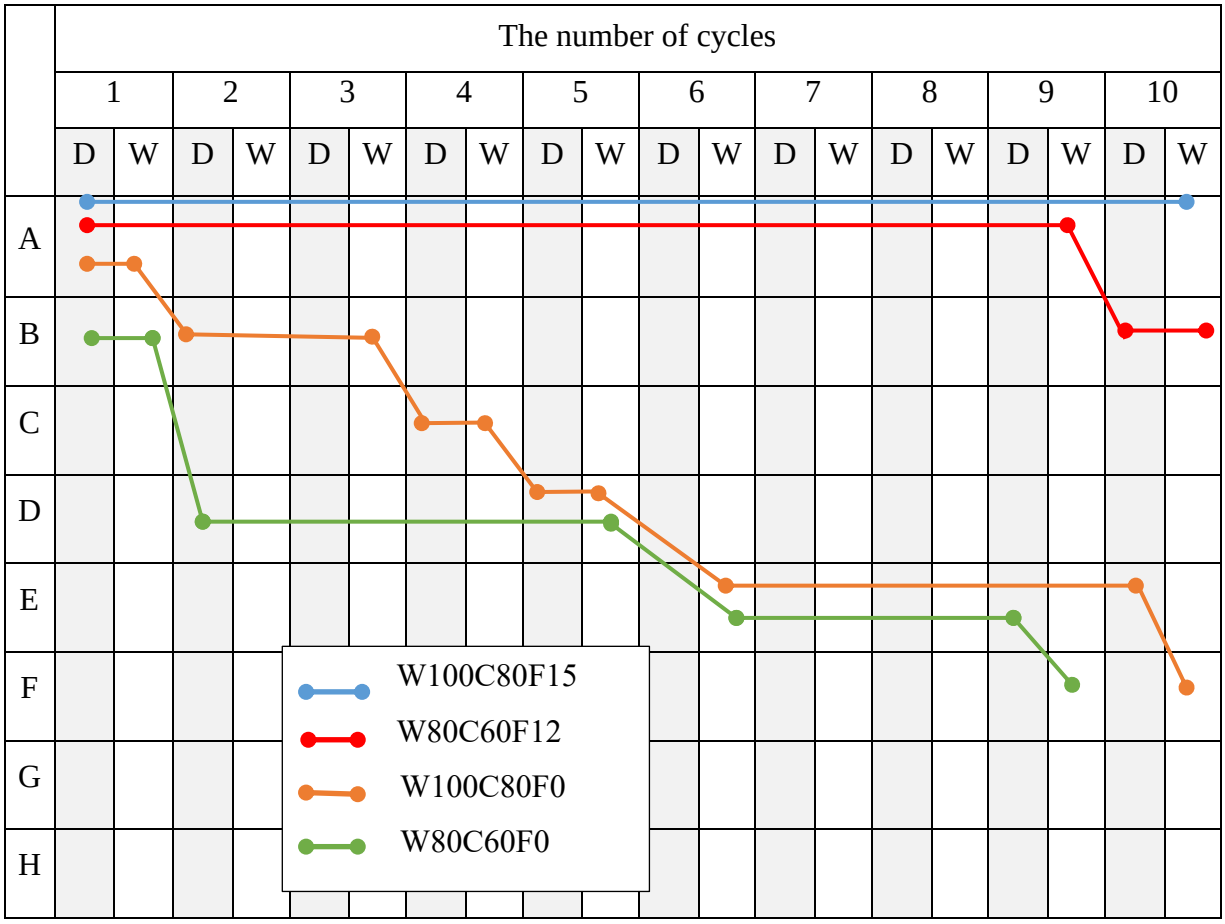

Fig. 3-29 The soundness evaluation under cycles of drying (D) and wetting (W)

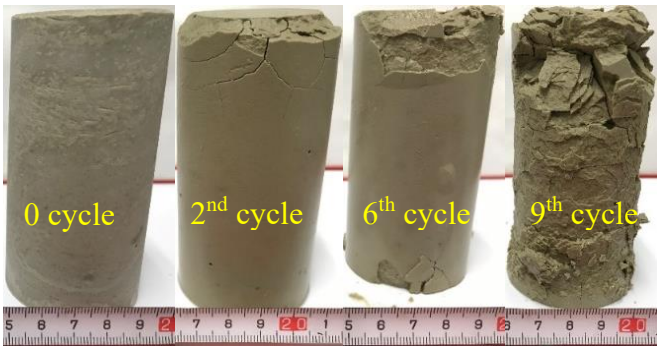

a) W80C60

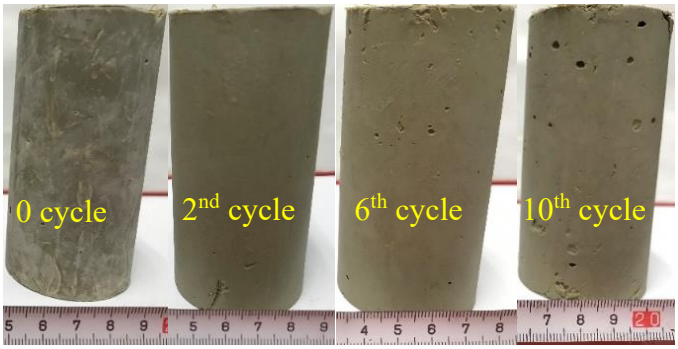

b) W80C60W12

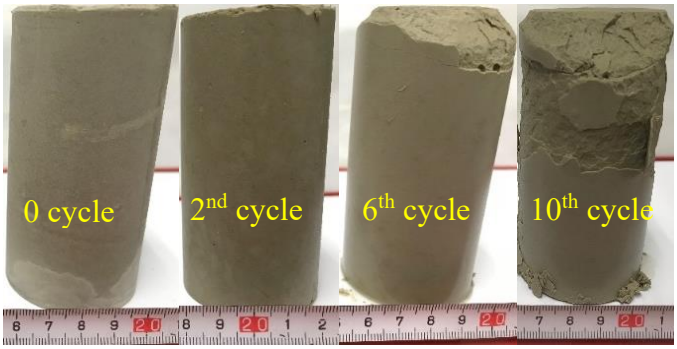

c) W100C80

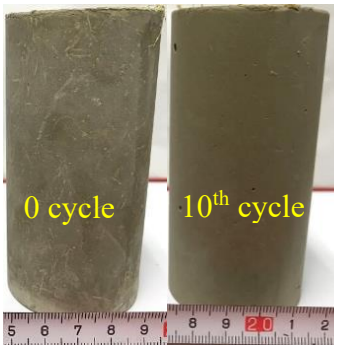

d) W100C80F15

Fig. 3-30 Specimen status throughout cyclic tests for drying and wetting

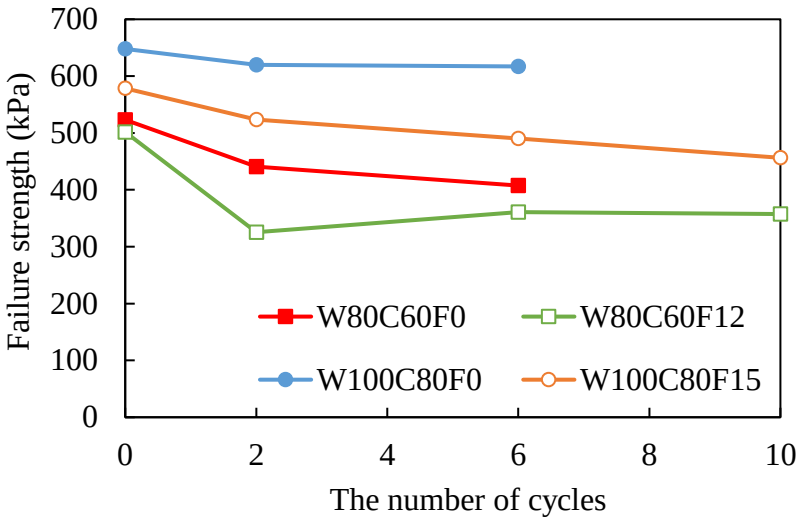

Fig. 3-31 Failure strength of specimens throughout cyclic tests for drying and wetting

3.4.6 Relationship between tensile strength and failure strength

Fig. 3-32 shows the relationship between failure strength and tensile strength of cemented specimens and fiber-cement stabilized specimens with various water, cement, and fiber contents. The figure simulates that tensile strength increases with the increase in failure strength. This result is in line with a previous study [92]. It is observed that the points are not scattered and closely concentrate along the straight line. Besides, tensile strength and failure strength perform a very strong linear relationship with a coefficient of 0.191 and a correlation coefficient of 0.99.

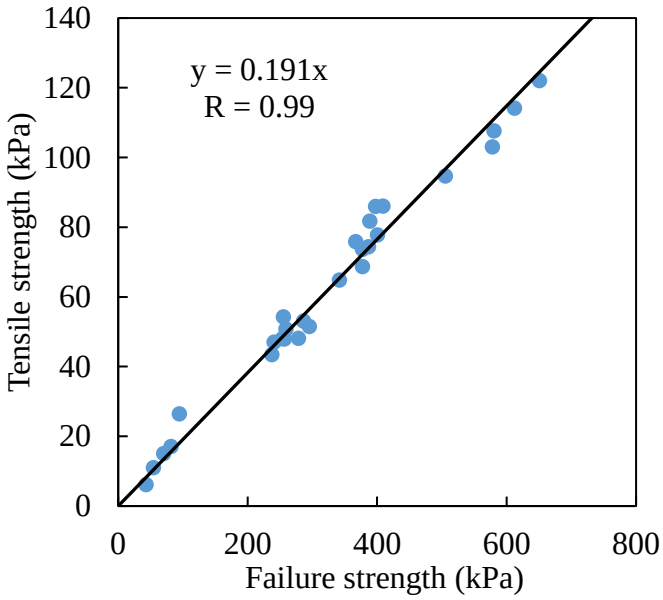

Fig. 3-32 Relationship between failure strength and tensile strength

3.5 Conclusions

The objective of this chapter is to investigate the effect of corn husk fiber on the properties of cemented soil with high water content. Five laboratory experiments including bleeding, flow, unconfined compression, splitting tension, and durability tests are conducted. Besides, tensile strength of corn husk fiber is studied to understand more clearly corn husk property. The experimental results are briefed below.

- Tensile strength of corn husk fiber decreases and initial modulus increases with the increase of gage length. However, the cross-sectional area of fiber has a trivial impact on tensile strength and initial modulus.

- Fiber and cement inclusion contribute to the reduction of bleeding ratio and flow value. For bleeding test, all mixtures with 80% water content satisfy the target value of bleeding ratio. With mixtures of 100% water content, bleeding rate of admixture with 80 and 100 kg/m^3 cement is less than 1% when fiber content is from 6 and 9 kg/m^3, respectively. For flow test, all mixing conditions obtain the target value.

- At water content of 80% and cement content of 40 kg/m^3, tensile strength and failure strength of cemented specimens increase from 79% to 330% and from 26% to 119% when adding fiber from 3 to 15 kg/m^3, respectively. For higher cement content, the addition of fiber changes failure strength and tensile strength slightly.

- In cases of W100C80, and W100C100, the addition of fiber from 15 kg/m^3 increases failure strength 44% and 38%, respectively. As for tensile strength, when adding fiber of 15 kg/m^3 to W100C80 and W100C100, tensile strength increases 49% and 24% in comparison with that of specimens without fiber, respectively.

- Corn husk inclusion makes a contribution to the decrease of loss of post-peak stress of cemented soil.

- The second tensile strength appears due to the presence of corn husk fiber.

- In cases of W80C40 and all cases of admixtures with 100% water content, stiffness increases with increasing fiber content for a given strain value. For the other cases, the effect of fiber on stiffness-strain curves is presented in the final phase of the curve.

- The more strain increases, the more clearly the effect of fiber on energy absorption shows. The increase in fiber content leads to an increase in energy absorption.

- Specimens with fiber inclusion experience 10 cycles of drying and wetting with slight damage. In contrast, specimens without fiber inclusion are gradually broken during durability tests.
- A strong linear relationship is confirmed between tensile strength and failure strength values.

CHAPTER 4

STUDY ON MECHANICAL PROPERTIES OF CORN HUSK FIBER-CEMENT STABILIZED SOIL WITH LOW WATER CONTENT PRODUCED BY FIBER-CEMENT STABILIZED SOIL METHOD

4.1 Introduction

In developing countries like Viet Nam, the economy grows at a high speed and the living standard has been improving year by year. Therefore, more and more infrastructure has been being built to facilitate the development of economics such as the metro system, highway, high-rise building, etc. Consequently, a huge amount of excavated soft soil is produced from construction projects. However, it is unsuitable to directly reuse this soft soil again in construction (i.e., pavement, embankment, etc.) due to its poor strength properties, so soft soil becomes solid waste from construction. To cope with this issue, soil stabilization methods are developed to improve soft soil properties for reusing. Currently, mechanical stabilization, chemical stabilization, and mechanical-chemical stabilization method are the popular methods for soil stabilization.

In the chemical stabilization method, several kinds of chemical additives have been used to stabilize soft soil, for example, cement, lime, fly ash, rice husk ash, silica fume, meta-kaolin [12, 93–100]. These binders play an important role to enhance soft soil characteristics (i.e., tensile strength, failure strength, energy absorption, shear strength, stiffness, modulus, etc.) via the formation of cementitious products from a pozzolanic reaction in the soil matrix. However, the application of this method for soil improvement results in the increase of the brittleness of soil which leads to the sudden decline of structure. As for mechanical stabilized method, there are many approaches to improve soil properties such as compaction, fibrous reinforcement, etc. In mechanical stabilization method, the use of randomly distributed discrete fiber is the most popular over a few past decades. This method possesses many advantages such as limiting potential weak planes and no impact on the environment [55]. Both synthetic fiber (i.e., polypropylene, polyethylene terephthalate, polyester, scrap tire rubber fiber, etc.) [19, 101–104] and natural fiber (i.e., jute, sisal, hemp, oil palm fiber, rice straw, corn silt, rice husk, hay fiber, bagasse fiber, coconut fiber, etc.) [32, 44, 56, 71, 105–108] have been used for reinforcement in the approach of randomly distributed discrete fiber. Due to the addition of fiber, the mechanical behaviors of fiber-reinforced soil are much better than that of bare soil with the improvement of failure strength, tensile strength, energy absorption, ductility, etc. Unfortunately, it is difficult for fiber-reinforced soil to meet the requirement of many structures such as high compressive, high tensile strength, high durability, high stiffness, etc. As described above, both chemical and mechanical methods have weak points for soil improvement, so the combination of these two methods named the

mechanical-chemical method is developed. The combination method with the addition of both fiber and chemical additives is a perfect method for soil improvement due to the elimination of undesirable behaviors of modified soil produced from the separated method. In this method, fiber-cement stabilized soil is the most well-known and has been focused on by many researchers [22, 23, 29, 73–75, 91, 109–111].

Nowadays, in the construction field, the lack of eco-friendly materials receives more attention due to the high-speed degradation of the environment. Therefore, from an environmental viewpoint, natural fibers, especially by-products from agriculture, need to be utilized in Fiber-Cement Stabilized Soil methods to reduce environmental issues.

Therefore, this chapter focuses on the characteristics of corn husk fiber-reinforced cemented soil under the compacted condition in terms of unconfined compression, splitting tension, direct tension, and shear box tests. The workability of corn husk fiber is evaluated based on the influence of fiber length and fiber content on failure strength, energy absorption, secant modulus, splitting tensile strength, direct tensile strength, shear strength, cohesion, and angle of internal friction of cemented soil with different cement contents.

4.2 Materials

4.2.1 Soil

The imitated dry soil No. 1 is used in this chapter. It consists of 40% Kasaoka clay and 60% silt. The grain size distribution, properties of dry sludge are shown in Section 2.2.1.

4.2.2 Cement

Geoset 200 cement is used. The chemical and physical properties of cement are summarized in Section 2.2.2.

4.2.3 Fiber materials

Corn husk fiber is applied in this chapter. To extract fiber from raw corn husk, the segments of raw corn husk with 10 mm and 30 mm long are cut and blended with water to fibrous form. The wet fibers are dried before use (Fig. 4-1). The sizes of dry fiber are 0.32 mm in average longest diameter and 9.1 mm in average length for 10 mm segments, and 0.35 mm in average longest diameter and 23.4 mm in average length for 30 mm segments. The longest diameter and length distribution of 10 mm and 30 mm segments are provided in Fig. 4-2 and

Fig. 4-3, respectively. The chemical composition and other properties of corn husk fiber are listed in Section 2.2.3.

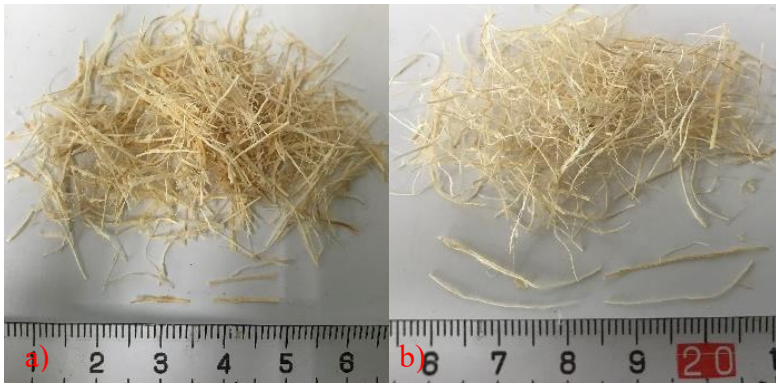

Fig. 4-1 Corn husk fiber

a) 10 mm; b) 30 mm

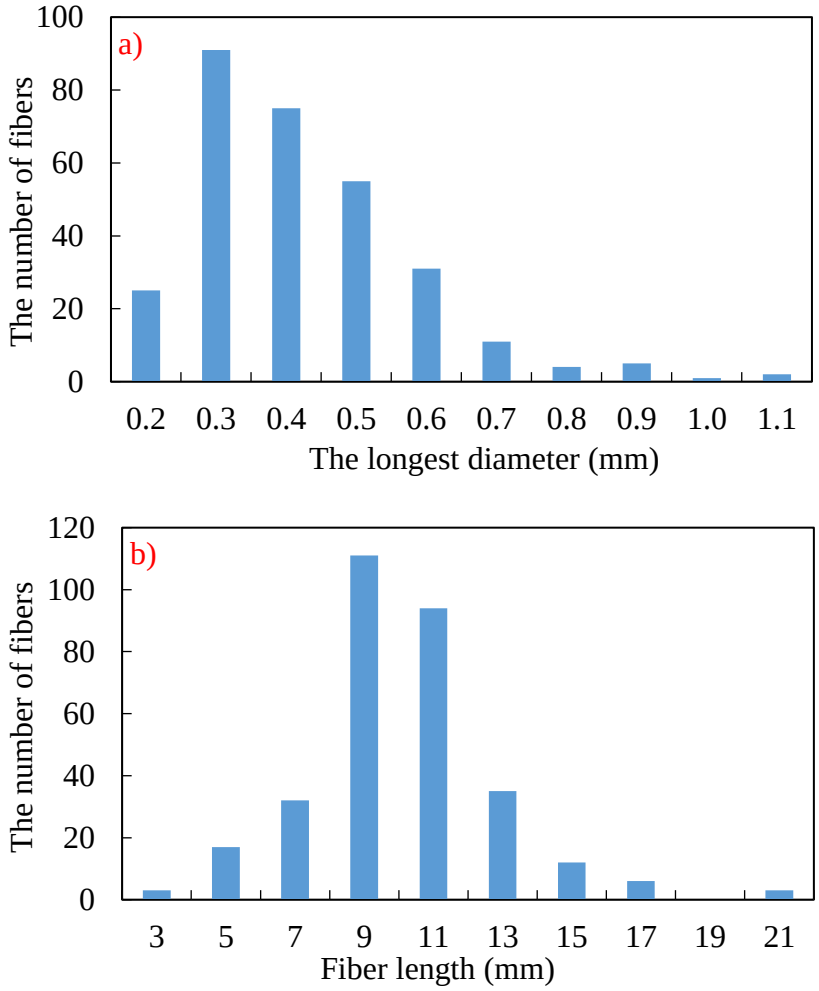

Fig. 4-2 The longest diameter and length distribution of 10 mm corn husk fiber

a) The longest diameter distribution; b) Length distribution

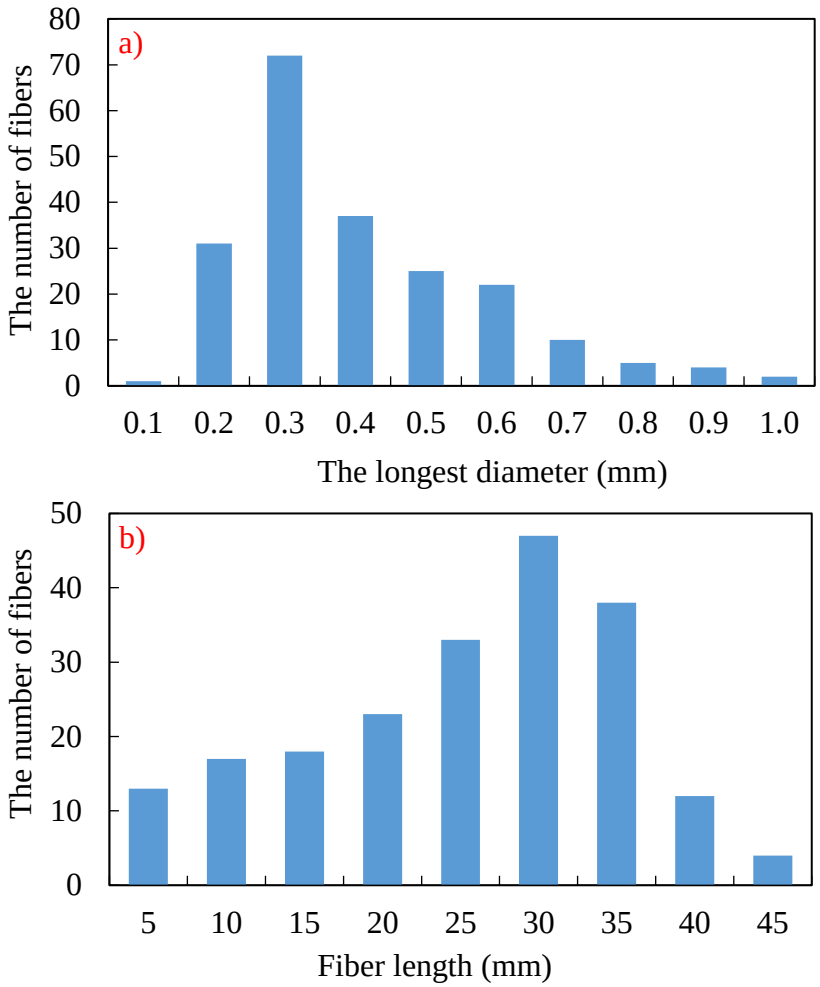

Fig. 4-3 The longest diameter and length distribution of 30 mm corn husk fiber

a) The longest diameter distribution; b) Length distribution

4.3 Specimen preparations

4.3.1 Specimen preparation apparatus

- Mixing machine

The mixing machine used to prepare the mixture is shown in Section 2.3.1

- Mold

The mold with 100 mm in height and 50 mm in inside diameter is used to make specimens for unconfined compression test, splitting tension test as shown in Section 2.3.1.

The mold used for direct tension test is an 8-shaped mold. The shape and dimension of mold for making specimens are presented in Fig. 4-4.

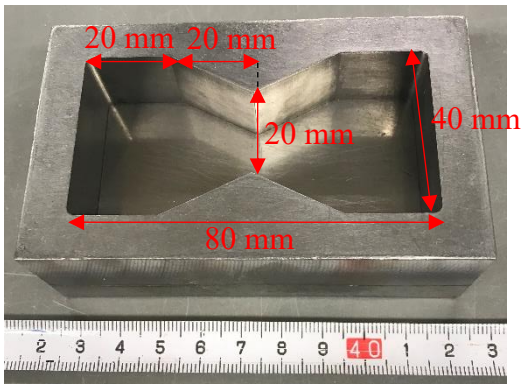

Fig. 4-4 8-shaped mold

Shear box test uses the cylindrical mold for making specimens. The dimension of the mold is 60 mm in inside diameter and 20 mm in height. The shape of the mold is shown in Fig. 4-5.

Fig. 4-5 Mold of shear box test

- Rammer

Rammer for compacting specimens includes the weight with 1.5 kg. Falling height of the weight is 200 mm for unconfined compression test, splitting tension test, direct tension test and 100 mm for shear box test. Rammer set for unconfined compression test, splitting tension test, and shear box test is shown in Section 2.3.1. Rammer set for direct tension test is shown in Fig. 4-6.

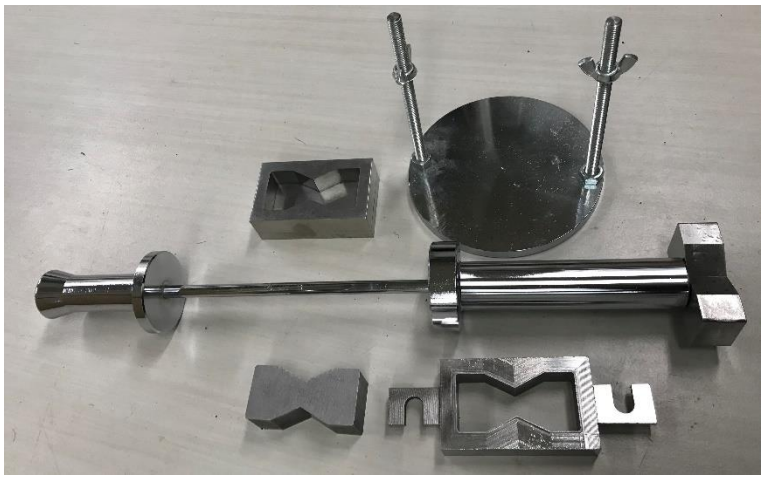

Fig. 4-6 Rammer set for direct tension test

- Dry oven

There is a 20 ± 3^{0}C oven kind in this chapter which is shown in Section 2.3.1.

4.3.2 Preparation process

The laboratory experiments including unconfined compression, direct tension, splitting tension, and shear box tests are carried out with various cement content, fiber content, and fiber length. All mixing conditions for each experiment are detailed in Table 4-1. Cement and fiber contents are determined by cement and fiber mass in 1 m^3 of total dry soil and water. The procedures for mixing admixture and making specimens are as follows.

1. Fiber, cement, and dry soil are mixed by hand until the dry admixture is homogeneous.

2. Then water at the optimum moisture content of 30.8% is added and the mixing machine is used to agitate the admixture homogenously. The mixing includes four times and 2 mins/time.

3. Specimens are produced under compacted condition. Specimens subjected to unconfined compression test and splitting tension test include four layers for compaction. The falling time of rammer is 5, 10, 10, and 20 times for four layers. For direct tension test and shear box test, there are three layers for compaction. The falling time of rammer for three layers is 4, 8, 8 times for direct tension test and 6, 10, 10 times for shear box test.

4. Specimens extruded from mold are covered by a cling film and cured in the 20 ± 3^{0}C oven for 7 days before being subjected to the experiments.

For unconfined compression and splitting tension test, the sizes of specimens are 100 mm in

length and 50 mm in diameter. In direct tension test, specimens in 8-shape are produced with the sizes of 20 mm thick, 40 mm wide, 80 mm long, and the neck of 20 mm wide (Fig. 4-7). The specimen of shear box test is cylindrical with 60 mm in diameter and 20 mm in height.

Table 4-1 Mixing conditions for each experiment

Cement content (kg/m^3)	Fiber content (kg/m^3)	Fiber length (mm)	Name
16	0	10	C16F0L10
16	4	10	C16F4L10
16	8	10	C16F8L10
16	16	10	C16F16L10
16	4	30	C16F4L30
16	8	30	C16F8L30
16	16	30	C16F16L30
32	0	10	C32F0L10
32	4	10	C32F4L10
32	8	10	C32F8L10
32	16	10	C32F16L10
32	4	30	C32F4L30
32	8	30	C32F8L30
32	16	30	C32F16L30

Note: C= cement content; F= fiber content; L= fiber length

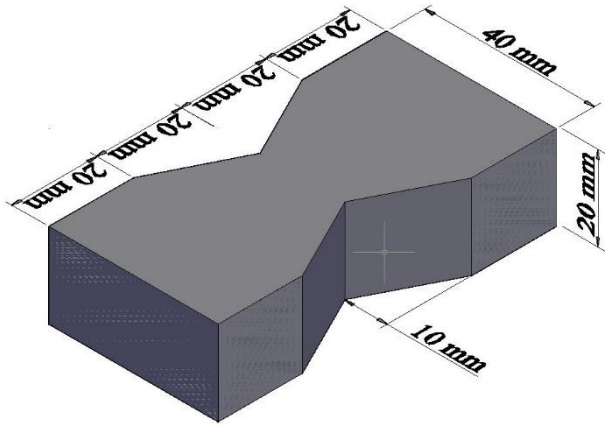

Fig. 4-7 8-shaped specimen dimension

4.4 Testing programs

4.4.1 Unconfined compression test

The testing machine and testing procedure of unconfined compression test are shown in Section 2.4.1.

4.4.2 Splitting tension test

The testing machine and testing procedure of splitting tension test are shown in Section 2.4.2.

4.4.3 Direct tension test

Fig. 4-8 illustrates the testing machine of direct tension test. The maximum load and displacement speed are 2 kN and 1 mm/min, respectively. The stress and strain value are continuously collected until achieving the desired value. To confirm the accuracy of the data, three samples for each mixing condition are tested. The variation between each data and mean data within 12% are accepted. Direct tensile strength from direct tension test is calculated following Eq. (4-1).

$$T = (N\text{-}W)/A \tag{4-1}$$

where N is the applied load (kN), W is the weight of the upper part including mold and specimens (kN), A is the failure section area at the neck of specimen (m^2), T is the direct tensile strength (kPa).

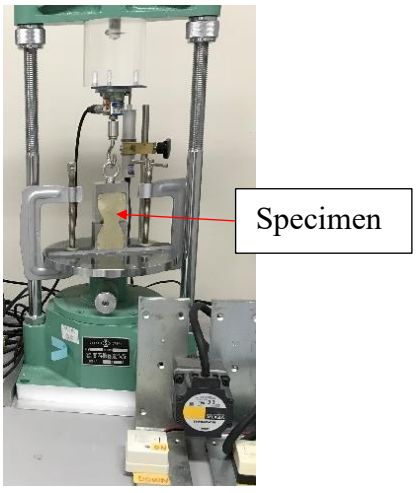

Fig. 4-8 Testing machine of direct tension test

4.4.4 Shear box test

Shear box test is carried out by using a shear box machine (Fig. 4-9). The maximum load and rate of displacement are 2 kN and 1mm/min, respectively. The normal stress is 50, 100, and 150 kPa. Load and displacement of specimens are recorded in PC until the horizontal displacement reaches 7 mm. To control the accuracy of the results, nine specimens are prepared for each mixing condition and three specimens are subjected to each normal stress. Shear strength is calculated by using Eq. (4-2).

$$S=N/A \tag{4-2}$$

where N is the applied load (kN), A is the cross-sectional area of specimen (m^2), S is the shear strength (kPa).

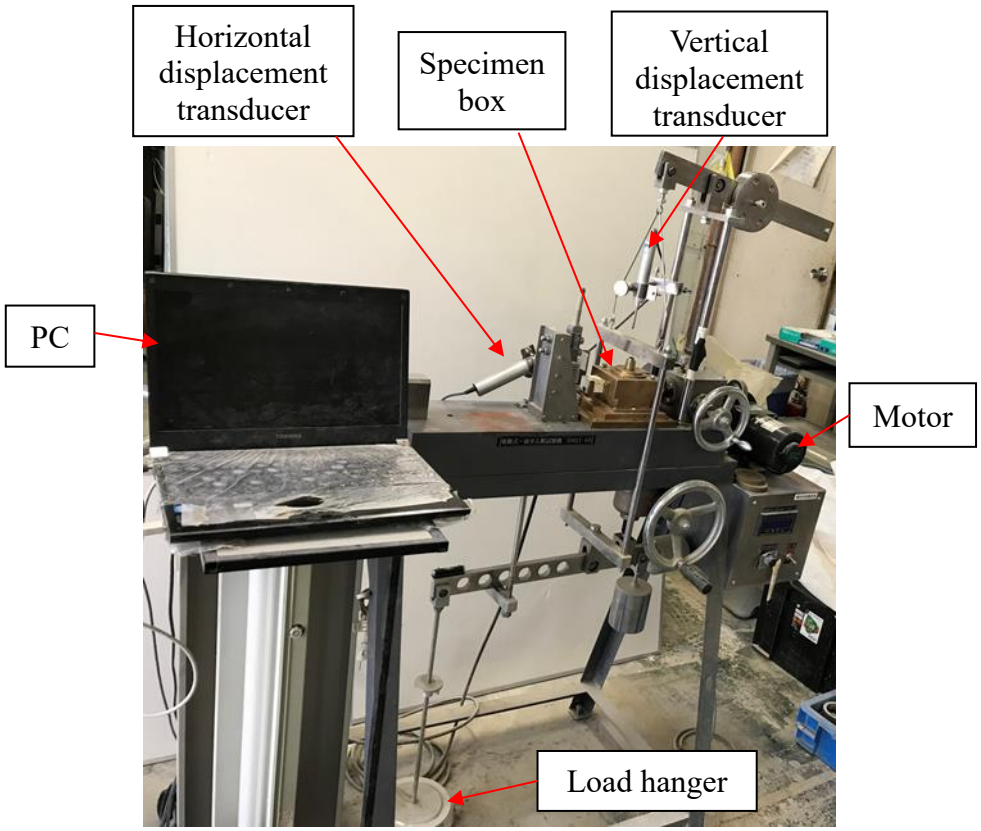

Fig. 4-9 Shear testing machine

4.5 Experimental results

4.5.1 Unconfined compression test

4.5.1.1 Compressive stress-strain curves

Fig. 4-10 depicts the typical compressive stress-strain curves of cemented soil and fiber-reinforced cemented soil. As indicated in the figures, fiber inclusion improves the loss of post-peak stress of cemented soil. Fiber-unreinforced cemented soil performs brittle behavior with the dramatic decrease of the compressive stress after maximum stress. Consequently, specimens are destroyed soon after maximum stress. However, with fiber inclusion, the failure process of specimens is delayed with the diminution of the slope of stress-strain curves after the peak point. Both fiber length and fiber content have an effect on the slope of the curves. The slope reduces with the increase of length and content of fiber. Besides, the figures also display that failure strain of fiber-unreinforced cemented soil increases due to the addition of fiber. The diminution of loss of post-peak stress and the increase of strain to failure translate that fiber-unreinforced cemented soil performs more ductile behavior when fiber is added.

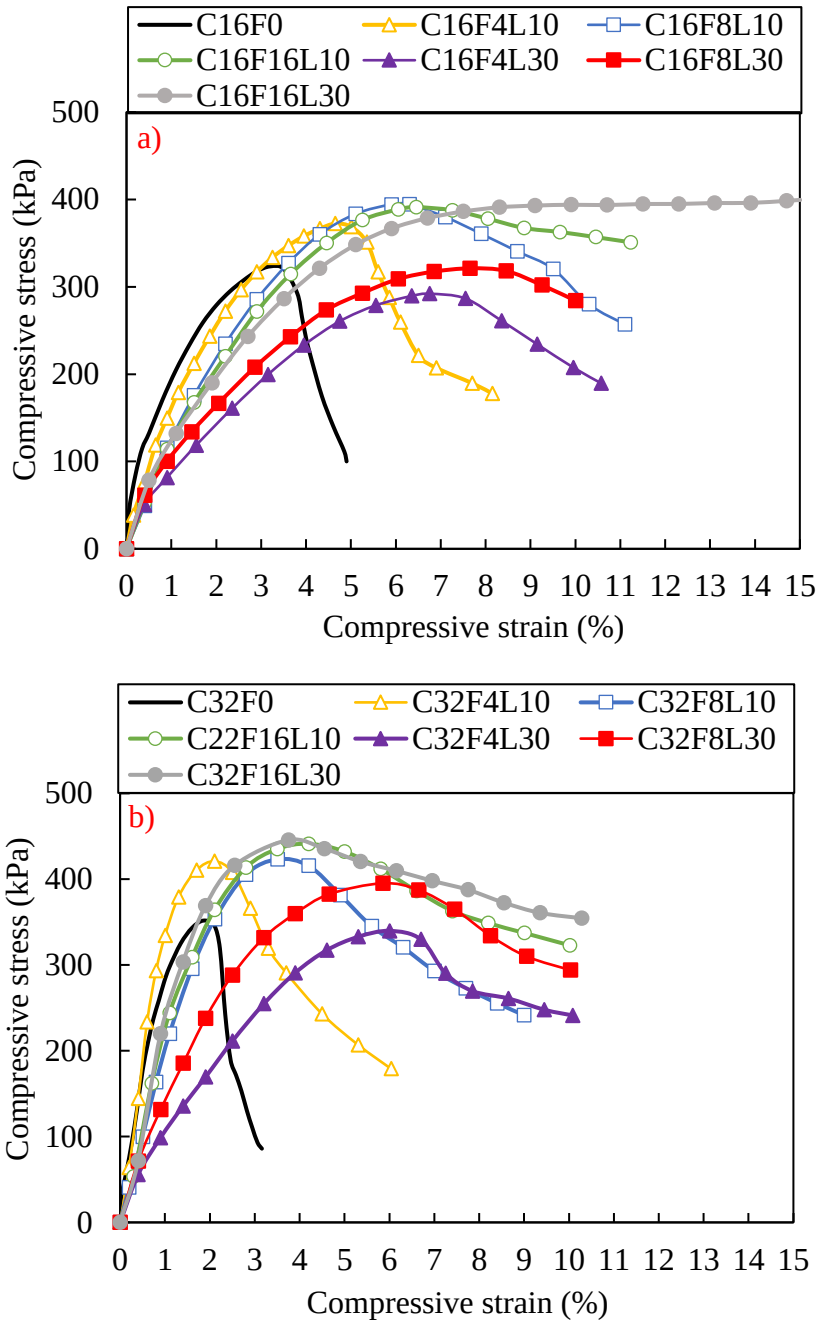

Fig. 4-10 Typical compressive stress-strain curves

a) Cement content 16 kg/m^3; b) Cement content 32 kg/m^3

4.5.1.2 Failure strength

The development of failure strengths according to fiber content is presented in Fig. 4-11. The plot illustrates that corn husk enhances failure strength of fiber-unreinforced cemented soil in general. In the mixing conditions of 30 mm fiber, the influence of fiber on failure strength at the low content of fiber (4 kg/m^3 and 8 kg/m^3) is insignificant. However, further

fiber inclusion (16 kg/m^3), failure strength of cemented soil in cases of 16 kg/m^3 and 32 kg/m^3 cement content improves 24.2% and 30.4%, respectively. With mixtures including 10 mm fiber, failure strength at cement level of 16 kg/m^3 increases according to the enlargement of fiber from 0 to 8 kg/m^3 and then reduces slightly when fiber content is from 8 kg/m^3 to 16 kg/m^3. In these cases, failure strength of fiber-unreinforced cemented soil is improved the most with 21.5% at fiber content of 8 kg/m^3. For 32 kg/m^3 cement content, the enlargement of fiber content contributes to the increase of failure strength and the most improvement is 30.6% at 16 kg/m^3 fiber content. Besides, fiber length has an influence on failure strength. Failure strength of the mixture including 10 mm fiber is higher than that of the mixture including 30 mm fiber at 4 kg/m^3 and 8 kg/m^3 fiber content. Nevertheless, there is an insignificant difference in failure strength between cemented soil with 10 mm and 30 mm fiber in the case of 16 kg/m^3 fiber content.

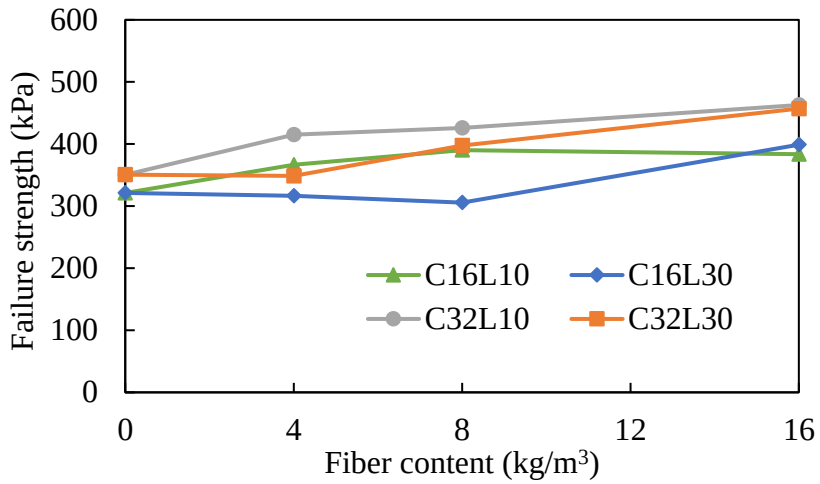

Fig. 4-11 The development of failure strength according to fiber content

The concept of fiber-reinforced cemented soil is inspired from the interaction mechanism between plant roots and soil matrix. Plant roots embedding in the soil matrix prevent soil movement under the loading to prevent erosion. Like plant roots, the role of fiber is to enhance cemented soil properties in Fiber-Cement Stabilized Soil method. In this method, the improvement of cemented soil when adding fiber is linked to interfacial interaction of fiber with soil-cement matrix and interlocking force of fiber [54]. Compared with raw corn husk fiber in Fig. 12a and b, Fig. 12c, d, and e indicate that there is a layer of soil-cement particles on the surface of fiber embed in specimen after 7 days. This interfacial interaction results in the bonding strength between them to prevent the slide of soil-cement particles on the surface of fiber as well as pull-out of fiber from the soil-cement matrix under loading.

Besides, fiber is flexible and randomly distributed, so fibers interact together to generate networks as shown in Fig. 4-12f. These grids hold soil-cement particles (Fig. 4-12g) to limit the movement of fiber and soil-cement particles. Therefore, the complete failure of fiber-reinforced cemented soil is delayed, and failure strength is improved.

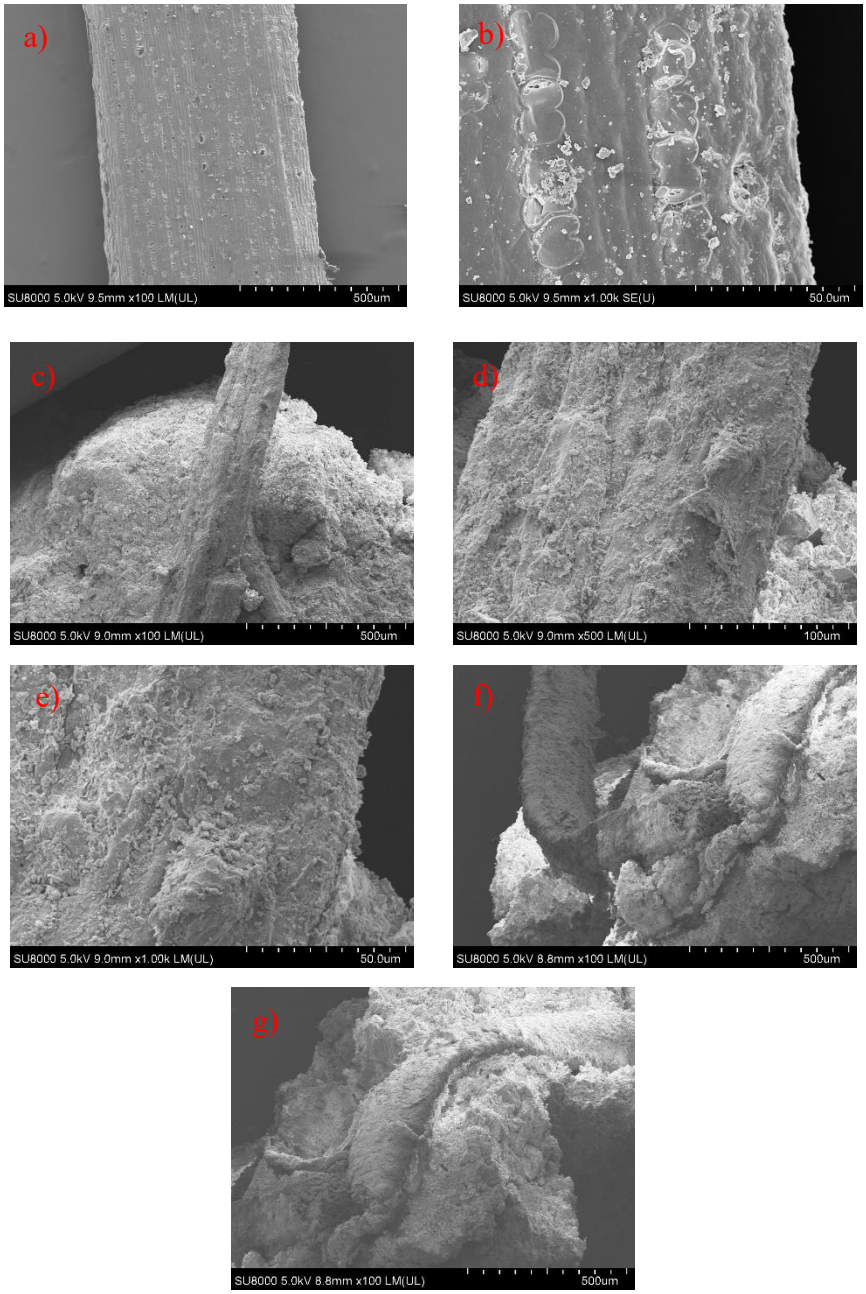

Fig. 4-12 SEM images of fiber and fiber-cement stabilized soil

a and b) Raw fiber status; c, d and e) Fiber status in cement-soil matrix;

f and g) Fiber generating grid and holding cement-soil particles

4.5.1.3 Energy absorption

Energy absorption is the energy that specimens absorb to destroy themselves when load is applied. In this chapter, energy absorption is calculated by totaling the area from origin to maximum stress or strain value of 15%. Fig. 4-13 displays the relationship between the ratio of energy absorption of fiber-reinforced cemented soil to fiber-unreinforced cemented soil and fiber content. The figure provides that energy absorption capacity of cemented soil expands when adding fiber, namely fiber-cement stabilized soil shows greater energy absorption than cemented soil with all ratios larger than 1. Moreover, the ratio of energy absorption of fiber-reinforced cemented soil to fiber-unreinforced cemented soil increases with the increase of fiber from 0 to 16 kg/m^3. The mixture including 16 kg/m^3 fiber shows the highest ratio. Besides, as can be seen from the plots, the ratio value of 10 mm fiber is lower than that of 30 mm fiber. It means that fiber length also has an effect on energy absorption and cemented soil with 30 mm fiber absorbs more energy than that with 10 mm fiber.

4.5.1.4 Secant modulus

Secant modulus is determined as the modulus at 50% of maximum stress. The plot of secant modulus versus fiber content is displayed in Fig. 4-14. As evidenced in the figure, the addition of fiber results in the decline of modulus of fiber-unreinforced cemented soil. The developing tendency of modulus of cemented soil including 10 mm and 30 mm fiber is different. With 10 mm fiber, secant modulus declines with the increase of fiber from 0 to 16 kg/m^3. However, with 30 mm fiber, after decreasing significantly when adding 4 kg/m^3 fiber, the enlargement of fiber from 4 kg/m^3 to 16 kg/m^3 contributes to the increase of secant modulus. Also, fiber length impacts on secant modulus, namely, secant modulus of specimens with 10 mm fiber is higher than that of specimens with 30 mm fiber.

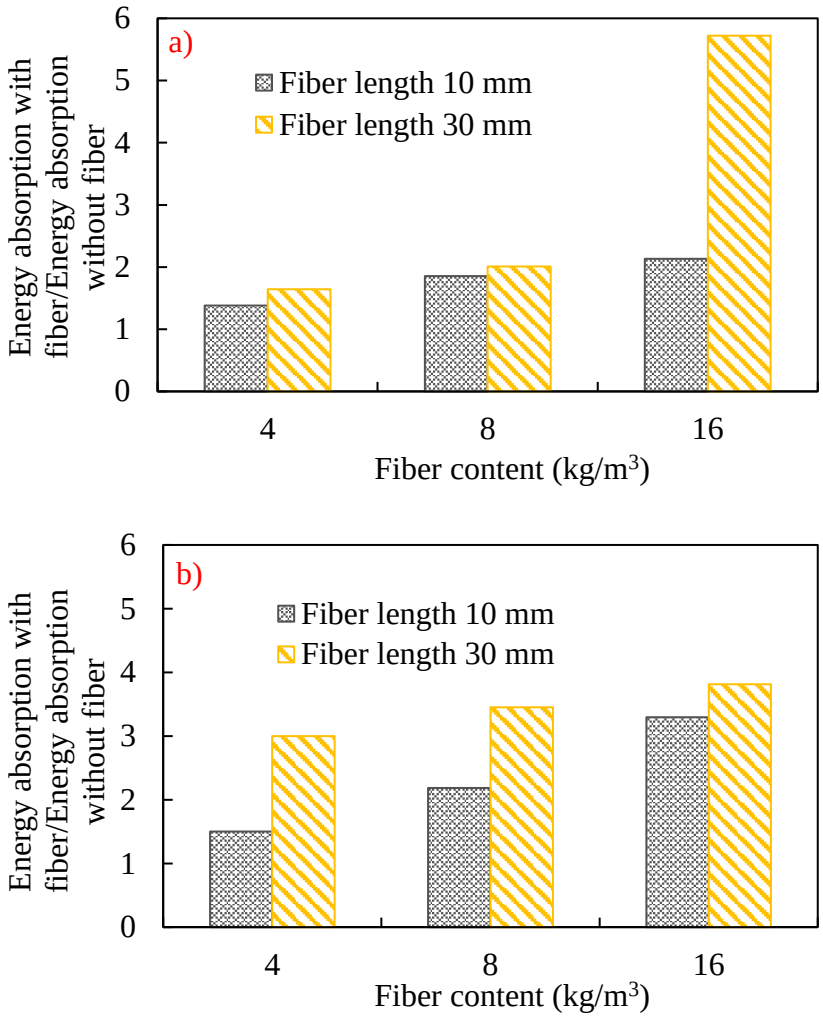

Fig. 4-13 Energy absorption behavior of specimens

a) Cement content 16 kg/m^3; b) Cement content 32 kg/m^3

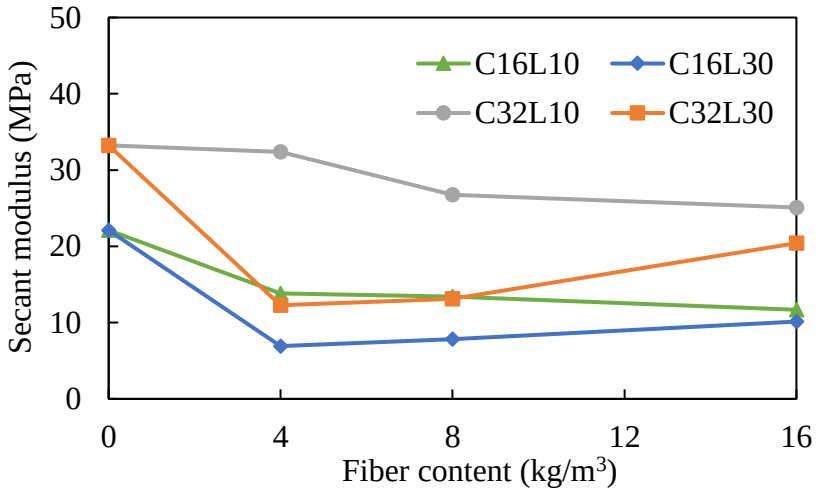

Fig. 4-14 The change of secant modulus according to fiber content

4.5.2 Splitting tension test

4.5.2.1 Splitting tensile stress-strain curves

Splitting tensile stress-strain curves of cemented soil and fiber-reinforced cemented soil are plotted in Fig. 4-15. Figures report that corn husk fiber changes the behavior of fiber-unreinforced cemented soil in terms of tensile stress. Tensile stress-strain curve of fiber-unreinforced cemented soil immediately drops to zero after maximum tensile stress. In contrast, with fiber inclusion, after reaching yield tensile strength, tensile stress either decreases slightly and increases again (in cases of 4 and 8 kg/m^3 fiber) or changes slope and keeps increasing until obtaining ultimate tensile strength (in some cases of 16 kg/m^3 fiber). Like the results obtaining from unconfined compression test, fiber content and fiber length impact stress behavior after ultimate tensile strength (loss of post-peak tensile stress). The drop speed of tensile stress following ultimate strength decreases with the increase in content of fiber. Besides, the increase of fiber length results in the decrease of loss of post-peak tensile stress. Also, the enlargement of length and content of corn husk leads to the increase of strain to failure of cemented soil. These behaviors of specimens in terms of tensile stress-strain curve strengthen the comment in the previous section that cemented specimen is more ductile with the addition of fiber.

4.5.2.2 Splitting tensile strength

Fig. 4-16 depicts the yield tensile strength and ultimate tensile strength versus fiber content. The results reveal that corn husk fiber improves both ultimate tensile strength and yield tensile strength in general. In comparison to fiber-unreinforced cemented soil, yield tensile strength of specimens with 10 mm fiber and 16 kg/m^3 cement content changes slightly. For other mixing conditions, the addition of 4 and 8 kg/m^3 fiber affects trivially yield tensile strength. However, further fiber inclusion (16 kg/m^3), yield tensile strength of specimens is 83.9%, 32.2%, and 62.8% higher than tensile strength of cemented soil for mixing conditions of C16L30, C32L10, and C32L30, respectively. Compared to yield tensile strength, the improvement effect of fiber on ultimate tensile strength is more remarkable. The increase in fiber from 4 to 16 kg/m^3 contributes to the increase in ultimate tensile strength. The most enhancement of ultimate tensile strength is 63.7%, 206.1%, 72.6%, and 155.1% concerning C16F16L10, C16F16L30, C32 F16L10, and C32F16L30 in comparison to that of fiber-unreinforced cemented soil. The development of tensile strength of fiber-unreinforced specimens when adding fiber can be explained as follows. Under loading, the yield point

coincides with the first crack during tensile stress development. After the first crack, the increase of tensile stress until failure is attributed to the presence of fiber at the crack. In the fiber-soil-cement matrix, bonding between soil-cement particles and the surface of fiber contributes to the transfer of tensile load in the soil-cement matrix to fiber at the cracks. Also, fiber performs like a bridge at the cracks to retain the spread of cracks, as presented in Fig. 4-17. As a result, fiber carries the tensile load at the crack to improve the tensile strength.

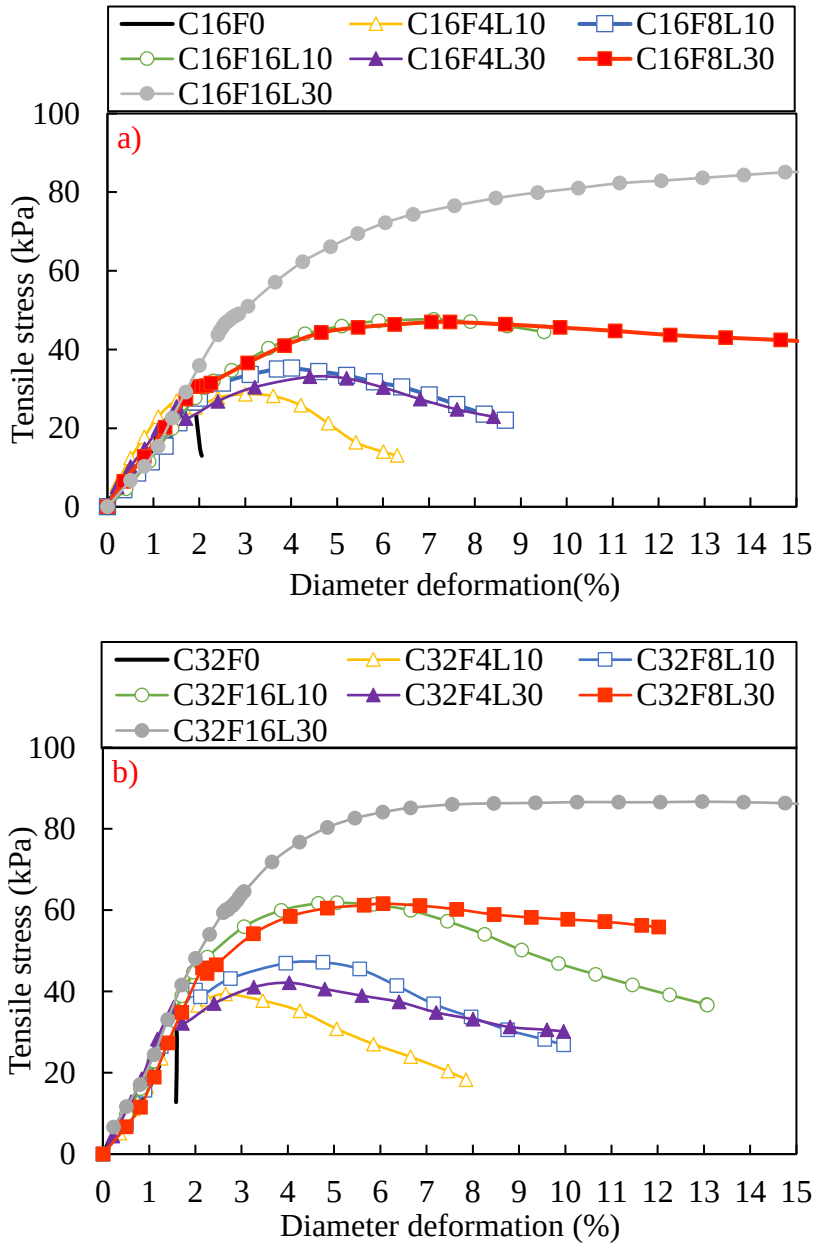

Fig. 4-15 Typical tensile stress-strain curves of specimens

a) Cement content 16 kg/m^3; b) Cement content 32 kg/m^3

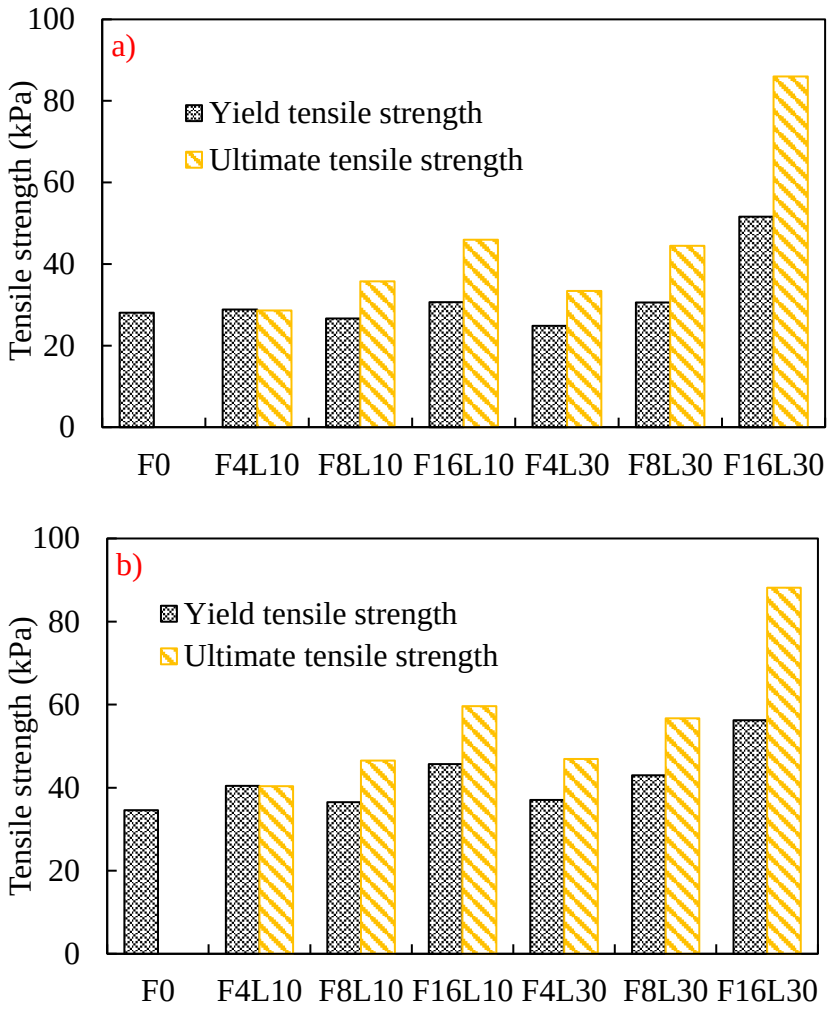

Fig. 4-16 Splitting tensile strength of specimens with and without fiber inclusion

a) Cement content 16 kg/m^3; b) Cement content 32 kg/m^3

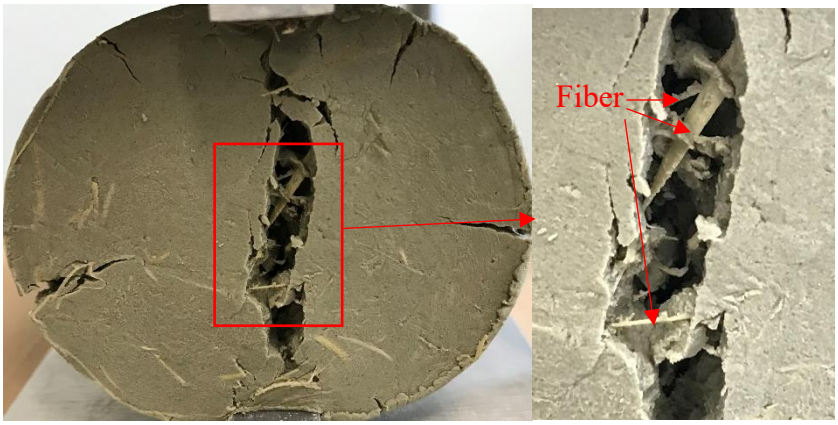

Fig. 4-17 The presence of fiber at the crack

4.5.3 Direct tension test

4.5.3.1 Direct tensile stress-strain curves

Fig. 4-18 depicts the typical direct tensile stress-strain curves obtained from direct tension test. The results illustrate that tensile stress of cemented soil sharply declines after achieving peak point. However, the presence of fiber prevents specimens from dropping to zero by the appearance of the residual phase. Residual stress either gradually reduces or increases and then gradually reduces according to the increase of strain. Besides, the plot depicts that there is a difference in residual stress behavior of specimens with different fiber content and fiber length. Residual stress increases with enlargement of fiber length and fiber content at a given strain value. The residual stress of 10 mm fiber decreases to zero more quickly than that of 30 mm fiber. The difference in direct tensile stress-strain behavior of specimens with and without fiber could be explained as follows. After the first crack, specimens without fiber are divided into two separate parts including the upper and lower parts. However, for specimens with fiber inclusion, these two parts are still connected by fiber after cracking. Under loading, the bonding between fiber and soil-cement particles limits the displacement of fiber to restrain the pull-out of fiber from the soil-cement matrix. Hence, at the crack, fiber plays a role as a bridge to limit the spread of the crack (Fig. 4-19) and carries more tensile load. This leads to the development of residual stress after direct tensile strength. Besides, the embed fiber length of 30 mm fiber in two parts of specimens after the crack is more than that of 10 mm, so the pull-out of 10 mm fiber is faster than that of 30 mm fiber. As a result, the decrease speed of residual stress of 30 mm fiber is lower and residual stress at a given strain is higher than that of 10 mm fiber.

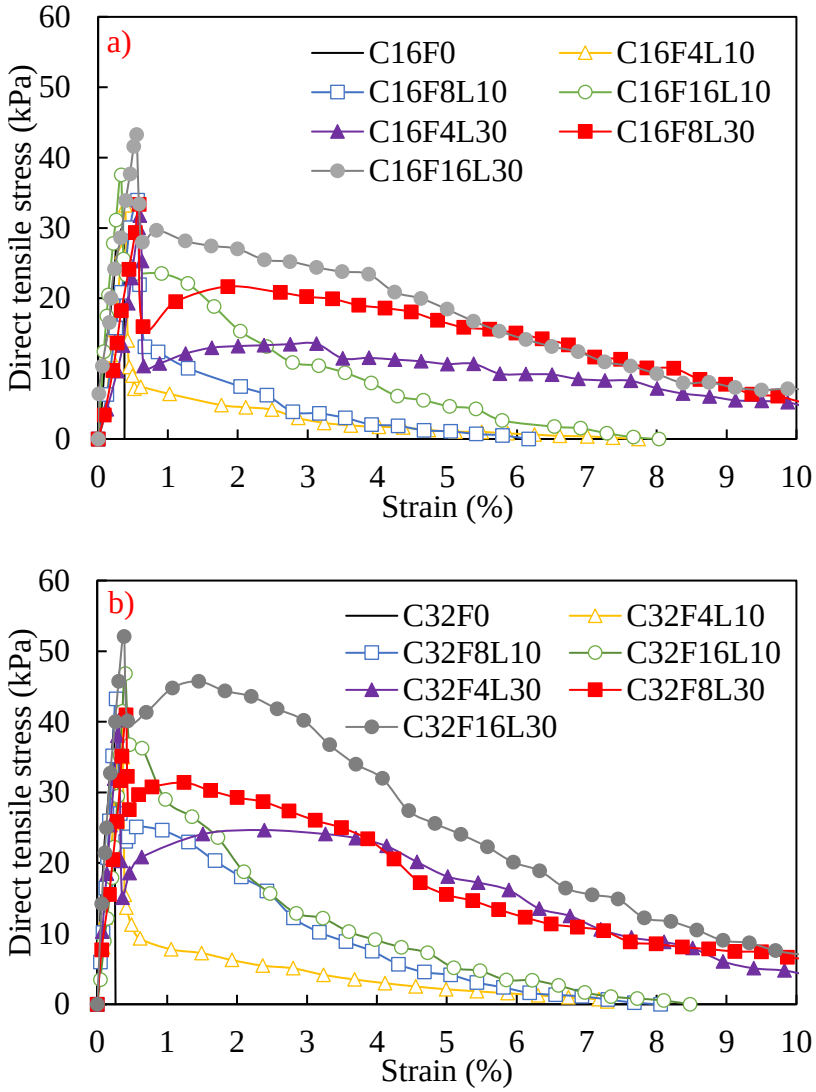

Fig. 4-18 Typical tensile stress-strain curves of direct tension test

a) Cement content 16 kg/m^3; b) Cement content 32 kg/m^3

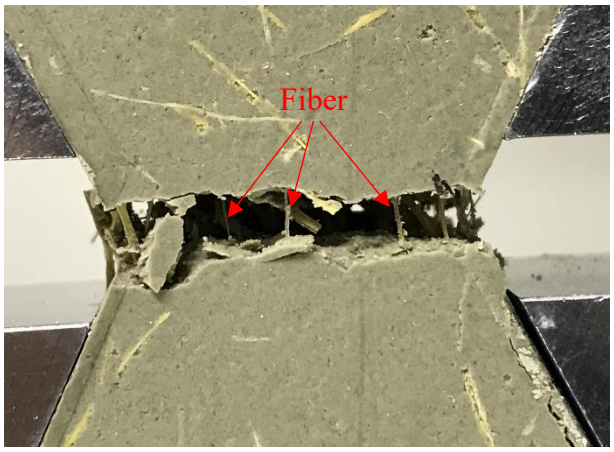

Fig. 4-19 Fiber presenting at the crack

4.5.3.2 Direct tensile strength

The relationship between direct tensile strength and fiber content is presented in Fig. 4-20. The plot illustrates that fiber inclusion leads to the increase of direct tensile strength in general. The addition of fiber from 4 to 8 kg/m^3 has an insignificant effect on tensile strength of fiber-unreinforced cemented soil. Nevertheless, the addition of 16 kg/m^3 fiber content increases tensile strength of cemented specimen. The improvements of direct tensile strength of fiber-unreinforced cemented specimens when adding 10 mm and 30 mm fiber is 19.5% and 26.7% for mixing conditions of 16 kg/m^3 cement content, 20.6% and 27.9% for mixing conditions of 32 kg/m^3 cement content, respectively. Besides, it could be seen that fiber length impacts trivially on tensile strength in terms of direct tensile strength.

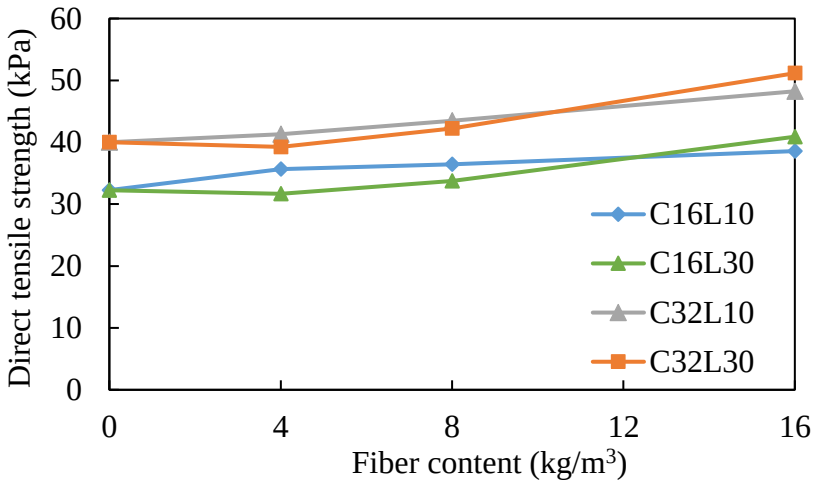

Fig. 4-20 Relationship between direct tensile strength and fiber content

4.5.3.3 Energy absorption

In this direct tension test, energy absorption of fiber-cement stabilized specimens includes peak energy and residual energy which are calculated from origin to maximum direct tensile stress and the beginning of residual phase to strain value of 5%, respectively, as shown in Fig. 4-21. The residual energy plays an important role in an anti-earthquake of structure. After failure, the structures without residual energy collapse immediately. However, structures with residual energy still withstand the load after the first crack and gradually destroy. Fig. 4-22 displays energy absorption of the mixtures from direct tension test. As can be identified from the plot, the energy absorption of cemented soil increases when adding fiber. The peak energy and residual energy increase when increasing in fiber content. Besides, it is clear that the change of fiber length remarkably influents on residual energy. Residual

energy of the mixture including 30 mm fiber is much higher than that of the mixture including 10 mm fiber for the same fiber content.

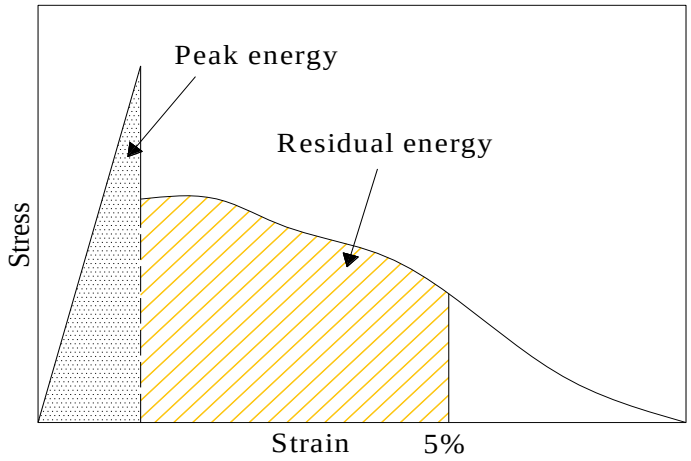

Fig. 4-21 Definition of peak energy and residual energy

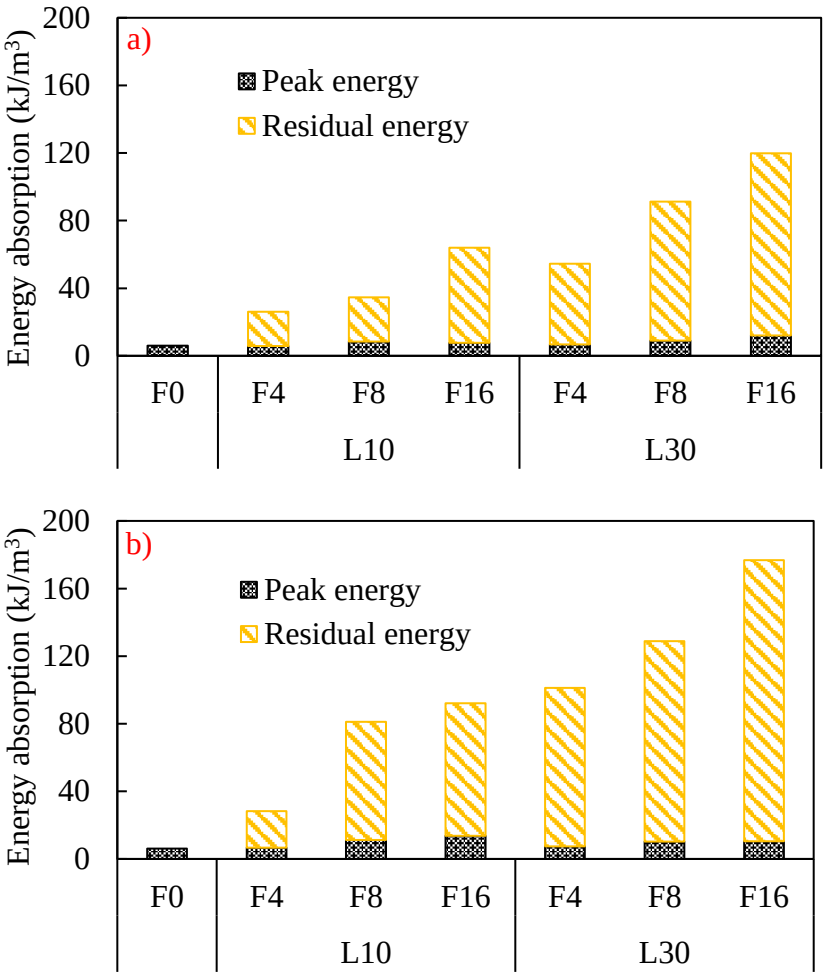

Fig. 4-22 Energy absorption of cemented soil with and without fiber inclusion

a) Cement content 16 kg/m^3; b) Cement content 32 kg/m^3

4.5.4 Shear box test

4.5.4.1 Shear stress-displacement curves

The typical shear stress-displacement curves of specimens with and without fiber inclusion at normal stress of 50, 100, and 150 kPa for 16 and 32 kg/m^3 cement content are plotted in Fig. 4-23 and Fig. 4-24, respectively. These figures show that the slope of the curve from origin to peak stress develops in a different tendency between mixing conditions of 16 and 32 kg/m^3 cement. In the cases of 16 kg/m^3 cement content, after reaching shear stress of about 50 kPa, the slope of curves with high fiber content (F8L10 at normal stress 50 and 150 kPa, F8L30 at normal stress 100 kPa, F16L10, and F16L30) is higher than that of curves with lower fiber content. In contrast, for the mixing condition of 32 kg/m^3 cement content, the slope of all mixing conditions is equal from origin to maximum shear stress. Besides, the inclusion of fiber improves residual stress of cemented soil, namely, residual stress of fiber-unreinforced cemented soil increases with the increase of fiber content. The residual stress is highest at 16 kg/m^3 fiber content. In general, the increase of fiber length results in the increase of residual stress except for the cases of 16 kg/m^3 cement content at a normal stress of 150 kPa. The increase of residual stress due to the addition of fiber could be attributed to the interfacial interaction between fiber and soil-cement matrix. At residual phase, the bonding between the surface of fiber and soil-cement particles at the shearing plane limits movement of fiber in soil-cement matrix. As a result, the slide of two parts of specimen is restrained and the residual stress is improved when adding fiber.

4.5.4.2 Shear strength

The relationship between shear strength and fiber content at normal stress of 50, 100, and 150 kPa is displayed in Fig. 4-25. As can be observed from the figures, fiber inclusion results in the enhancement of shear strength in general. The inclusion of 4 kg/m^3 fiber content has an insignificant effect on shear strength. Further fiber inclusion (8 and 16 kg/m^3 fiber content), fiber inclusion leads to the increase in shear strength to some extent. In cases of 16 kg/m^3 cement content, the most improvement of shear strength of fiber-unreinforced cemented soil when adding fiber with 10 and 30 mm in length is at 16 kg/m^3 cement content with 40.2%, 35.8% at normal stress of 50 kPa, 40.5%, 29.9% at normal stress of 100 kPa, 25.5%, 24.3% at normal stress of 150 kPa, respectively. For 32 kg/m^3 cement content, the effect of fiber on shear strength reduces. Shear strength of cemented soil improves the most at 16 kg/m^3 cement content with 17.8% and 21.9% for 10 mm and 30 mm fiber at normal

stress of 100 kPa, respectively. The figures also present that fiber length has an insignificant effect on shear strength of fiber-cement stabilized soil.

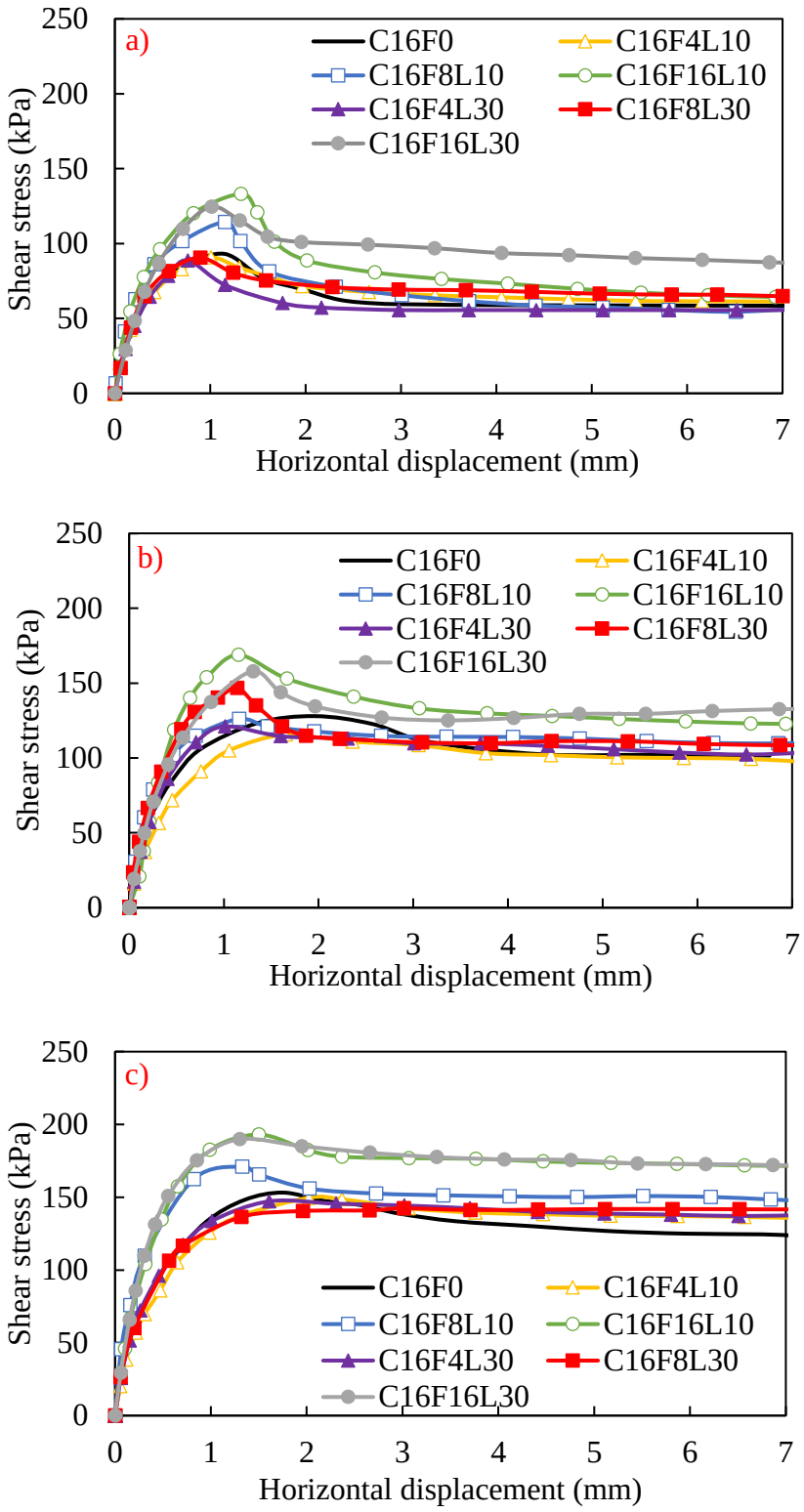

Fig. 4-23 Typical shear stress-displacement curves of specimens with 16 kg/m^3 cement

a) Normal stress 50 kPa; b) Normal stress 100 kPa; c) Normal stress 150 kPa

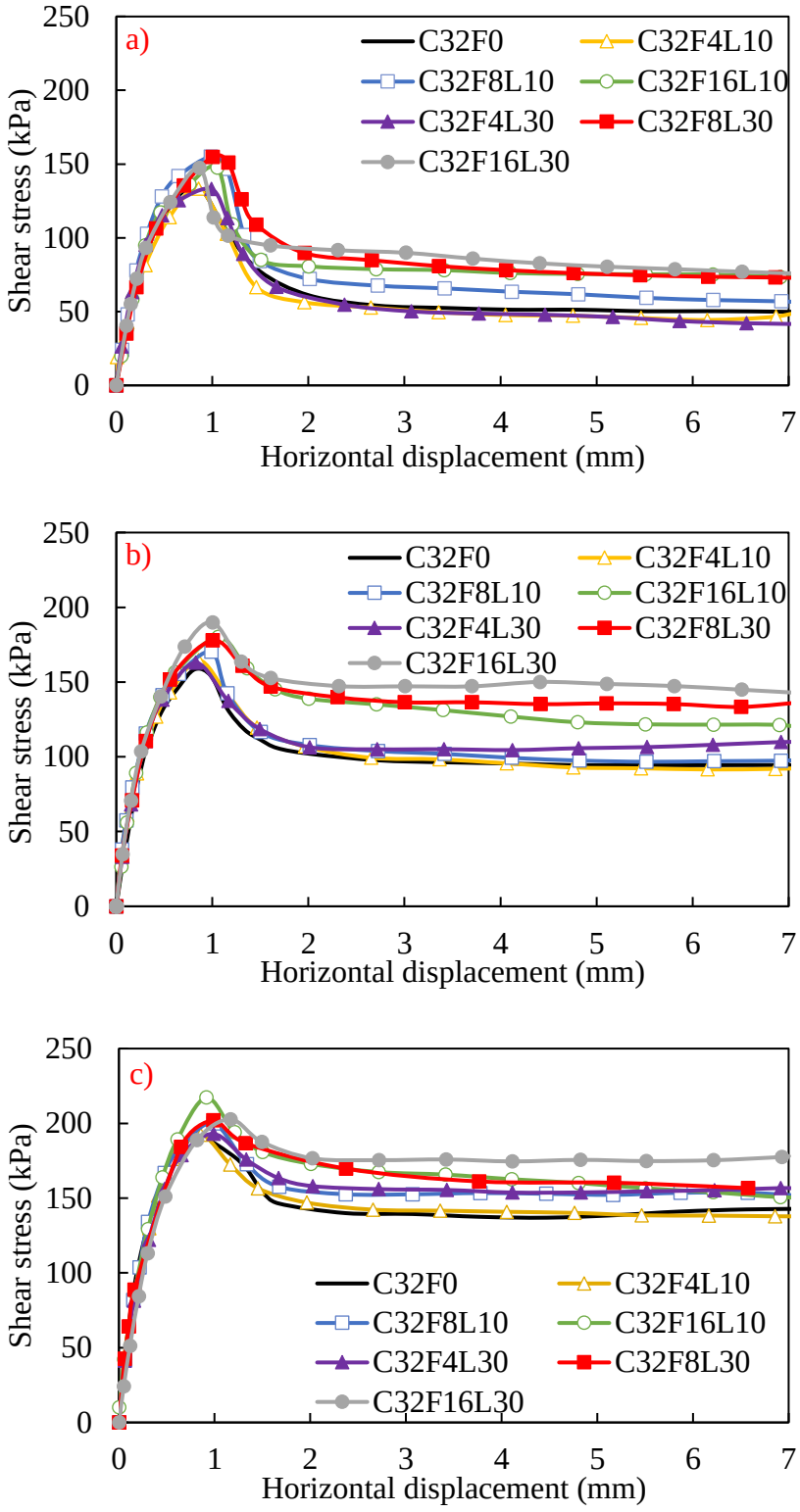

Fig. 4-24 Typical shear stress-displacement curves of specimens with 32 kg/m^3 cement

a) Normal stress 50 kPa; b) Normal stress 100 kPa; Normal stress 150 kPa

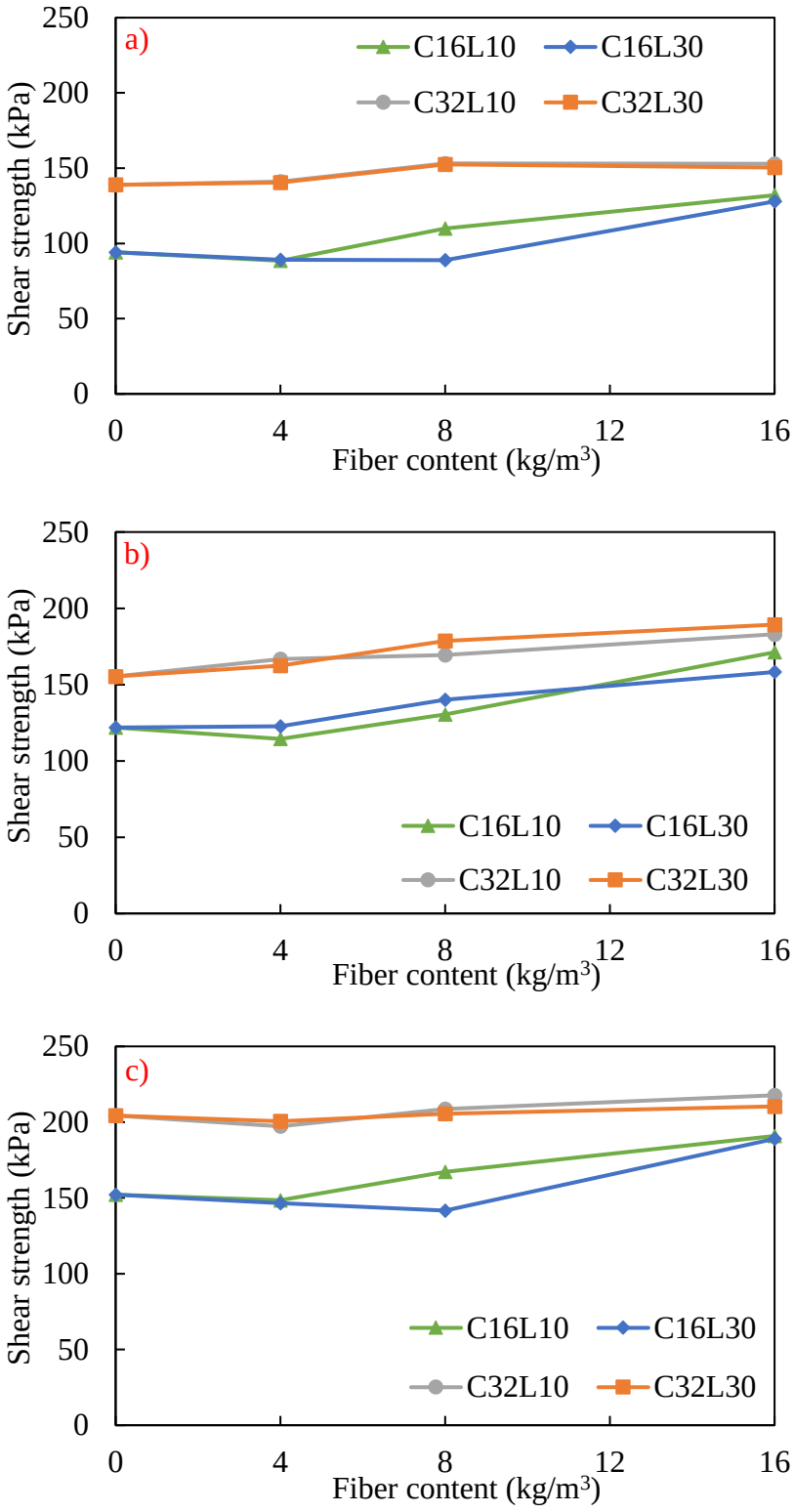

Fig. 4-25 Relationship between shear strength and fiber content

a) Normal stress 50 kPa; b) Normal stress 100 kPa; c) Normal stress 150 kPa

4.5.4.3 Angle of internal friction and cohesion

The plot of shear strength at three normal stress values performs the straight line with the intercept of cohesion (c) and the slope of angle of internal friction (ϕ) as shown in Fig. 4-26.

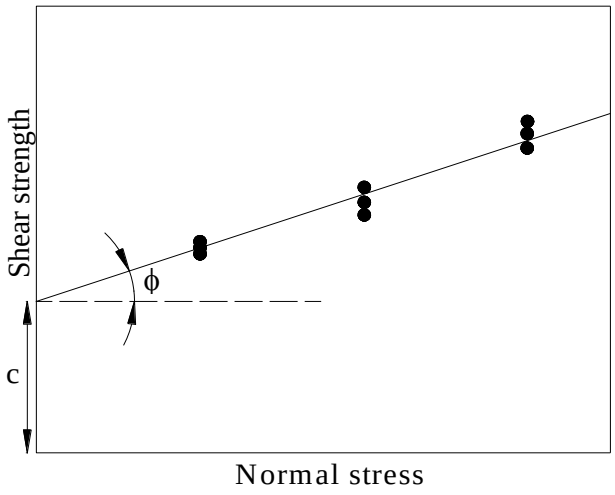

Fig. 4-26 Definition of angle of internal friction and cohesion

Fig. 4-29 displays the relationship between fiber content with angle of internal friction. Angle of internal friction is determined as the slope of the trend lines in Fig. 4-27 and Fig. 4-28. The results show that with fiber inclusion, angle of internal friction of cemented soil seems not to change for mixing conditions of 16 kg/m^3 cement content. As for 32 kg/m^3 cement content, fiber inclusion results in a slight decrease when adding 4 and 8 kg/m^3 fiber content. Further fiber inclusion (16 kg/m^3), angle of internal friction of cemented soil increases slightly.

Fig. 4-30 illustrates the relationship between fiber and cohesion which is determined as the intercept of the trend lines in Fig. 4-27 and Fig. 4-28. The plot presents that fiber inclusion leads to the improvement of cohesion in general. At 16 kg/m^3 cement content, the inclusion of 4 kg/m^3 fiber content has an insignificant effect on cohesion, namely, cohesion of cemented soil decreases slightly. Further fiber inclusion (8 kg/m^3), cohesion of cemented soil enhances slightly when adding 30 mm fiber, while the addition of 10 mm fiber improves cohesion of cemented soil by 21%. The addition of 16 kg/m^3 fiber shows the highest cohesion, namely, cohesion of cemented soil enhances 63.4% and 55% concerning the inclusion of 10 mm and 30 mm fiber. In the case of 32 kg/m^3 cement content, like the results of 16 kg/m^3 cement content, fiber content of 4 kg/m^3 changes cohesion of cemented soil slightly. However, further fiber inclusion, cohesion increases when adding 8 kg/m^3 fiber

content and then decreases slightly when adding fiber of 16 kg/m^3. Therefore, with 32 kg/m^3 cement content, the most improvement of cohesion is 20.7% and 25.9% at 8 kg/m^3 fiber content for mixing conditions of 10 mm and 30 mm fiber, respectively. As can be seen from the figure, fiber length affects trivially cohesion for both cement content of 16 kg/m^3 and 32 kg/m^3.

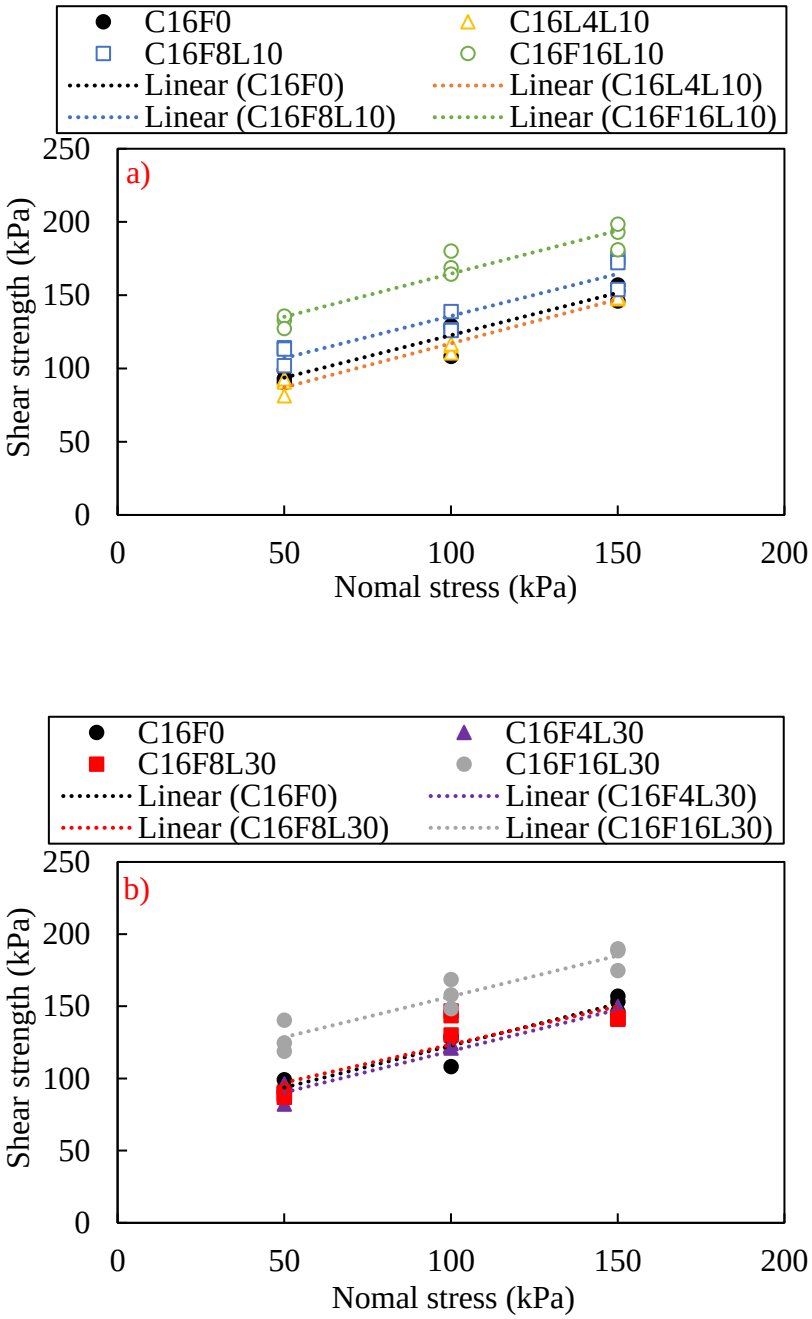

Fig. 4-27 Shear strength versus normal stress at 16 kg/m^3 cement content

a) Fiber length 10 mm; b) Fiber length 30 mm

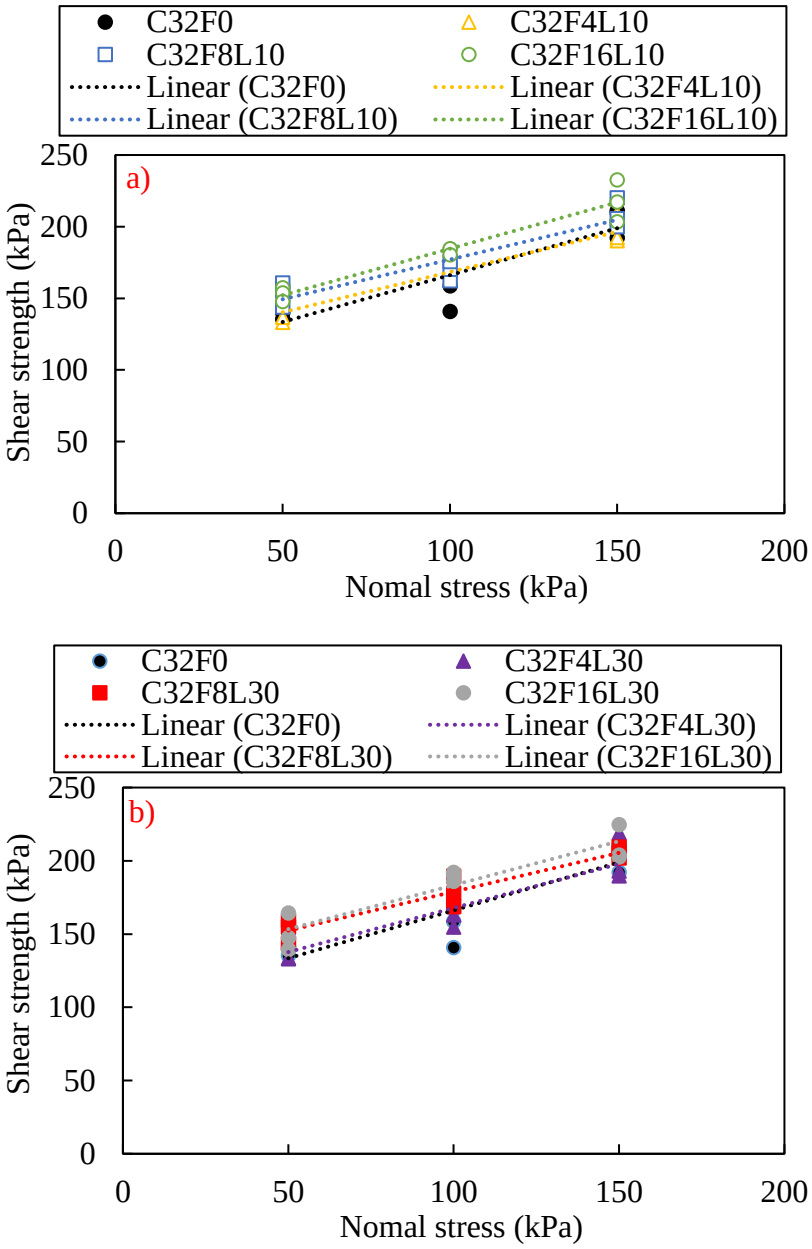

Fig. 4-28 Shear strength versus normal stress at 32kg/m^3 cement content

a) Fiber length 10 mm; b) Fiber length 30 mm

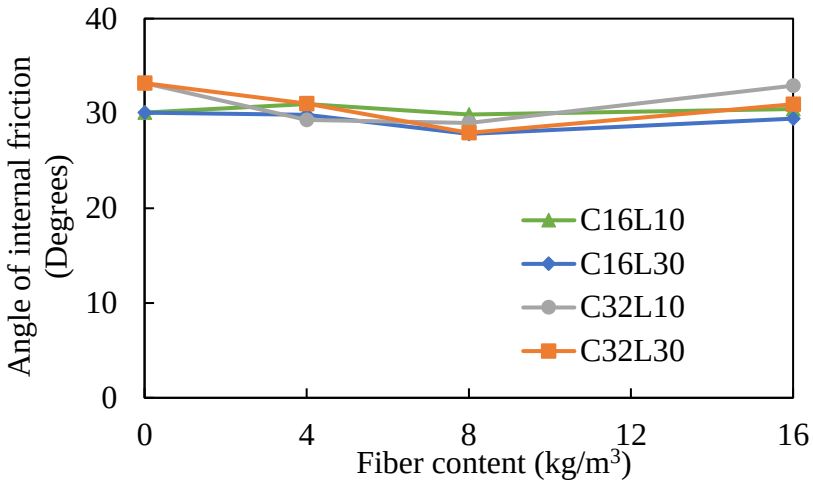

Fig. 4-29 Relationship between angle of internal friction and fiber content

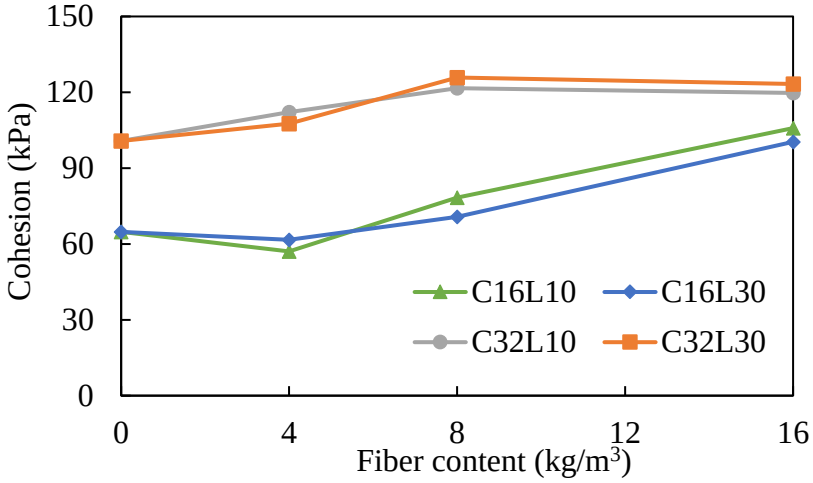

Fig. 4-30 Relationship between cohesion and fiber content

4.5.5 Relationships among strengths from experiments

Fig. 4-31, Fig. 4-32, Fig. 4-33, and Fig. 4-34 depict the relationships among failure strength, ultimate tensile strength, yield tensile strength, direct tensile strength, shear strength, and cohesion. The plots present that the strengths from unconfined compression, splitting tension, shear box, and direct tension test have good relationships with a high coefficient of determination. Besides, the coefficient of determination between yield tensile strength with failure strength, direct tensile strength, and cohesion (coefficient of determination of 0.972, 0.980, and 0.972, respectively) are higher than that between ultimate tensile strength with failure strength, direct tensile strength, and cohesion (coefficient of determination of 0.910, 0.920, and 0.919, respectively). It means that yield tensile strength performs a stronger relationship with failure strength, direct tensile strength, and cohesion than ultimate tensile

strength. From Fig. 4-32a, it is obvious that direct tensile strength values are nearly equal to yield tensile strength values for the same mixing condition with the coefficient of 1.054. Furthermore, failure strength and direct tensile strength show the best linear relationship, namely, the coefficient of determination (0.997) is highest, and the value points are the most closed to the straight line (Fig. 4-33).

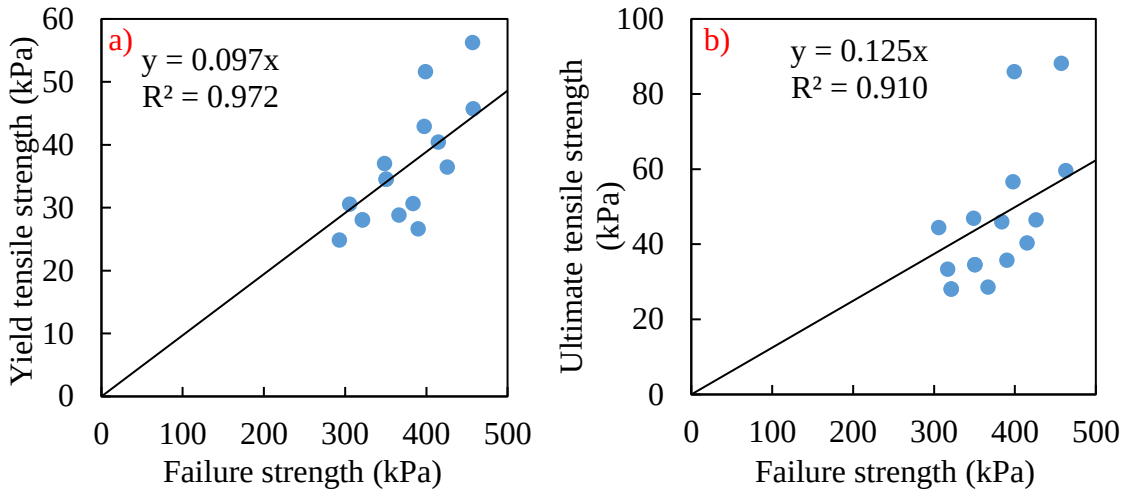

Fig. 4-31 Relationship between splitting tensile strength and failure strength

a) Yield tensile strength versus failure strength;

b) Ultimate tensile strength versus failure strength

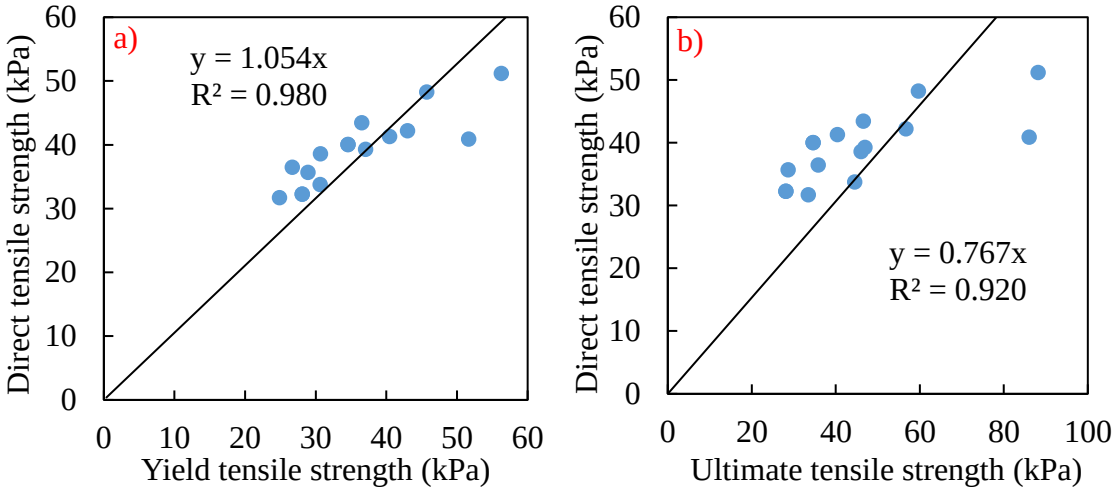

Fig. 4-32 Relationship between direct tensile strength and splitting tensile strength

a) Direct tensile strength versus yield tensile strength;

b) Direct tensile strength versus ultimate tensile strength

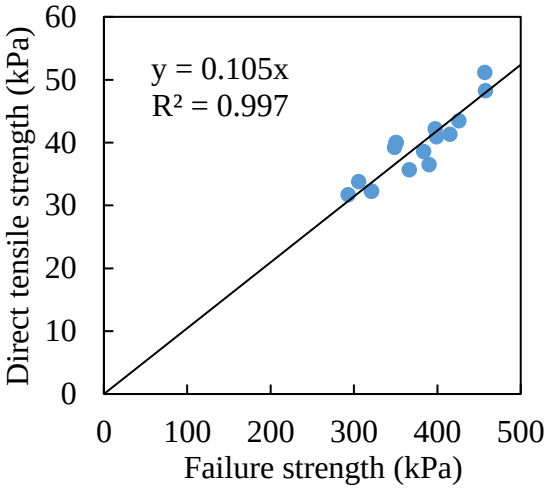

Fig. 4-33 Relationship between direct tensile strength and failure strength

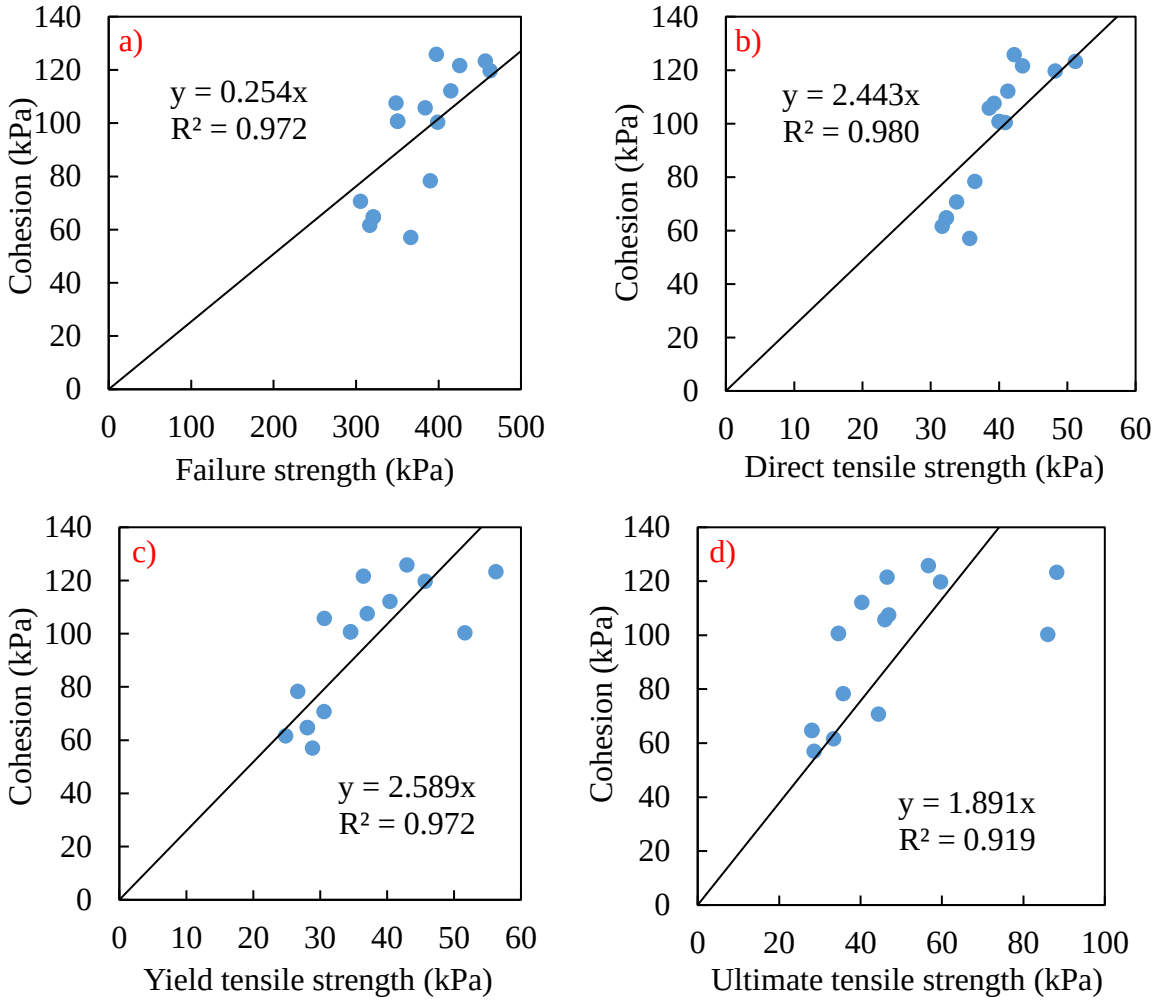

Fig. 4-34 Relationship between cohesion with and other strengths

a) Cohesion versus failure strength; b) Cohesion versus direct tensile strength;

c) Cohesion versus yield tensile strength; d) Cohesion versus ultimate tensile strength

4.6 Conclusions

This chapter focuses on the impact of corn husk fiber on the cemented soil properties at low water content with different contents and lengths of fiber. Unconfined compression, splitting tension, shear box, and direct tension tests are conducted to evaluate the behavior of fiber-reinforced cemented soil. Some conclusions from the experimental results are summarized as follows.

- The inclusion of 30 mm fiber and 16 kg/m^3 fiber content increases 24.2% and 30.4% failure strengths of cemented soil in cases of 16 kg/m^3 and 32 kg/m^3 cement content, respectively. With the mixtures including 10 mm fiber, failure strength increases with the increase of fiber content. In these cases of 16 kg/m^3 cement, failure strength of fiber-unreinforced cemented soil with 10 mm fiber is improved the most with 21.5% at fiber content of 8 kg/m^3. For 32 kg/m^3 cement content, strength of fiber-unreinforced cemented soil with 10 mm fiber is improved the most with 30.6% at fiber content of 16 kg/m^3.

- Energy absorption from unconfined compression test significantly increases with the increase of fiber content. Besides, specimens with 30 mm fiber absorb much higher energy than that with 10 mm fiber.

- Secant modulus of specimens in unconfined compression test decreases due to the addition of fiber. When adding fiber from 0 to 16 kg/m^3, secant modulus of 10 mm fiber is higher than that of 30 mm fiber.

- The addition of fiber results in the appearance of ultimate and yield tensile strength. Tensile stress increases from origin to yield tensile strength and then either decreases slightly and then increases again or changes the slope and then increases to ultimate tensile strength. Ultimate tensile strength increases with the increase of fiber content and fiber length.

- Loss of post-peak stress decreases with the increase of fiber length and fiber content.

- Direct tensile strength of cemented specimens increases the most when adding 16 kg/m^3 fiber content. The addition of fiber leads to the appearance of residual stress after peak stress. The residual stress increases with the increase of fiber content and fiber length.

- In direct tension test, the energy absorption of fiber-cement stabilized soil is much higher than that of cemented soil. The residual energy increases with the increase of fiber length and fiber content.

- Residual stress from shear box test increases when fiber length and fiber content increase in general. Furthermore, fiber inclusion improves shear strength to some extent, and shear strength of cemented soil is highest when adding 16 kg/m^3 fiber.

- Cohesion increases when adding corn husk fiber from 8 to 16 kg/m^3 for mixing conditions of 16 kg/m^3 cement content. However, for cement content of 32 kg/m^3, cohesion increases when adding corn husk fiber from 0 to 8 kg/m^{3,} and further fiber inclusion (16 kg/m^3) cohesion decreases slightly. As for angle of internal friction, fiber inclusion either slightly changes or slightly decreases the angle of internal friction of cemented soil. The difference in cohesion and angle of internal friction between two fiber lengths is insignificant.

- Failure strength and direct tensile strength show the strongest relationship when compared with other relationships among strengths. Besides, the relationships between yield tensile strength and other parameters (i.e., failure strength, direct tensile strength, and cohesion) are stronger than those between ultimate tensile strength and other parameters.

CHAPTER 5

REGRESSION MODELS FOR PREDICTING MECHANICAL PROPERTIES OF CORN HUSK FIBER-CEMENT STABILIZED SOIL

5.1 Introduction

Regression analysis is an effective method to investigate and analyze the relationship between two or more independent variables in many engineering and scientific problems. If regression models can be developed to predict output variables, it will contribute to saving time and cost for laboratory experiments. There are two kinds of regression analysis including simple linear regression and multiple regression. In the simple regression model, there is only one independent variable. In contrast, if there are more than one variable, it is called a multiple regression model. Besides, the multiple regression model is classified into two models: multiple linear regression and multiple non-linear regression model. Until now, many researchers used regression model in soil improvement field. G. L. Sivakumar Babu et al. (2008) [112] predicted seepage velocity and piping resistance of sand and red soil reinforced by coir fiber by using multiple linear and non-linear regression models. The results showed a quite high coefficient of correlation between input variables (i.e., fiber content, fiber length, and hydraulic gradient) and output variables (i.e., seepage velocity and piping resistance). A. R. Estabragh et al. (2016) [113] applied a regression model to predict the seepage velocity and seepage force of fiber-reinforced silty soil from fiber content, fiber length, and gradient hydraulic. In that study, both multiple linear and multiple non-linear regression models are used to compare their errors and find out the best model. They reported that multiple non-linear regression models showed better results. A. Ahmed (2012) [114] used a multiple linear regression model to estimate splitting tensile strength and failure strength of reinforced sand by waste polystyrene plastic. There are two kinds of model including first and second-order multiple linear regression model. The researcher based on relative bias and relative root mean square error to propose the best model for predicting. Also, they concluded that the developed regression model is a powerful method to predict strength in terms of sand improvement by waste polystyrene plastic.

In this research, cement and corn husk are used to improve soft soil and sludge properties. Water content, cement content, fiber content, and fiber length are four parameters affecting the mechanical properties of soil. Therefore, it is necessary to investigate the relationship between these four parameters and soil characteristics. The purpose of this chapter is to develop regression models for predicting soil properties including failure strength, splitting tensile strength, direct tensile strength, shear strength, and cohesion obtained from Chapters 3 and 4 using water content, cement content, fiber content, and fiber length.

5.2 Data collection and methodology

To understand the effect of water content, cement content, fiber content, and fiber length on mechanical properties of soil with high and low water content, regression models are used to analyze the results from Chapters 3 and 4. In Chapter 3, the relationship between the input parameters including water content, cement content, and fiber content with output parameters including failure strength and splitting tensile strength is investigated. In Chapter 4, strengths consisting of failure strength, splitting tensile strength, direct tensile strength, shear strength, and cohesion are predicted from cement content, fiber content, fiber length, and normal stress.

In this research, there is more than one independent variable, so the multiple linear regression (MLR) and multiple non-linear regression (MNLR) models are applied to predict the mechanical properties of modified soil. The general forms of MLR and MNLR are as follows.

$$y = \beta_0 + \sum_{1}^{n} \beta_n x_n \tag{5-1}$$

$$y = \beta_0 + \sum_{i=1}^{n} \beta_i x_i + \sum_{i=1}^{n} \beta_{ii} x_i^2 + \sum_{i=1}^{n-1} \sum_{j=i+1}^{n} \beta_{ij} x_i x_j \tag{5-2}$$

where y is the output variable, n is the number of the input variable, β_0, β_n, β_i, β_{ii}, and β_{ij} are the coefficients of regression model, x_n, x_i , and x_j are the input variable. The coefficients of regression model are determined by dealing with the matrix form of input and output variables. In geotechnical engineering, these two forms of regression models are popular for predicting some problems such as failure strength, splitting tensile strength, etc. Both MLR and MNLR forms are used to predict output data, but a model giving the best results is selected for predicting based on the evaluation of adjusted coefficient of determination (R^2_a) and root mean square error (RMSE). Eqs. (5-3) and (5-4) show the formulas for calculating an adjusted coefficient of determination and root mean square error, respectively.

$$R_a^2 = 1 - \left[\left(1 - \frac{\sum_{i=1}^{m} \left(y_{Pi} - \overline{y_M} \right)^2}{\sum_{i=1}^{m} \left(y_{Mi} - \overline{y_M} \right)^2} \right) \times \frac{m-1}{m-n-1} \right] \tag{5-3}$$

$$RMSE = \sqrt{\frac{\sum_{i=1}^{m} \left(y_{Pi} - y_{Mi} \right)^2}{m}} \tag{5-4}$$

where R^2_a is the adjusted coefficient of determination, *RMSE* is the root mean square error between measured data and predicted data, m is the number of data, y_{Pi} is the predicted output data of ith data, y_{Mi} is the measured data of ith data, $\overline{y_M}$ is the mean value of measured data, n is the number of input variables.

There are many independent input variables for predicting output variables, and the effective degree of each variable on each output variable is different, so it is necessary to evaluate the contribution of each input variable to the output variable. In this study, the weight of each variable is determined by sensitive analysis [115]. The sensitivity of each independent parameter is determined as follows.

$$N_i = f_{x_i}^{max} - f_{x_i}^{min} \tag{5-5}$$

$$S_i = \frac{N_i}{\sum_{i=1}^{n} N_i} \times 100 \tag{5-6}$$

where $f_{x_i}^{max}$ and $f_{x_i}^{min}$ are the highest and lowest value of predicted output data over the i^{th} input domain, while the other input data are equal to the average value, S_i is the contribution of i^{th} input variable, n is the number of the independent input variable.

5.3 Analysis results

5.3.1 Modified soil produced by Liquified-Stabilized Soil method

As described in Section 5.2, a regression model is applied to predict dependent variables (i.e., failure strength (FS) and splitting tensile strength (STS)) from three independent variables (i.e., water content (W), cement content (C), and fiber content (F)). Therefore, the forms of MLR and MNLR models used to analyze the results of Chapter 3 are given as follows.

$$y = \beta_1 x_1 + \beta_2 x_2 + \beta_3 x_3 \tag{5-7}$$

$$y = \beta_1 x_1 + \beta_2 x_2 + \beta_3 x_3 + \beta_{11} x_1^2 + \beta_{22} x_2^2 + \beta_{33} x_3^2 + \beta_{12} x_1 x_2 + \beta_{13} x_1 x_3 + \beta_{23} x_2 x_3 \tag{5-8}$$

where y is the output variable (FS or STS), β_1 to β_{23} are the coefficients of regression model, x_1 to x_3 are the input variables (W, C, and F).

The MLR and MNLR for predicting FS and STS with their R^2_a and RMSE are shown in Table 5-1. The adjusted coefficient of determination of MLR and MNLR for predicting FS is 0.937 and 0.943 and for predicting STS is 0.936 and 0.942, respectively. It means that there is an insignificant variation of R^2_a between MLR and MNLR models. As listed in the table, the RMSE of MLR model is about 2.5 times higher than that of MNLR model for predicting both FS and STS. In the viewpoint of error between predicted data and measured data, MNLR models for estimating FS and STS show better results than MLR models. Therefore, in this research, MNLR models are selected to estimate FS and STS in terms of Liquified-Stabilized Soil method.

Fig. 5-1 shows experimental data versus predicted data. The figures show that data points are closed to the line of best fit. Furthermore, 90% of the data point is in the range of ±10% for both unconfined compression test and splitting tensile strength. MNLR models are empirical formulas, so these accuracies are very good. However, to verify MNLR model for prediction, some test data points (orange color) are used to confirm MNLR model for predicting failure strength which is a very important property of specimens. These data points are obtained from the additional experiments after empirical formulas were obtained. The additional experimental conditions are shown in Table 5-2. It can be seen from the figure that all test data is extremely closed or on the line of best fit and in the range of ±10%. It means that the selected MNLR model performs the expected output data from input data.

Table 5-1 MLR and MNLR models for predicting strengths

Output		Model	R^2_a	RMSE
Failure strength	MLR	$FS = -3.9553W + 8.3739C + 5.0655F$	0.937	52.6
	MNLR	$FS = -6.1509W + 17.5322C - 14.4085F + 0.0319W^2 - 0.0023C^2 + 0.5273F^2 - 0.1067WC + 0.1014WF + 0.0437FC$	0.943	20.2
Splitting tensile strength	MLR	$STS = -0.7044W + 1.5563C + 0.8682F$	0.936	10.5
	MNLR	$STS = -0.0959W + 2.3416C + -3.4178F - 0.0101W^2 - 0.0047C^2 + 0.1266F^2 - 0.0002WC + 0.0328WF - 0.0051CF$	0.942	4.1

Table 5-2 Additional experimental conditions

Water content (%)	Cement content (kg/m^3)	Fiber content (kg/m^3)
80	70	3
	80	4
	90	8
	90	10
90	70	5
	80	0
	85	7
100	90	5

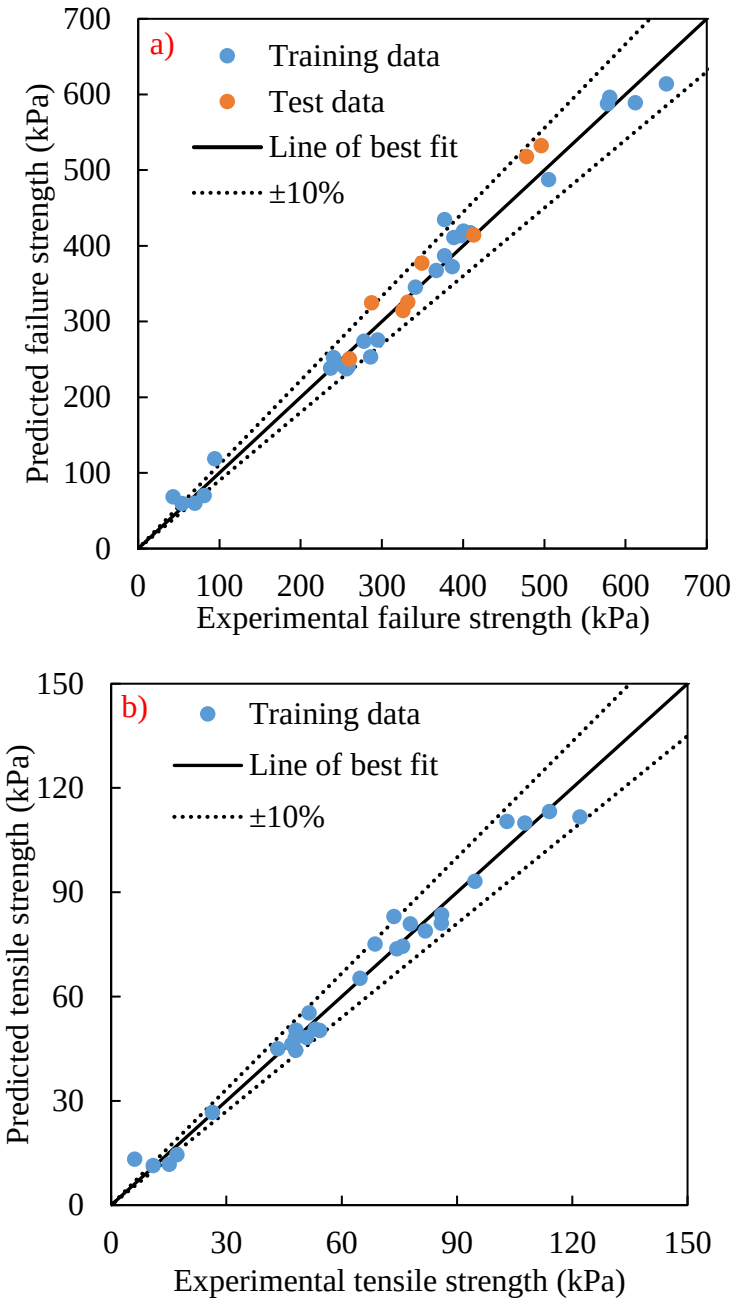

Fig. 5-1 Predicted data versus experimental data

a) Failure strength; b) Splitting tensile strength

Table 5-3 provides the effective degree of independent variables on failure strength and splitting tensile strength. The results display that cement content plays an important role in failure strength and tensile strength with 66.7% and 65.9%, respectively. Fiber content shows the lowest effect on failure strength and tensile strength with 11.8% and 10.7%, respectively. This could be explained by the fact that in Liquified-Stabilized Soil method, cement is added with a great amount to produce cementitious product due to high water content in soil (80%

and 100%). Therefore, a large amount of cement product is mainly responsible for loading. Furthermore, in this method due to no compaction effort, bonding between fiber and soil-cement particles for reinforcing cemented soil is weak. As a result, the addition of fiber has the lowest effect on failure strength and splitting tensile strength.

Table 5-3 The contribution of each input variable to output variable

Output	W (%)	C (%)	F (%)
Failure strength	21.5	66.7	11.8
Splitting tensile strength	23.3	65.9	10.7

5.3.2 Modified soil produced by Fiber-Cement Stabilized Soil method

In this section, the data collection from Chapter 4 is used for prediction. There are three independent variables including cement content (C), fiber content (F), and fiber length (L) for predicting failure strength (FS), splitting tensile strength (STS), direct tensile strength (DTS), and cohesion (CO). The form of MLR and MNLR model of Fiber-Cement Stabilized Soil method are shown in Eqs. (5-9) and (5-10) with three input data. For estimating shear strength (SS), four variables embracing cement content (C), fiber content (F), fiber length (L), and normal stress (N) are used as input data. The forms of model for predicting shear strength are shown in Eqs. (5-11) and (5-12).

$$y = \beta_0 + \beta_1 x_1 + \beta_2 x_2 + \beta_3 x_3 \tag{5-9}$$

$$\begin{aligned} y = {} & \beta_0 + \beta_1 x_1 + \beta_2 x_2 + \beta_3 x_3 + \beta_{11} x_1^2 + \beta_{22} x_2^2 \\ & + \beta_{33} x_3^2 + \beta_{12} x_1 x_2 + \beta_{13} x_1 x_3 + \beta_{23} x_2 x_3 \end{aligned} \tag{5-10}$$

$$y = \beta_0 + \beta_1 x_1 + \beta_2 x_2 + \beta_3 x_3 + \beta_4 x_4 \tag{5-11}$$

$$\begin{aligned} y = {} & \beta_0 + \beta_1 x_1 + \beta_2 x_2 + \beta_3 x_3 + \beta_4 x_4 + \beta_{11} x_1^2 + \beta_{22} x_2^2 + \beta_{33} x_3^2 + \beta_{44} x_4^2 \\ & + \beta_{12} x_1 x_2 + \beta_{13} x_1 x_3 + \beta_{14} x_1 x_4 + \beta_{23} x_2 x_3 + \beta_{24} x_2 x_4 + \beta_{34} x_3 x_4 \end{aligned} \tag{5-12}$$

where y is the output variable (FS, STS, STS, SS, or CO), β_0 to β_{34} are the coefficients of regression model, x_1 to x_4 are the input variables (C, F, L, and N). Table 5-4 lists the MLR and MNLR model, R^2_a, and RMSE of all models for estimating failure strength, splitting tensile strength, direct tensile strength, shear strength, and cohesion. As provided from the table, the adjusted coefficient of determination of MNLR models is higher than that of MLR

models. Especially, in the cases of failure strength, splitting tensile strength, and direct tensile strength, there is a significant variation of R^2_a between MLR and MNLR models. Besides, the RMSE of MNLR model for failure strength, splitting tensile strength, direct tensile strength, shear strength, and cohesion (8.6, 2.3, 0.5, 5.5, and 4.3, respectively) is much lower than that of MLR models (44.8, 8.3, 2.8, 8.0, and 7.7, respectively). It means that the predicted data from MNLR models are more closed to experimental data. Therefore, MNLR models are used for prediction in terms of Fiber-Cement Stabilized Soil method based on a comparison of R^2_a and RMSE.

Fig. 5-2 depicts the estimated data versus experimental data of failure strength, splitting tensile strength, direct tensile strength, shear strength, and cohesion. The figures display that all data points are closed or on the line of best fit. Especially, all data points of direct tension test are on the line of best fit. Besides, almost all data are in the range of ± 10%, so the accuracy of selected MNLR models is quite high. However, to confirm MNLR model for prediction, the model for predicting failure strength is verified by some test data (orange color) like the previous section, as seen from Fig. 5-2a. These data points are obtained from the additional experiments after empirical formulas were obtained. The experimental conditions are shown in Table 5-5. The results show that all test data is closed to the line of best fit and in the range of ±10%. Therefore, like the test results of MNLR model for predicting failure strength of Liquified-Stabilized Soil method, it is concluded that MNLR model for predicting failure strength of Fiber-Cement Stabilized Soil method performs very good prediction.

The weight of all variables in MNLR models is reported in Table 5-6. As given from the table, the effect of fiber length and fiber content on failure strength and splitting tensile strength is more significant than that of cement content. Fiber length and fiber content perform the highest weight to failure strength (39.4%) and splitting tensile strength (47.7%), respectively. In the case of direct tension test, the effect of cement content and fiber content on direct tensile strength is the same (40.0% and 39.9%, respectively) and is much higher than that of fiber length (20.1%). In shear box test, normal stress and fiber content make the highest distribution to shear strength (34.7%) and cohesion (45.2%), respectively. Fiber length performs the lowest effective degree on shear strength and cohesion. In general, fiber content has an important effect on output parameters with a very high percentage of contribution in terms of Fiber-Cement Stabilized Soil method.

Table 5-4 MLR and MNLR models for predicting strengths

Output		Model	R^2_a	RMSE
Failure strength	MLR	$FS = 171.1703 + 6.2272C + 7.8026F - 0.5434L$	0.717	44.8
	MNLR	$FS = 63.5010 + 23.1651C - 5.5485F + 8.3596L - 0.4432C^2 + 0.1016F^2 - 0.3326L^2 + 0.1362CF + 0.0212CL + 0.2788FL$	0.971	9.6
Splitting tensile strength	MLR	$STS = 5.8440 + 0.6603C + 2.1926F + 0.5201L$	0.808	8.3
	MNLR	$STS = 4.7350 + 1.6410C - 1.0424F + 0.5199L - 0.0200C^2 + 0.0731F^2 - 0.0218L^2 - 0.0077CF - 0.0006CL + 0.1242FL$	0.968	2.3
Direct tensile strength	MLR	$DTS = 17.4398 + 0.6779C + 0.0780F - 0.0116L$	0.881	2.8
	MNLR	$DTS = 10.9000 + 1.8782C - 0.4913F + 0.3435L - 0.0310C^2 + 0.0185F^2 - 0.0159L^2 + 0.0117CF + 0.0011CL + 0.0243FL$	0.992	0.5
Shear strength	MLR	$SS = 21.4461 + 2.5522C + 2.2484F - 0.2425L + 0.5829N$	0.953	8.0
	MNLR	$SS = 25.224 + 1.992C + 6.184F - 2.2639L + 0.5389N + 0.0209C^2 - 0.0250F^2 + 0.0429L^2 + 0.0002N^2 - 0.1288CF + 0.0290CL + 0.0008CN - 0.0153FL + 0.0018FN - 0.0014LN$	0.970	5.5
Cohesion	MLR	$CO = 24.1626 + 2.3930C + 2.0964F - 0.1072L$	0.917	7.7
	MNLR	$CO = 25.5850 + 1.7088C + 8.9192F - 3.1922L + 0.0253C^2 - 0.1651F^2 + 0.0586L^2 - 0.1356CF + 0.0346CL - 0.0027FL$	0.942	4.3

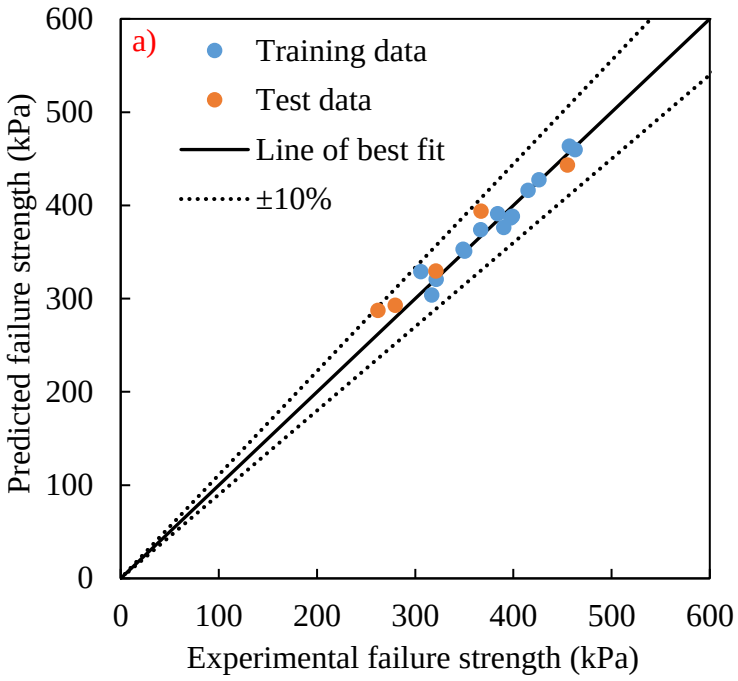
a)
Training data
Test data
Line of best fit
±10%
Predicted failure strength (kPa)
Experimental failure strength (kPa)
0
100
200
300
400
500
600

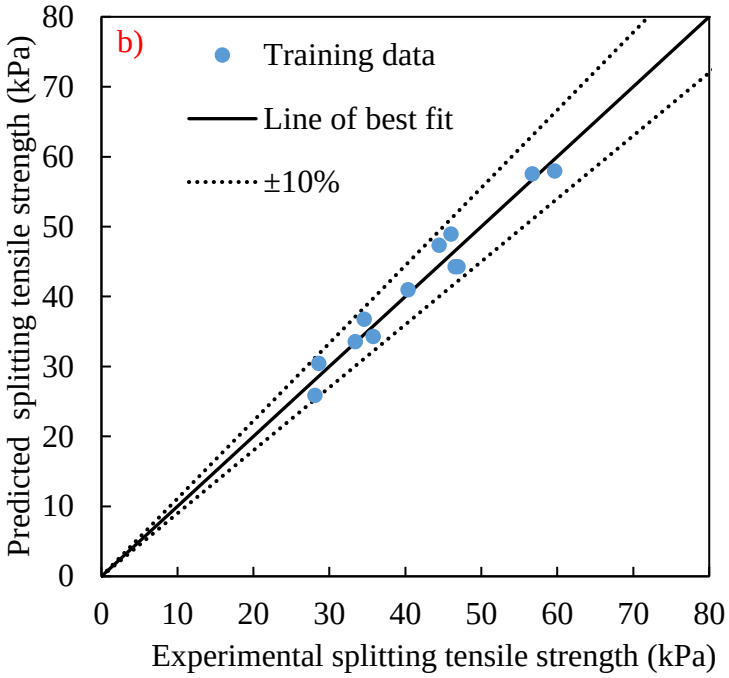
b)
Training data
Line of best fit
±10%
Predicted splitting tensile strength (kPa)
Experimental splitting tensile strength (kPa)
0
10
20
30
40
50
60
70
80

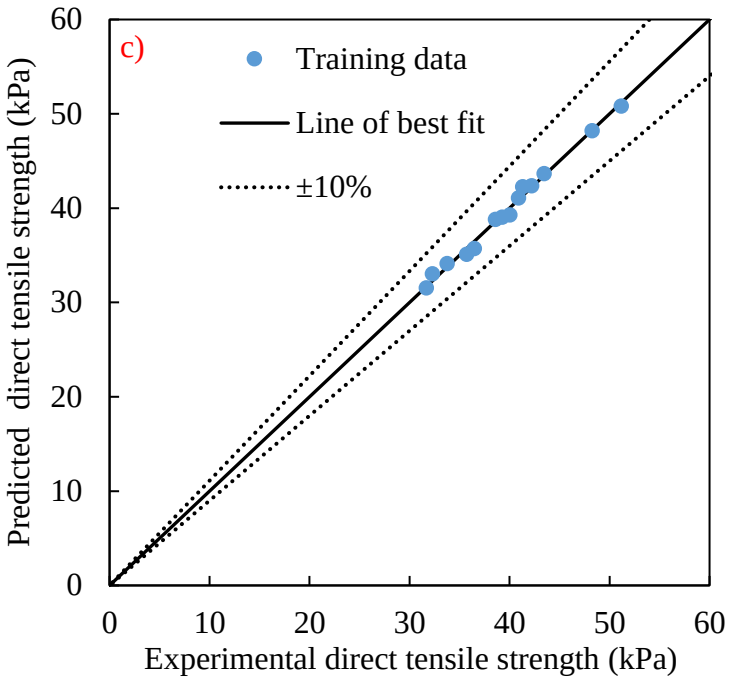
c)
Training data
Line of best fit
±10%
Predicted direct tensile strength (kPa)
Experimental direct tensile strength (kPa)
0
10
20
30
40
50
60

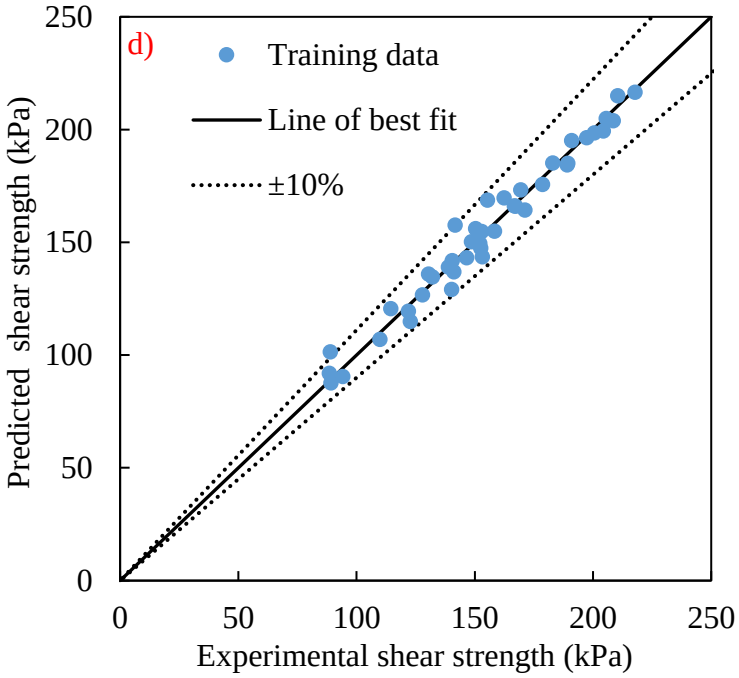
d)
Training data
Line of best fit
±10%
Predicted shear strength (kPa)
Experimental shear strength (kPa)
0
50
100
150
200
250

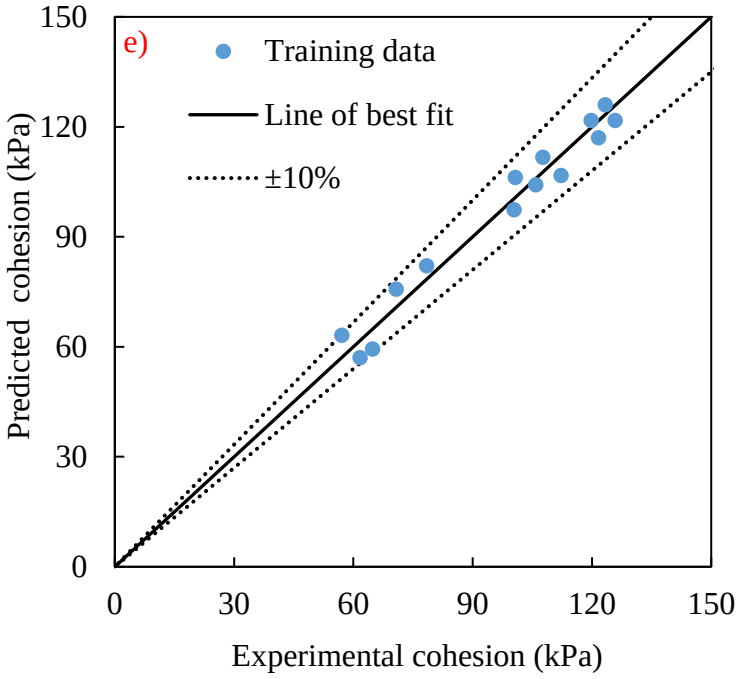

Fig. 5-2 Predicted data versus experimental data

a) Failure strength; b) Splitting tensile strength;

c) Direct tensile strength; d) Shear strength; e) Cohesion

Table 5-5 Additional experimental conditions

Cement content (kg/m^3)	Fiber content (kg/m^3)	Fiber length (mm)
12	10	10
14	5	30
16	2	30
18	5	20
32	14	30

Table 5-6 The contribution of each input variable to output variable

Output	C (%)	F (%)	L (%)	S (%)
Failure strength	27.1	33.5	39.4	-
Splitting tensile strength	14.5	47.7	37.8	-
Direct tensile strength	40.0	39.9	20.1	-
Shear strength	26.3	27.3	11.7	34.7
Cohesion	36.9	45.2	17.8	-

5.4 Conclusions

This chapter applies regression model including multiple linear and non-linear regression models to predict output data and evaluate the relationship between input data and output data obtained from Chapters 3 and 4. The best models are determined based on the comparison of adjusted coefficient of determination and root mean square error. Some conclusions are shown below.

- Input and output variables in terms of both Liquified-Stabilized Soil method and Fiber-Cement Stabilized Soil method perform the good relationships.
- The form of MNLR models is more complicated than that of MLR models.
- For Liquified-Stabilized Soil method, there is an insignificant variation of R^2_a between MLR and MNLR models. However, for Fiber-Cement Stabilized Soil method, R^2_a of MNLR models is much higher than that of MLR models.
- MNLR models perform better results of RMSE than MLR models in terms of both two methods for soil stabilization.
- MNLR models show a better prediction than MLR models based on the evaluation of adjusted coefficient of determination and root mean square error.
- Cement content and fiber content perform the highest and lowest effective degree to output variables in Liquified-Stabilized Soil method.
- Fiber length and fiber content show the highest effective degree on failure strength and splitting tensile strength, respectively. For direct tensile strength, cement content and fiber content perform the same contribution. In shear box test, normal stress and fiber content show the highest contribution to shear strength and cohesion, respectively.

CHAPTER 6
CONCLUSIONS

6.1 Conclusions

In Viet Nam, not only the construction sludge and soft soil produced from construction sites but also crop residue burning from agriculture cause environmental and economic problems. The Fiber-Cement-Stabilized Soil method and Liquified-Stabilized Soil method are the effective solutions to reduce the amount of construction sludge and soft soil discharged to the final disposal by modifying sludge and soft soil for reusing in construction. Besides, the use of by-products as a fiber material replacing paper debris for soil improvement in Viet Nam also contributes to the solution of crop residue burning problems. However, it is not clear about the suitable kind of by-product and workability of by-products for soil improvement in Viet Nam. Therefore, a series of experiments is carried out in this study to find out fiber giving good performance in terms of fiber-cement stabilized soil. The selected fiber is used to reinforce cemented soil with high water content in terms of the Liquified-Stabilized Soil method and low water content in terms of the Fiber-Cement Stabilized Soil method. The summary of this research is as follows.

Chapter 1 is an introduction.

In Chapter 2, to find out the best by-product for soil improvement, a series of laboratory experiments including unconfined compression, splitting tension, permeability, and durability tests are carried out. The workability of five kinds of fiber (i.e., corn husk, corn silk, rice straw, rice husk, and paper debris) is evaluated using two kinds of imitated sludge (sludge No.1 including 40% Kasaoka clay and 60% silk, sludge No.2 including 40% sand and 60% Kasaoka clay). The results show that fiber inclusions improve failure strength and tensile strength of cement soil. The general order of fiber according to the ascending order of failure strength and tensile strength is rice husk, paper debris, corn silk, rice straw, and corn husk. The hydraulic conductivity of specimens is highest when adding paper debris and lowest when adding rice straw to sludge No. 1 and corn husk to sludge No.2. Besides, cemented sludge with the inclusion of rice straw, corn silk, and corn husk survives after 10^{th} cycle of drying and wetting. Based on the experimental results, mixing conditions with corn husk inclusion show the best performance in general. Therefore, corn husk fiber is selected for soil improvement. The mechanical properties of corn husk fiber-cement stabilized soil are evaluated in terms of Liquified-Stabilized Soil method for soil with high water content and Fiber-Cement Soil Stabilized Soil method for soil with low water content in next chapters.

In Chapter 3, bleeding, flow, unconfined compression, splitting tension, and durability tests are conducted to investigate properties of corn husk fiber-cement stabilized soil with high water content produced by Liquified-Stabilized Soil method. Besides, tensile strength of corn husk fiber is studied to understand more clearly corn husk fiber property. The experimental results show that cement and fiber content are the important parameters affecting bleeding ratio and flow value. The increase in cement and fiber content results in the reduction of bleeding ratio and flow value. Fiber inclusion improves failure strength and tensile strength to some extent. With low cement content, failure strength and tensile strength increase with the increase in fiber content. However, the improvement effect of corn husk fiber on cemented soil decreases for mixing conditions of high cement content. Fiber inclusion diminishes loss of post-peak stress and results in the appearance of second tensile strength in some cases of splitting tension test. It translates that the behavior of cemented soil changes from ductile to brittle when adding corn husk fiber. Besides, the increase of fiber content leads to an increase in energy absorption and stiffness to some extent. The addition of fiber contributes to the limitation of the appearance and propagation of cracks under cycle of drying and wetting. As a result, specimens with fiber inclusion show trivial damage under cycle of drying and wetting, meanwhile, the cracks appear and propagate strongly for specimens without fiber inclusion.

In Chapter 4, the laboratory tests consisting of unconfined compression, splitting tension, direct tension, and shear box tests are carried out to evaluate the behavior of corn husk fiber-reinforced cemented soil with low water content produced by Fiber-Cement Stabilized Soil method. This research focuses on the impact of corn husk fiber on the cemented soil properties with different fiber contents and fiber lengths. The results show that corn husk inclusion improves failure strength, splitting tensile strength, direct tensile strength, shear strength, and cohesion in general. The increase of failure strain and the decrease of loss of post-peak stress due to the presence of fiber translate that cemented soil becomes more ductile when added fiber. Moreover, the increase in fiber content contributes to the markable enlargement of energy absorption, the decrease of secant modulus, and the decrease of loss of post-peak stress. In splitting tension test, the improvement effect of fiber on ultimate tensile strength is higher than that on yield tensile strength. Besides, fiber at the crack carrying the load leads to the appearance of residual stress to delay the complete destruction of specimens in terms of direct tension test. In shear box test, both residual stress and cohesion of specimens without fiber inclusion are enhanced due to the addition of corn husk

fiber in some cases.

In Chapter 5, regression models consisting of MNLR and MLR models are applied to Chapters 3 and 4 to analyze the relationships between input parameters and output parameters. Furthermore, the models for predicting output variables including failure strength, splitting tensile strength, direct tensile strength, shear strength, and cohesion are proposed from input variables including water content, cement content, fiber content, fiber length, and normal stress. The analysis results indicate that MNLR models show a better prediction than MLR models based on the comparison of adjusted coefficient with determination and root mean square error. In Liquified-Stabilized Soil method, the contribution of fiber content to output parameters is lowest. However, for Fiber-Cement Stabilized Soil method, fiber content makes an important contribution to output variables.

Finally, Chapter 6 is conclusions and future perspective of this research.

6.2 Future perspective and practical application

The stabilization of soft soil and sludge by cement shows good performance such as high failure strength and tensile strength. However, there are some unwanted properties of stabilized soil in this method such as brittle behavior and low durability [116]. Especially, the durability of material against water and weather effect is very vital in the practical application. In geotechnical engineering, the inclusion of fiber leads to the improvement of durability and ductility of cemented soil. Therefore, the addition of fiber is an effective solution for the weakness of cemented soil. A review by Hejazi et al. (2012) [117] showed that natural fiber or synthetic fiber use is feasible in six fields of geotechnical engineering: protection of slope, railway embankment, road construction, retaining walls, soil-foundation engineering, and earthquake. Moreover, it is feasible to apply Liquified-Stabilized Soil method at narrow construction sites or underground without compaction energy. These reasons provide an incentive to enlarge its application field. In Japan, cement-treated dredged soil was used for pavement upon subsoil for traffic, backfill as seep-proof structure, widening dike for leak prevention of muddy water, and embankment inside reclamation [67]. Besides, many researchers reported several applications of modified sludge in construction including filling a cavity under pavement, backfilling of void under floor due to subsidence, underwater seawall, abutment, underground pipe, and building foundation [79, 118, 119].

In this study, corn husk, new material in this field, is used to enhance its properties. The

results show that fiber works well in cemented soil with a significant improvement of failure strength, ductility, energy absorption, stiffness, and durability. Especially, the inclusion of corn husk leads to the enhancement of ductile property and energy absorption which play an important role in an ani-earthquake. It means that corn husk seems to be a new promising material in geotechnical engineering. This study is the premise of application in practice and the following studies on corn husk fiber-cement stabilized soil with high and low water content.

From an environmental viewpoint, soft soil and sludge reinforced by cement and corn husk bring several advantages. A large amount of crop residue of maize, soft soil and sludge from construction sites are treated without environmental effect. These make a very important contribution to the development of Viet Nam. Viet Nam is an agricultural and developing country. The treatment of by-products from agriculture is a serious issue causing many environmental problems. The application of this method in practice is meaningful in decreasing the impacts of crop residue treatment on environment in Viet Nam. Besides, the developing speed of Viet Nam is quite high with more and more infrastructure established for the present and in the future. Treatment of a large amount of excavated soil and sludge from construction sites becomes a big problem. For example, Viet Nam had a plan to build Metro Rail System with many six lines in Ho Chi Minh City. A large amount of excavated soft soil and sludge would be discharged from this project. Therefore, the soft soil and sludge recycled by Fiber-Cement Stabilized Soil method and Liquified-Stabilized Soil method using agricultural by-product make an important contribution to solution of soft soil and sludge discharge problems.

6.3 Future study

- In practice, many kinds of soft soil and sludge are discharged into the environment. The improvement effect of corn husk fiber on different kinds of soft soil and sludge is significantly different due to variation of grain size distribution. Therefore, it is necessary to investigate the workability of corn husk fiber in different kinds of soft soil and sludge.

- In this study, the durability of specimens was carried out with 10 cycles for drying and wetting. This is the test with the severe conditions in 30 days. However, it is unclear about the behaviors of specimens after 30 days. Thus, in the next study, the durability of specimens for the long term is investigated. For example, 3 months, 6 months, 1 year, etc.

- Acid and base environments have a significant effect on failure strength and durability of fiber-cement stabilized soil. Hence, the behaviors of fiber-cement stabilized soil in acid and base environments need to be studied.

REFERENCES

1. Viet, N.T., Dieu, T.T.M., Loan, N.T.P.: Current Status of Sludge Collection, Transportation and Treatment in Ho Chi Minh City. J. Environ. Prot. (Irvine,. Calif). 04, 1329–1335 (2013). https://doi.org/10.4236/jep.2013.412154.
2. Ho Chi Minh City People's Committee Management Authority for Urban Railways: Environmental Impact Assessment. (2012).
3. Johnson, O.A., Napiah, M., Kamaruddin, I.: Potential uses of Waste Sludge in Construction Industry: A Review. Res. J. Appl. Sci. Eng. Technol. 8, 565–570 (2014). https://doi.org/10.19026/rjaset.8.1006.
4. Movilla-Quesada, D., Vega-Zamanillo, Á., Castro-Fresno, D., Calzada-Pérez, M.A., Raposeiras, A.C.: Sustainability in construction works: Reuse of sludge from tunnel boring in lime mortars. Appl. Clay Sci. 114, 402–406 (2015). https://doi.org/10.1016/j.clay.2015.05.019.
5. Liew, A.G., Idris, A., Wong, C.H.K., Samad, A.A., Noor, M.J.M.M., Baki, A.M.: Incorporation of sewage sludge in clay brick and its characterization. Waste Manag. Res. 22, 226–233 (2004). https://doi.org/10.1177/0734242X04044989.
6. Chiang, K.Y., Chou, P.H., Hua, C.R., Chien, K.L., Cheeseman, C.: Lightweight bricks manufactured from water treatment sludge and rice husks. J. Hazard. Mater. 171, 76–82 (2009). https://doi.org/10.1016/j.jhazmat.2009.05.144.
7. Nam, G.S.O. of V.: Agriculture, Forestry, & Fishing. Stat. Yearb. Viet Nam 2016. 421–530 (2016).
8. Koopmans, A., Koppejan, J.: Agricultural and forest residues - Generation, utilization and availability. Reg. Consult. Mod. Appl. Biomass Energy. 6–10 (1997). https://doi.org/10.1016/S0251-1088(83)90310-8.
9. The Project for Capacity Building for National Greenhouse Gas Inventory in Viet Nam: Inventory National GHG Report of Vietnam. (2010).
10. Takahashi, H.: Waste materials in construction: Sludge and recycling. Top. Themes Energy Resour. A Cross-Disciplinary Educ. Train. Progr. Environ. Leaders. 177–194 (2015). https://doi.org/10.1007/978-4-431-55309-0_10.
11. Sasanian, S., Newson, T.A.: Basic parameters governing the behaviour of cement-treated clays. Soils Found. 54, 209–224 (2014). https://doi.org/10.1016/j.sandf.2014.02.011.
12. Chew, S.H., Kamruzzaman, A.H.M., Lee, F.H.: Physicochemical and Engineering Behavior of Cement Treated Clays. J. Geotech. Geoenvironmental Eng. 130, 696–706 (2004). https://doi.org/10.1061/(asce)1090-0241(2004)130:7(696).
13. Sariosseiri, F., Muhunthan, B.: Effect of cement treatment on geotechnical properties of some Washington State soils. Eng. Geol. 104, 119–125 (2009). https://doi.org/10.1016/j.enggeo.2008.09.003.
14. Dafalla, M.A., Moghal, A.A.B., Al-Obaid, A.K.: Enhancing tensile strength in clays using polypropylene fibers. Int. J. Geomate. 12, 33–37 (2017). https://doi.org/10.21660/2017.29.5263.
15. Correia, A.A.S., Venda Oliveira, P.J., Custódio, D.G.: Effect of polypropylene fibres on the compressive and tensile strength of a soft soil, artificially stabilised with binders. Geotext. Geomembranes. 43, 97–106 (2015). https://doi.org/10.1016/j.geotexmem.2014.11.008.
16. Venda Oliveira, P.J., Correia, A.A.S., Teles, J.M.N.P.C., Custódio, D.G.: Effect of fibre type on the compressive and tensile strength of a soft soil chemically stabilised. Geosynth. Int. 23, 171–182 (2015). https://doi.org/10.1680/jgein.15.00040.
17. Chen, M., Shen, S.L., Arulrajah, A., Wu, H.N., Hou, D.W., Xu, Y.S.: Laboratory

evaluation on the effectiveness of polypropylene fibers on the strength of fiber-reinforced and cement-stabilized Shanghai soft clay. Geotext. Geomembranes. 43, 515–523 (2015). https://doi.org/10.1016/j.geotexmem.2015.05.004.
18. Tang, C.-S., Shi, B., Cui, Y.-J., Liu, C., Gu, K.: Desiccation cracking behavior of polypropylene fiber–reinforced clayey soil. Can. Geotech. J. 49, 1088–1101 (2012). https://doi.org/10.1139/t2012-067.
19. Botero, E., Ossa, A., Sherwell, G., Ovando-Shelley, E.: Stress-strain behavior of a silty soil reinforced with polyethylene terephthalate (PET). Geotext. Geomembranes. 43, 363–369 (2015). https://doi.org/10.1016/j.geotexmem.2015.04.003.
20. Estabragh, A.R., Namdar, P., Javadi, A.A.: Behavior of cement-stabilized clay reinforced with nylon fiber. Geosynth. Int. 19, 85–92 (2012). https://doi.org/10.1680/gein.2012.19.1.85.
21. Consoli, N.C., Prietto, P.D.M., Ulbrich, L.A.: Influence of Fiber and Cement Addition. J. Geotech. Geoenvironmental Eng. 124, 1211–1214 (1998).
22. Consoli, N.C., Vendruscolo, M.A., Fonini, A., Rosa, F.D.: Fiber reinforcement effects on sand considering a wide cementation range. Geotext. Geomembranes. 27, 196–203 (2009). https://doi.org/10.1016/j.geotexmem.2008.11.005.
23. Consoli, N.C., Arcari Bassani, M.A., Festugato, L.: Effect of fiber-reinforcement on the strength of cemented soils. Geotext. Geomembranes. 28, 344–351 (2010). https://doi.org/10.1016/j.geotexmem.2010.01.005.
24. Freitag, D.R.: Soil Randomly Reinforced with Fibers. J. Geotech. Eng. 112, 823–826 (1986). https://doi.org/10.1061/(ASCE)0733-9410(1986)112:8(823).
25. Tubiello, F.N., Salvatore, M., Cóndor Golec, R.D., Ferrara, A., Rossi, S., Biancalani, R., Federici, S., Jacobs, H., Flammini, A.: Agriculture , Forestry and Other Land Use Emissions by Sources and Removals by Sinks. ESS Work. Pap. No.2. 2, 4–89 (2014). https://doi.org/10.13140/2.1.4143.4245.
26. Mohammed, L., Ansari, M.N.M., Pua, G., Jawaid, M., Islam, M.S.: A Review on Natural Fiber Reinforced Polymer Composite and Its Applications. Int. J. Polym. Sci. 2015, (2015). https://doi.org/10.1155/2015/243947.
27. Ardanuy, M., Claramunt, J., Toledo Filho, R.D.: Cellulosic fiber reinforced cement-based composites: A review of recent research. Constr. Build. Mater. 79, 115–128 (2015). https://doi.org/10.1016/j.conbuildmat.2015.01.035.
28. Yan, L., Kasal, B., Huang, L.: A review of recent research on the use of cellulosic fibres, their fibre fabric reinforced cementitious, geo-polymer and polymer composites in civil engineering. Compos. Part B Eng. 92, 94–132 (2016). https://doi.org/10.1016/j.compositesb.2016.02.002.
29. Lenoir, T., Preteseille, M., Ricordel, S.: Contribution of the fiber reinforcement on the fatigue behavior of two cement-modified soils. Int. J. Fatigue. 93, 71–81 (2016). https://doi.org/10.1016/j.ijfatigue.2016.08.007.
30. Prabakar, J., Sridhar, R.S.: Effect of random inclusion of sisal fibre on strength behaviour of soil. Constr. Build. Mater. 16, 123–131 (2002). https://doi.org/10.1016/S0950-0618(02)00008-9.
31. Wu, Y., Li, Y., Nui, B.: Assessment of the Mechanical Properties of Sisal Fiber-Reinforced Silty Clay Using Triaxial Shear Tests. ScientificWorldJournal. 2014, 9 (2014). https://doi.org/10.1155/2014/436231.
32. Yixian, W., Panpan, G., Shengbiao, S., Haiping, Y., Binxiang, Y.: Study on Strength Influence Mechanism of Fiber-Reinforced Expansive Soil Using Jute. Geotech. Geol. Eng. 34, 1079–1088 (2016). https://doi.org/10.1007/s10706-016-0028-4.
33. Mostafa, M., Uddin, N.: Effect of Banana Fibers on the Compressive and Flexural Strength of Compressed Earth Blocks. Buildings. 5, 282–296 (2015).

https://doi.org/10.3390/buildings5010282.
34. Mori, M., Takahashi, H., Kumakura, K.: An Experimental Study on the Durability of Fiber-Cement-Stabilized Mud by Repeated Cycle Test of Drying and Wetting. J. Min. Mater. Process. Inst. Japan. 121, 37–43 (2005). https://doi.org/10.2473/shigentosozai.121.37.
35. Satomi, T., Kuribara, H., Takahashi, H.: Evaluation of Failure Strength Property and Permeability of Fiber-Cement-Stabilized Soil Made of Tsunami Sludge. J. JSEM. 14, 303–308 (2014). https://doi.org/10.1117/12.2076716.
36. Tran, K.Q., Satomi, T., Takahashi, H.: Study on strength behavior of cement stabilized sludge reinforced with waste cornsilk fiber. Int. J. Geomate. 13, 140–147 (2017). https://doi.org/10.21660/2017.39.28994.
37. Youssef, A.M., El-Gendy, A., Kamel, S.: Evaluation of corn husk fibers reinforced recycled low density polyethylene composites. Mater. Chem. Phys. 152, 26–33 (2015). https://doi.org/10.1016/j.matchemphys.2014.12.004.
38. Tachaapaikoon, C., Kyu, K.L., Ratanakhanokchai, K.: Purification of xylanase from alkaliphilic Bacillus sp. K-8 by using corn husk column. Process Biochem. 41, 2441–2445 (2006). https://doi.org/10.1016/j.procbio.2006.07.004.
39. Alves Fidelis, M.E., Pereira, T.V.C., Gomes, O.D.F.M., De Andrade Silva, F., Toledo Filho, R.D.: The effect of fiber morphology on the tensile strength of natural fibers. J. Mater. Res. Technol. 2, 149–157 (2013). https://doi.org/10.1016/j.jmrt.2013.02.003.
40. Defoirdt, N., Biswas, S., Vriese, L. De, Tran, L.Q.N., Acker, J. Van, Ahsan, Q., Gorbatikh, L., Vuure, A. Van, Verpoest, I.: Assessment of the tensile properties of coir, bamboo and jute fibre. Compos. Part A Appl. Sci. Manuf. 41, 588–595 (2010). https://doi.org/10.1016/j.compositesa.2010.01.005.
41. Wei, J., Ma, S., Thomas, D.G.: Correlation between hydration of cement and durability of natural fiber-reinforced cement composites. Corros. Sci. 106, 1–15 (2016). https://doi.org/10.1016/j.corsci.2016.01.020.
42. Wei, J., Meyer, C.: Utilization of rice husk ash in green natural fiber-reinforced cement composites: Mitigating degradation of sisal fiber. Cem. Concr. Res. 81, 94–111 (2016). https://doi.org/10.1016/j.cemconres.2015.12.001.
43. Wei, J., Meyer, C.: Degradation mechanisms of natural fiber in the matrix of cement composites. Cem. Concr. Res. 73, 1–16 (2015). https://doi.org/10.1016/j.cemconres.2015.02.019.
44. Vatani Oskouei, A., Afzali, M., Madadipour, M.: Experimental investigation on mud bricks reinforced with natural additives under compressive and tensile tests. Constr. Build. Mater. 142, 137–147 (2017). https://doi.org/10.1016/j.conbuildmat.2017.03.065.
45. Chien, P.T., Satomi, T., Takahashi, H.: Study on strength characteristics of rice straw fiber-cement-reinforced sludge. Int. J. Soc. Mater. Eng. Resour. 23, 147–151 (2018). https://doi.org/10.5188/ijsmer.23.147.
46. Ho Chi Minh City Urban Railway Construction Project, B.T.-S.T. (Line 1): Geotechnical Investigation Report for Design Package 1. (2013).
47. De Carvalho Mendes, C.A., De Oliveira Adnet, F.A., Leite, M.C.A.M., Furtado, C.R.G., De Sousa, A.M.F.: Chemical, physical, mechanical, thermal and morphological characterization of corn husk residue. Cellul. Chem. Technol. 49, 727–735 (2015).
48. Rahman, N.A., Wan Rosli, W.I.: Nutritional compositions and antioxidative capacity of the silk obtained from immature and mature corn. J. King Saud Univ. - Sci. 26, 119–127 (2014). https://doi.org/10.1016/j.jksus.2013.11.002.
49. Chandrasekhar, S., Satyanarayana, K.G., Pramada, P.N., Raghavan, P., Gupta, T.N.:

Review Processing, properties and applications of reactive silica from rice husk—an overview. J. Mater. Sci. 38, 3159–3168 (2003). https://doi.org/10.1023/A:1025157114800.
50. Bakker, R., Elbersen, W., Ronald Poppens, J., Lesschen, P.: Rice straw and Wheat straw Potential feedstocks for the Biobased Economy Colofon. NL Agency Minist. Econ. Aff. 1–31 (2013).
51. Tejado, A., Van De Ven, T.G.M.: Why does paper get stronger as it dries? Mater. Today. 13, 42–49 (2010). https://doi.org/10.1016/S1369-7021(10)70164-4.
52. ASTM D2166/D2166M: Standard Test Method for Unconfined Compressive Strength of Cohesive Soil. ASTM Int. 04, 1–6 (2016).
53. ASTM C496: Standard Test Method for Splitting Tensile Strength of Cylindrical Concrete Specimens, ASTM International, West Conshohocken, PA, USA. (2017). https://doi.org/10.1520/C0496_C0496M-17.
54. Tang, C., Shi, B., Gao, W., Chen, F., Cai, Y.: Strength and mechanical behavior of short polypropylene fiber reinforced and cement stabilized clayey soil. Geotext. Geomembranes. 25, 194–202 (2007). https://doi.org/10.1016/j.geotexmem.2006.11.002.
55. Li, J., Tang, C., Wang, D., Pei, X., Shi, B.: Effect of discrete fibre reinforcement on soil tensile strength. J. Rock Mech. Geotech. Eng. 6, 133–137 (2014). https://doi.org/10.1016/j.jrmge.2014.01.003.
56. Mesbah, A., Morel, J.C., Walker, P., Ghavami, K.: Development of a Direct Tensile Test for Compacted Earth Blocks Reinforced with Natural Fibers. J. Mater. Civ. Eng. 16, 95–98 (2004). https://doi.org/10.1061/(asce)0899-1561(2004)16:1(95).
57. Yan, G., Zhang, H., Wang, X., Li, M., Zhao, T.: Study on the permeability of reinforced soil with herb fiber under different salt solution concentration. Adv. Mater. Res. 308–310, 2291–2296 (2011). https://doi.org/10.4028/www.scientific.net/AMR.308-310.2291.
58. Xiao, H., Liu, Y.: A prediction model for the tensile strength of cement-admixed clay with randomly orientated fibres. Eur. J. Environ. Civ. Eng. 22, 1131–1145 (2018). https://doi.org/10.1080/19648189.2016.1232662.
59. Tran, K.Q., Satomi, T., Takahashi, H.: Improvement of mechanical behavior of cemented soil reinforced with waste cornsilk fibers. Constr. Build. Mater. 178, 204–210 (2018). https://doi.org/10.1016/j.conbuildmat.2018.05.104.
60. Zhu, W., Zhang, C.L., Chiu, A.C.F.: Soil–Water Transfer Mechanism for Solidified Dredged Materials. J. Geotech. Geoenvironmental Eng. 133, 588–598 (2007). https://doi.org/10.1061/(asce)1090-0241(2007)133:5(588).
61. Kamruzzaman, A.H., Chew, S.H., Lee, F.H.: Structuration and destructuration behavior of cement-treated Singapore marine clay. J. Geotech. Geoenvironmental Eng. 135, 573–589 (2009). https://doi.org/10.1061/(ASCE)1090-0241(2009)135:4(573).
62. Farzana, F.H., Rafizul, I.M., Alamgir, M.: Engineering behaviour of cement treated soft clay at high water content. Proc. 3rd Int. Conf. Civ. Eng. Sustain. Dev. (ICCESD 2016). 960–969 (2016).
63. Horpibulsuk, S., Miura, N., Bergado, D.T.: Undrained Shear Behavior of Cement Admixed Clay at High Water Content. J. Geotech. Geoenvironmental Eng. 130, 1096–1105 (2004). https://doi.org/10.1061/(asce)1090-0241(2004)130:10(1096).
64. Chiu, C.F., Zhu, W., Zhang, C.L.: Yielding and shear behaviour of cement-treated dredged materials. Eng. Geol. 103, 1–12 (2009). https://doi.org/10.1016/j.enggeo.2008.07.007.
65. Lee, F.-H., Lee, Y., Chew, S.-H., Yong, K.-Y.: Strength and Modulus of Marine Clay-Cement Mixes. J. Geotech. Geoenvironmental Eng. 131, 178–186 (2005).

https://doi.org/10.1061/(asce)1090-0241(2005)131:2(178).
66. Zhang, R.J., Santoso, A.M., Tan, T.S., Phoon, K.K.: Strength of High Water-Content Marine Clay Stabilized by Low Amount of Cement. J. Geotech. Geoenvironmental Eng. 139, 2170–2181 (2013). https://doi.org/10.1061/(asce)gt.1943-5606.0000951.
67. Tang, Y.X., Miyazaki, Y., Tsuchida, T.: Practices of reused dredgings by cement treatment. Soils Found. 41, 129–143 (2001). https://doi.org/10.3208/sandf.41.5_129.
68. Kitazume, M., Hayano, K.: Strength properties and variance of cement-treated ground using the pneumatic flow mixing method. Proc. Inst. Civ. Eng. - Gr. Improv. 11, 21–26 (2007). https://doi.org/10.1680/grim.2007.11.1.21.
69. Jongpradist, P., Jumlongrach, N., Youwai, S., Chucheepsakul, S.: Influence of Fly Ash on Unconfined Compressive Strength of Cement-Admixed Clay at High Water Content. J. Mater. Civ. Eng. 22, 49–58 (2009). https://doi.org/10.1061/(asce)0899-1561(2010)22:1(49).
70. Miura, N., Horpibulsuk, S., Nagaraj, T.S.: Engineering behavior of cement stabilized clay at high water content. Soils Found. 41, 33–45 (2001). https://doi.org/10.3208/sandf.41.5_33.
71. Tran, K.Q., Satomi, T., Takahashi, H.: Effect of waste cornsilk fiber reinforcement on mechanical properties of soft soils. Transp. Geotech. 16, 76–84 (2018). https://doi.org/10.1016/j.trgeo.2018.07.003.
72. Bordoloi, S., Kashyap, V., Garg, A., Sreedeep, S., Wei, L., Andriyas, S.: Measurement of mechanical characteristics of fiber from a novel invasive weed: A comprehensive comparison with fibers from agricultural crops. Meas. J. Int. Meas. Confed. 113, 62–70 (2018). https://doi.org/10.1016/j.measurement.2017.08.044.
73. Park, S.S.: Unconfined compressive strength and ductility of fiber-reinforced cemented sand. Constr. Build. Mater. 25, 1134–1138 (2011). https://doi.org/10.1016/j.conbuildmat.2010.07.017.
74. Sharma, V., Vinayak, H.K., Marwaha, B.M.: Enhancing compressive strength of soil using natural fibers. Constr. Build. Mater. 93, 943–949 (2015). https://doi.org/10.1016/j.conbuildmat.2015.05.065.
75. Hamidi, A., Hooresfand, M.: Effect of fiber reinforcement on triaxial shear behavior of cement treated sand. Geotext. Geomembranes. 36, 1–9 (2013). https://doi.org/10.1016/j.geotexmem.2012.10.005.
76. Cai, Y., Shi, B., Ng, C.W.W., Tang, C. sheng: Effect of polypropylene fibre and lime admixture on engineering properties of clayey soil. Eng. Geol. 87, 230–240 (2006). https://doi.org/10.1016/j.enggeo.2006.07.007.
77. Ilankeeran, P.K., Mohite, P.M., Kamle, S.: Axial Tensile Testing of Single Fibres. Mod. Mech. Eng. 02, 151–156 (2012). https://doi.org/10.4236/mme.2012.24020.
78. ASTM C1557: Standard Test Method for Tensile Strength and Young's Modulus of Fibers, https://www.astm.org/Standards/C1557, (2008).
79. Institute Public Works Research, LSS General Management. Co.Ltd: Utilization manual of liquified stabilized soil. 51 (2008).
80. Japan Society of Civil Engineering: JSCE Standard Specifications for Concrete Structures: Test Methods and Specifications. (2008).
81. Mukherjee, P.S., Satyanarayana, K.G.: Structure and properties of some vegetable fibres Part 1 Sisal fibre. J. Mater. Sci. 19, 3925–3934 (1984).
82. Silva, F. de A., Chawla, N., Filho, R.D. de T.: Tensile behavior of high performance natural (sisal) fibers. Compos. Sci. Technol. 68, 3438–3443 (2008). https://doi.org/10.1016/j.compscitech.2008.10.001.
83. De Silva, F.A., Chawla, N., Filho, R.D.T.: Mechanical behavior of natural sisal fibers. J. Biobased Mater. Bioenergy. 4, 106–113 (2010).

https://doi.org/10.1166/jbmb.2010.1074.
84. Tripathy, S.S., Landro, L. Di, Fontanelli, D., Marchetti, A., Levita, G.: Mechanical properties of jute fibers and interface strength with an epoxy resin. J. Appl. Polym. Sci. 75, 1585–1596 (2000). https://doi.org/10.1002/(SICI)1097-4628(20000328)75:13<1585::AID-APP4>3.0.CO;2-Q.
85. Fothergill, J.C.: Estimating the Cumulative Probability of Failure Data Points to be Plotted on Weibull and other Probability Paper. IEEE Trans. Electr. Insul. 25, 489–492 (1990). https://doi.org/10.1109/14.55721.
86. Satomi, T., Takahashi, H.: Setting of Optimum Conditions for Creating Fiber-Cement Stabilized Soil by Recycling Tsunami Sludge. J. Japanese Soc. Exp. Mech. 15, 225–230 (2015). https://doi.org/10.11395/jjsem.15.225.
87. Tachihana, S., Satomi, T., Takahashi, H.: Experimental Evaluation on Strength Properties of Placing Type Fiber-Cement-Stabilized Soil. Proc. Int. Symp. Earth Sci. Technol. 2016. 79–84 (2016).
88. Ateş, A.: Mechanical properties of sandy soils reinforced with cement and randomly distributed glass fibers (GRC). Compos. Part B Eng. 96, 295–304 (2016). https://doi.org/10.1016/j.compositesb.2016.04.049.
89. Sivakumar Babu, G.L., Vasudevan, A.K.: Strength and stiffness response of coir fiber-reinforced tropical soil. J. Mater. Civ. Eng. 20, 571–577 (2008). https://doi.org/10.1061/(ASCE)0899-1561(2008)20:9(571).
90. Sobhan, K., Mashnad, M.: Tensile Strength and Toughness of Soil–Cement–Fly-Ash Composite Reinforced with Recycled High-Density Polyethylene Strips. J. Mater. Civ. Eng. 14, 177–184 (2002). https://doi.org/10.1061/(asce)0899-1561(2002)14:2(177).
91. Cristelo, N., Cunha, V.M.C.F., Topa Gomes, A., Araújo, N., Miranda, T., Lurdes Lopes, M. de: Influence of fibre reinforcement on the post-cracking behaviour of a cement-stabilised sandy-clay subjected to indirect tensile stress. Constr. Build. Mater. 138, 163–173 (2017). https://doi.org/10.1016/j.conbuildmat.2017.02.010.
92. Anggraini, V., Asadi, A., Huat, B.B.K., Nahazanan, H.: Effects of coir fibers on tensile and compressive strength of lime treated soft soil. Meas. J. Int. Meas. Confed. 59, 372–381 (2015). https://doi.org/10.1016/j.measurement.2014.09.059.
93. Horpibulsuk, S., Rachan, R., Raksachon, Y.: Role of fly ash on strength and microstructure development in blended cement stabilized silty clay. Soils Found. 49, 85–98 (2009). https://doi.org/10.3208/sandf.49.85.
94. Mousavi, S.E.: Utilization of Silica Fume to Maximize the Filler and Pozzolanic Effects of Stabilized Soil with Cement. Geotech. Geol. Eng. 36, 77–87 (2018). https://doi.org/10.1007/s10706-017-0305-x.
95. Kolovos, K.G., Asteris, P.G., Cotsovos, D.M., Badogiannis, E., Tsivilis, S.: Mechanical properties of soilcrete mixtures modified with metakaolin. Constr. Build. Mater. 47, 1026–1036 (2013). https://doi.org/10.1016/j.conbuildmat.2013.06.008.
96. Goodarzi, A.R., Akbari, H.R., Salimi, M.: Enhanced stabilization of highly expansive clays by mixing cement and silica fume. Appl. Clay Sci. 132–133, 675–684 (2016). https://doi.org/10.1016/j.clay.2016.08.023.
97. Cuisinier, O., Auriol, J.C., Le Borgne, T., Deneele, D.: Microstructure and hydraulic conductivity of a compacted lime-treated soil. Eng. Geol. 123, 187–193 (2011). https://doi.org/10.1016/j.enggeo.2011.07.010.
98. Consoli, N.C., Rosa, A.D., Saldanha, R.B.: Variables Governing Strength of Compacted Soil–Fly Ash–Lime Mixtures. J. Mater. Civ. Eng. 23, 432–440 (2011). https://doi.org/10.1061/(asce)mt.1943-5533.0000186.
99. Tariq, K.A., Maki, T.: Mechanical behaviour of cement-treated sand. Constr. Build. Mater. 58, 54–63 (2014). https://doi.org/10.1016/j.conbuildmat.2014.02.017.

100. Basha, E.A., Hashim, R., Mahmud, H.B., Muntohar, A.S.: Stabilization of residual soil with rice husk ash and cement. Constr. Build. Mater. 19, 448–453 (2005). https://doi.org/10.1016/j.conbuildmat.2004.08.001.
101. Maher, M.H., Ho, Y.C., Members, A.: Mechanical properties of kaolinite/fiber soil composite. J. Geotech. Eng. 120, 1381–1393 (1994). https://doi.org/10.1061/(ASCE)0733-9410(1994)120:8(1381).
102. Choo, H., Yoon, B., Lee, W., Lee, C.: Evaluation of compressibility and small strain stiffness characteristics of sand reinforced with discrete synthetic fibers. Geotext. Geomembranes. 45, 331–338 (2017). https://doi.org/10.1016/j.geotexmem.2017.04.005.
103. Kumar, A., Walia, B.S., Mohan, J.: Compressive strength of fiber reinforced highly compressible clay. Constr. Build. Mater. 20, 1063–1068 (2006). https://doi.org/10.1016/j.conbuildmat.2005.02.027.
104. Akbulut, S., Arasan, S., Kalkan, E.: Modification of clayey soils using scrap tire rubber and synthetic fibers. Appl. Clay Sci. 38, 23–32 (2007). https://doi.org/10.1016/j.clay.2007.02.001.
105. Ahmad, F., Bateni, F., Azmi, M.: Performance evaluation of silty sand reinforced with fibres. Geotext. Geomembranes. 28, 93–99 (2010). https://doi.org/10.1016/j.geotexmem.2009.09.017.
106. Ghavami, K., Toledo Filho, R.D., Barbosa, N.P.: Behaviour of composite soil reinforced with natural fibres. Cem. Concr. Compos. 21, 39–48 (1999). https://doi.org/10.1016/S0958-9465(98)00033-X.
107. Mohamed, A.E.M.K.: Improvement of swelling clay properties using hay fibers. Constr. Build. Mater. 38, 242–247 (2013). https://doi.org/10.1016/j.conbuildmat.2012.08.031.
108. Danso, H., Martinson, D.B., Ali, M., Williams, J.: Effect of fibre aspect ratio on mechanical properties of soil building blocks. Constr. Build. Mater. 83, 314–319 (2015). https://doi.org/10.1016/j.conbuildmat.2015.03.039.
109. Consoli, N.C., Montardo, J.P., Prietto, P.D.M., Pasa, G.S.: Engineering Behavior of a Sand Reinforced with Plastic Waste. J. Geotech. Geoenvironmental Eng. 128, 462–472 (2002). https://doi.org/10.1061/(asce)1090-0241(2002)128:6(462).
110. Wei, L., Chai, S.X., Zhang, H.Y., Shi, Q.: Mechanical properties of soil reinforced with both lime and four kinds of fiber. Constr. Build. Mater. 172, 300–308 (2018). https://doi.org/10.1016/j.conbuildmat.2018.03.248.
111. Consoli, N.C., de Moraes, R.R., Festugato, L.: Variables controlling strength of fibre-reinforced cemented soils. Proc. Inst. Civ. Eng. Gr. Improv. 166, 221–232 (2013). https://doi.org/10.1680/grim.12.00004.
112. Sivakumar Babu, G.L., Vasudevan, A.K.: Seepage Velocity and Piping Resistance of Coir Fiber Mixed Soils. J. Irrig. Drain. Eng. 134, 485–492 (2008). https://doi.org/10.1061/(asce)0733-9437(2008)134:4(485).
113. Estabragh, A.R., Soltani, A., Javadi, A.A.: Models for predicting the seepage velocity and seepage force in a fiber reinforced silty soil. Comput. Geotech. 75, 174–181 (2016). https://doi.org/10.1016/j.compgeo.2016.02.002.
114. Ahmed, A.: Simplified Regression Model to Predict the Strength of Reinforced Sand with Waste Polystyrene Plastic Type. Geotech. Geol. Eng. 30, 963–973 (2012). https://doi.org/10.1007/s10706-012-9519-0.
115. Gandomi, A.H., Yun, G.J., Alavi, A.H.: An evolutionary approach for modeling of shear strength of RC deep beams. Mater. Struct. Constr. 46, 2109–2119 (2013). https://doi.org/10.1617/s11527-013-0039-z.
116. Kuno, G., Okamoto, S., Shibata, Y., Irishima, F., Taniguchi, T., Iwabuchi, J.:

Recycling Excavated Soil to Back-Filling Material with Liquefied Stabilized Soil Method. Proc. CIB World Build. Congr. Gaevle, Sweden. (1998).
117. Hejazi, S.M., Sheikhzadeh, M., Abtahi, S.M., Zadhoush, A.: A simple review of soil reinforcement by using natural and synthetic fibers. Constr. Build. Mater. 30, 100–116 (2012). https://doi.org/10.1016/j.conbuildmat.2011.11.045.
118. Kuno, G., Miki, H., Mori, N.: Filling a Cavity Under Pavement of Urban Road with Liquefied Stabilized Soil. XIIIth World Meet. Int. Road Fed. (1997).
119. Kawabata, T., Sawada, Y., Kashiwagi, A., Izumi, A., Uchida, K., Mohri, Y., Nakashima, H.: The Effect of liquefied stabilized soil with geosynthetics against thrust force of buried bend. Proc. Int. Offshore Polar Eng. Conf. 660–664 (2008).

LIST OF PUBLICATIONS

❖ **Peer-reviewed journals**

- **Thanh Nga DUONG**, Tomoaki SATOMI and Hiroshi TAKAHASHI. Potential of corn husk fiber for reinforcing cemented soil with high water content, Construction and Building Materials, Vol. 271 (2021). https://doi.org/10.1016/j.conbuildmat.2020.121848.
- **Thanh Nga DUONG**, Tomoaki SATOMI and Hiroshi TAKAHASHI. Mechanical Behavior Comparison of Cemented Sludge Reinforced by Waste Material and Several Crop Residues, Journal of Advanced Experimental Mechanics, Vol.4 pp.186-191 (2019).

❖ **International conferences**

- **Thanh Nga DUONG**, Tomoaki SATOMI and Hiroshi TAKAHASHI. Study on Strength Properties of Fiber-Liquefied Stabilization Soil Produced by Using Corn Husk Fiber, Proc. of 14th International Symposium on Advanced Science and Technology in Experimental Mechanics, USB (2019).
- **Thanh Nga DUONG**, Tomoaki SATOMI and Hiroshi TAKAHASHI. Study on the Compressive and Tensile Strength Behaviors of Corn Husk Fiber-Cement Stabilized Soil, Proc. of the International Conference GTSD2020 (2020).

ACKNOWLEDGMENTS

During three years of Doctor Course, there are many great difficulties, but this research was established with many helps and support from my professors, seniors, friends, and family.

First and foremost, I wish to express my gratefulness to my supervisor, Professor Takahashi Hiroshi, Graduate School of Environmental Studies, Tohoku University, for the continuous support of my Doctor Course study, for his patience, motivation, and immense knowledge. He gave me a lot of the invaluable assistance, supports, and guidance which make a tremendous contribution to my research and Doctor thesis. I could not have imagined having a better advisor and mentor for my study.

Secondly, I would like to express my gratitude to Professor Komai Takeshi and Professor Okamoto Atsushi, Graduate School of Environmental Studies, Tohoku University, who gave me many recommendations for my research and Doctor thesis. Their insightful comments and encouragement made a contribution to evaluate and improve my research, but also for the hard question which incented me to widen my research from various perspectives.

Next, my sincere thanks also go to Assistant Professor Satomi Tomoaki, Graduate School of Environmental Studies, Tohoku University, who created a good condition, support, and gave access to the laboratory and research facilities. Without his precious support, it would not be possible to conduct this research.

I take this opportunity to express gratitude to all members of Takahashi Laboratory, Kohei Ueno, Delima Canny Valentine Simarmata, Masahide Ishida, Hina Omuro, Kanna Kaji, Moeka Kuse, Rina Kasai, Yu Sato, Hiroaki Nakao, Nguyen Truong Van Loc, Ryohei Suzuki, Naoya Yaguchi, Misaki Yamashita, for their help and support. Especially, I am also grateful to my senior, Dr. Tran Quang Khiem, who directly and indirectly helped and gave me a lot of recommendations, assistances, and advices to finish my experiment, research, and thesis.

Finally, I would like to thank my parent and my husband. They continuous supported and created the good condition for me to study. Especially, my husband who followed all my step, helped and encouraged me during three years. Thank you so much.

The author

Duong Thanh Nga